Charles University
Second Faculty of Medicine

Doctoral study program: Biochemistry and Patobiochemistry


Mgr. Michaela Dvořáková

Molecular mechanism of Cannabinoid receptor 1 regulation by SGIP1

Molekulární mechanismus regulace signalizace kanabinoidního receptoru 1 proteinem SGIP1

Dissertation Thesis

Supervisor: doc. MUDr. Jaroslav Blahoš, Ph.D.

Prague, 2021

Declaration

I declare hereby that I made this dissertation thesis by myself and that I mentioned and cited properly all the sources and literature. At the same time, I declare that this thesis was not used to obtain another or the same title.

I agree with permanent deposition of an electronic version of my thesis in the system database of interuniversity project Thesis.cz for a permanent control of similarities of theses.

In Prague on February 1, 2021

Michaela Dvořáková

…….

Signature of the author

Acknowledgments

First of all, I would like to thank my supervisor, doc. MUDr. Jaroslav Blahoš, Ph.D. for the opportunity to become a long-term member of his team and for exciting projects. I would also like to thank prof. Ken Mackie, M.D. for the opportunity to work in his laboratory at the Department of Psychological and Brain Sciences at Indiana University in Bloomington and for his professional leadership and thoughtful approach. I would also like to thank Alex Straiker, Ph.D., for becoming my electrophysiological mentor and for his valuable advice and support by all means. Huge thanks belong to the excellent team of the Department of Molecular Pharmacology at the Institute of Molecular Genetics AS CR, v.i.i., namely to Alena Hájková, Irina Cheveleva, Judith Noda-Mayor, Matej Gazdarica, Lucie Pejšková, and Oleh Durydivka. Thanks to them, I will always think about my time in the lab with joy. I want to thank also to RNDr. Agnieszka Kubik-Zahorodná, Ph.D. and Ing. Vendula Novosádová, Ph.D. for their help with mouse phenotyping and data analysis. Many thanks also belong to my family and friends, without whose constant support this work would never have been possible. Many thanks belong to my mother, sister, and father, who were my most significant support and always listened to me patiently.

This work was created in the Laboratory of Molecular Pharmacology at the Institute of Molecular Genetics ASCR, with the support of grants GAČR 16-24210S, NIH DA009158, LM2015040 (Czech Center for Phenogenomics), CZ.1.05/2.1.00/19.0395 (Higher quality and capacity for transgenic models, Ministry of Education, Youth and Sports) and RVO 68378050 (Academy of Sciences of the Czech Republic). The work was also supported by the Fulbright Scholarship and the IMG International Mobility 2 (CZ.02.2.69/0.0/0.0/16_027/0008512, Ministry of Education, Youth and Sports).

Molecular mechanism of Cannabinoid receptor 1 regulation by SGIP1

Abstract

Src homology 3-domain growth factor receptor-bound 2-like endophilin interacting protein 1 (SGIP1) has been identified as an interacting partner of cannabinoid receptor 1 (CB1R). Their protein-protein interaction was confirmed by co-immunoprecipitation. SGIP1 hinders the internalization of activated CB1R and modulates its signaling in HEK293 cells. Employing whole-cell patch-clamp electrophysiology, we have shown that SGIP1 affects CB1R signaling in autaptic hippocampal neurons.

Using a battery of behavioral tests in SGIP1 constitutive knock-out (SGIP1$^{-/-}$) and WT mice, we investigated the consequences of SGIP1 deletion on behavior regulated by the endocannabinoid system. In SGIP1$^{-/-}$ mice, exploratory levels, working memory and sensorimotor gating were unaltered. SGIP1$^{-/-}$ mice showed decreased anxiety-like and depressive-like behaviors. Fear extinction to tone was enhanced in SGIP1$^{-/-}$ females. Several cannabinoid tetrad behaviors were altered in the absence of SGIP1. SGIP1$^{-/-}$ males exhibited abnormal THC withdrawal behaviors. SGIP1 deletion also reduced acute nociception, and SGIP1$^{-/-}$ mice were more sensitive to antinociceptive effects of CB1R agonists and morphine.

CB1R-SGIP1 interaction results in profound modification of CB1R signaling. Furthermore, *in vivo* findings suggest SGIP1 is a novel modulator of CB1R-related behavior.

Keywords

Anxiety, autaptic hippocampal neurons, cannabinoid receptor 1, endocannabinoid system, G protein coupled receptor, pain, SGIP1, tolerance, whole-cell patch-clamp electrophysiology

Molekulární mechanismus regulace signalizace kanabinoidního receptoru 1 proteinem SGIP1

Abstrakt

Src homology 3-domain growth factor receptor-bound 2-like endophilin interacting protein 1 (SGIP1) byl identifikován jako interakční partner kanabinoidního receptoru 1 (CB1R). Jejich protein-proteinová interakce byla potvrzena koimunoprecipitací. SGIP1 brání internalizaci aktivovaného CB1R a moduluje jeho signalizaci v buňkách HEK293. Pomocí elektrofyziologické metody terčíkového zámku jsme prokázali, že SGIP1 ovlivňuje signalizaci CB1R v autaptických hipokampálních neuronech.

Sadou behaviorálních testů jsme zkoumali důsledky delece SGIP1 na chování regulované endokanabinoidním systémem u myší s konstitutivní delecí SGIP1 (SGIP1$^{-/-}$) a myší WT. U myší SGIP1$^{-/-}$ nebylo změněno zkoumání prostředí, pracovní paměť a senzomotorické učení. Myši SGIP1$^{-/-}$ byly méně úzkostlivé a depresivní. U samic SGIP1$^{-/-}$ byla zrychlena extinkce averzivní vzpomínky. Projevy kanabinoidní tetrády byly delecí SGIP1 taktéž ovlivněny. Samci SGIP1$^{-/-}$ vykazovali abnormální příznaky závislosti na THC. Delece SGIP1 také snížila akutní nocicepci a myši SGIP1$^{-/-}$ byly citlivější na antinocicepční účinky agonistů CB1R a morfinu.

Interakce CB1R-SGIP1 vede k významné modifikaci signalizace CB1R. Pozorování *in vivo* dále naznačují, že SGIP1 ovlivňuje projevy chování souvisejícího s CB1R.

Klíčová slova

Autaptické hipokampální neurony, bolest, elektrofyziologie (metoda terčíkového zámku), endokanabinoidní systém, kanabinoidní receptor 1, receptor spojený s G proteinem, SGIP1, tolerance, úzkost

ABBREVIATIONS

%MPE	percents of the maximal possible effect
%ΔBT	percents of body temperature change
μHD	μ homology domain
2-AG	2-arachidonoylglycerol
AC	adenylate cyclase
AEA	N-arachidonoylethanolamine
AMPA	α-amino-3-hydroxy-5-methyl-4-isoxazole propionic acid
ANOVA	analysis of variance
AP-3	adaptor protein 3
APA	adaptor protein 2 activating domain
BRET	bioluminescence resonance energy transfer
cAMP	cyclic adenosine monophosphate
CB1R	cannabinoid receptor 1
$CB1R^{-/-}$	mouse with a deletion of CB1R gene in both alleles
CBD	cannabidiol
CHAPS	3-[(3-Cholamidopropyl)dimethylammonio]-1-propansulfonate
CNS	central nervous system
CRIP1	cannabinoid receptor 1 interacting protein 1
DAG	diacylglycerol
DAGL	diacylglycerol lipase
DNA	deoxyribonukleic acis
DSE	depolarization-induced suppression of excitation
DSI	depolarization-induced suppression of inhibition
ECS	endokanabinnoid system
EPM	elevated plus maze
ERK1/2	extracellular signal-regulated kinases 1/2
FAAH	fatty acid amide hydrolase
FC	fear conditioning

FCHO1/2	Fer/Cip4 homology domain only protein 1/2
GABA	γ-aminobutyric acid
$GABA_B$	γ-aminobutyric acid receptor B
GASP1	G protein-associated sorting protein 1
GDP	guanosine diphosphate
GFP	green fluorescent protein
GIRK	G protein-coupled inwardly-rectifying potassium channels
GPCR/s	G protein-coupled receptor/s
GRK	G protein-coupled receptor kinase
GTP	guan guanosine triphosphate
HEK293	human embryonic kidney cells 293
JNK	c-Jun N-terminal kinase
LTD	long-term depression
MGL	monoacylglycerol lipase
mGluR	metabotropic glutamate receptor
MOR	*mu* (μ) opioid receptor
MP	membrane phospholipid-binding domain
mRNA	mediator ribonucleic acid
MSE	metabotropic suppression of excitation
MSI	metabotropic suppression of inhibition
mTOR	mammalian target of rapamycin
NAPE-PLD	N-acyl-fosfatidylethanolamine phospholipase D
OF	open field
PAG	periaqueductal gray
PBS	phosphate-buffered saline
PCR	polymerase chain reaction
PI3K	phosphoinositide 3-kinase
PLC	phospholipase C
PPAR	peroxisome proliferator-activated receptor
PPI	prepulse inhibition
SA	spontaneous alteration

SDS	sodium dodecyl sulfate
SDS-PAGE	sodium dodecyl sulfate-polyacrylamide gel electrophoresis
SEM	anglického standard error of the mean
SGIP1	Src homology 3-domain growth factor receptor-bound 2-like (endophilin) interacting protein 1
SGIP1$^{-/-}$	mouse with a deletion of SGIP1 gene in both alleles
THC	Δ^9-tetrahydrocannabinol
TIT	tail immersion test
TMI-VII	transmembrane helix I-VII
TRPV1	transient receptor potential vanilloid subfamily member
TST	tail suspension test
VEH	vehicle
WIN	WIN 55, 212-2 mesylate
WT	wild-type

Contents

1. Introduction

Cell communication is a dynamic system mediated by secreted molecules serving as carriers of information and their receptors acting as acceptors and mediators. Receptors are protein molecules located either inside the cell or on the cell membrane. Membrane receptors are divided into ligand-gated ion channels (ionotropic receptors), receptors with intrinsic enzymatic activity (receptor tyrosine kinases), and G protein-coupled receptors (GPCRs), often referred to as metabotropic receptors (Alberts et al., 2014).

Receptors are a part of so-called signalosomes, complex systems that allow connection between receptors and protein molecules that transport them to specific cell sites and affect their properties and signaling activity (Burack and Shaw, 2000). Identification of new constituents of signalosomes provides a better understanding of receptor signaling.

This thesis focuses on the study of a newly described cannabinoid receptor 1 (CB1R)-associated protein called Src homology 3-domain growth factor receptor-bound 2-like (endophilin) interacting protein 1 (SGIP1). In the first publication concerning this topic, we characterized how SGIP1 modulates the CB1R signaling biochemically and pharmacologically *in vitro*. This thesis focuses on depicting the effect of SGIP1 on CB1R signaling in neurons and studying the consequences of SGIP1 modulation on mouse behavior by the reverse genetic approach.

1.1. G protein-coupled receptors

GPCRs are the largest and most diverse group of membrane receptors. GPCRs are encoded by 800 genes representing ~ 3 % of the total human genome and influence a vast number of physiological processes (Fredriksson et al., 2003). GPCRs are characterized by a conserved structure of an extracellular N-terminal domain followed by a heptahelical domain formed by seven transmembrane α-helices (TMI-VII) joined by three intracellular and three extracellular loops and an intracellular C-terminal domain (Pin et al., 2003). Intracellular loops and the C-terminus of the receptor are involved in the interaction with G proteins and other regulatory proteins. (Weis and Kobilka, 2018).

1.1.1. Classification of G protein-coupled receptors

GPCRs are classified into six families (denoted A-F) based on their sequence similarity and phylogenetic analysis (Fredriksson et al., 2003; Kolakowski, 1994). Approximately 80% of all GPCRs belong to family A. Characteristic for this family is an activation of its members by small ligands and the presence of an eighth intracellular helix in their structure. This family includes biogenic amine, rhodopsin, β adrenergic, chemokine, opioid, and cannabinoid receptors. Family B includes receptors for high molecular weight peptide hormones such as secretin, glucagon, corticotropin-releasing hormone, calcitonin, and parathyroid hormone. Family C receptors have a characteristic large extracellular N-terminal domain. Typical receptors of this family are metabotropic glutamate (mGluR) and γ-aminobutyric acid receptors B ($GABA_B$). Family D contains receptors for fungal pheromones and family E receptors for cyclic adenosine monophosphate (cAMP) (Luttrell, 2008; Pierce et al., 2002). The latter family F contains frizzled/smoothened receptors involved in cell proliferation and differentiation and tissue morphogenesis (Arensdorf et al., 2016; MacDonald and He, 2012).

1.1.2. Activation of G protein-coupled receptors

GPCRs recognize their ligands with distinguishable affinity and properties resulting in distinct outcomes for signaling. Based on the ability to elicit a specific response, GPCR ligands are divided into agonists, antagonists, and inverse agonists. An agonist is a ligand

that, by binding to the receptor, causes a biological response. A full agonist elicits the maximum possible response of a given signaling system. A partial agonist, on the other hand, can elicit only a weaker response. An antagonist does not elicit any response by binding to the receptor but prevents the binding of an agonist. The receptor can acquire an active conformation even without a ligand bound, causing so-called constitutive activity. An inverse agonist reduces constitutive, basal receptor activity (Berg and Clarke, 2018).

GPCR activation is accompanied by a conformational change in the receptor's transmembrane domain (Gether and Kobilka, 1998). This conformational change reveals a binding site for G protein. Subsequently, the G protein is activated by the receptor (Farrens et al., 1996). The information transmission via GPCRs typically involves such activation of G protein but also includes G protein-independent signaling (Pin et al., 2003). Those will be described in chapters 1.1.4 and 1.1.5.

1.1.3. G proteins and their role in signaling

Heterotrimeric G proteins serve as mediators between activated GPCRs and their intracellular signaling cascades. They consist of three subunits: α, β, and γ. In the inactive state, the α subunit binds guanosine diphosphate (GDP). Upon activation, GDP is exchanged for guanosine triphosphate (GTP), and the trimeric protein complex breaks down into an activated α subunit and a βγ dimer. Both of the isolated subunits subsequently bind to effector molecules and trigger cellular responses, e.g., phosphorylation of protein kinases. At the end of the signaling cycle, the α subunit hydrolyses GTP and reassembles into an inactivated trimeric G protein (de Oliveira et al., 2019). The G protein signaling cycle ensures tight regulation of G protein activity (**Fig. 1**).

Based on the structure and intracellular functions, α subunits of G proteins are classified into four families. The $G\alpha_s$ subunits stimulate adenylate cyclase (AC), which produces cAMP. Conversely, $G\alpha_{i/0}$ subunits inhibit AC. $G\alpha_{q/11}$ subunits activate beta isoform of phospholipase C (PLCβ), and $G\alpha_{12/13}$ subunits activate RhoA GTPase (Oldham and Hamm, 2008).

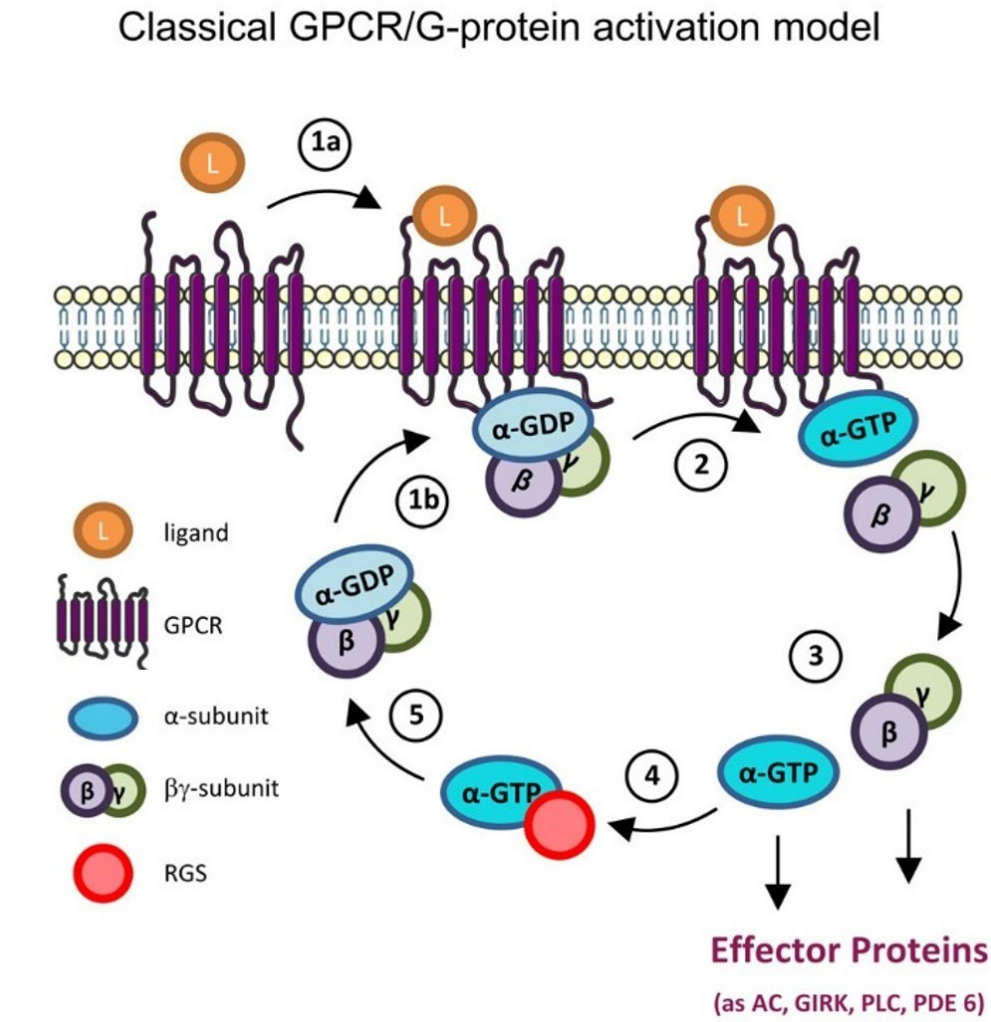

Fig. 1. Mechanism of activation of G protein-coupled receptors. In the inactive state, heterotrimeric G proteins form a complex consisting of α subunit with bound guanosine diphosphate (GDP) and βγ subunit. (**1a**) The binding of a ligand to a G protein-coupled receptor (GPCR) causes a conformational change in the receptor, (**1b**) which allows G protein to bind to the receptor. (**2**) G protein binding to a receptor causes another conformational change, this time in the α subunit of the G protein, followed by the exchange of GDP for guanosine triphosphate (GTP) and the separation of the βγ subunit. (**3**) In this step, the G protein is activated, and both subunits, α, and βγ, transmit a signal to the effector proteins, and the subsequent modulation of signaling pathways occurs. (**4**) G protein activation is terminated by the hydrolysis of GTP to GDP, which may additionally be affected by the binding of regulators of G protein signaling to the α subunit. (**5**) Hydrolysis of GTP causes the re-formation of the trimeric G protein complex, which is again inactive. AC - adenylate cyclase, GIRK - G protein-coupled inwardly-rectifying potassium channels, PDE 6 – phosphodiesterase 6, PLC - phospholipase C (de Oliveira et al., 2019).

1.1.4. Desensitization of G protein-coupled receptors

Signaling via GPCRs is modulated and terminated in a controlled manner. One possible change in signaling occurs via desensitization. Desensitization is a process in which the receptor's response to an external stimulus is altered, reduced, or stopped. The receptor can be desensitized after long-term exposure to an agonist or repeated short-term agonist administration (homologous desensitization - desensitization only for that receptor). Desensitization can also occur heterologously if the downstream signaling molecules in the receptor signaling pathway are over-activated through other receptors (Kelly et al., 2008).

During desensitization, the activated βγ subunit of a G protein facilitates the recruitment of G protein-coupled receptor kinases (GRK) and protein kinases A and C to the GPCR (Delom and Fessart, 2011; Smrcka, 2008). The kinases phosphorylate intracellular portions of the receptor, chiefly the C-terminus. GPCR phosphorylation increases the receptor affinity for proteins from the β-arrestin family. The β-arrestin binding to the activated GPCR causes uncoupling of the G protein, thereby terminating the G protein signaling. At the same time, β-arrestins allow the binding of several other adaptor proteins. The newly formed complexes of receptor and adaptor proteins trigger multiple downstream signaling pathways (Gainetdinov et al., 2004). Phosphorylation of the GPCR C-terminus encodes the bound β-arrestin's conformation, which then determines what signaling pathway/s will be activated. Therefore, different phosphorylation patterns serve as barcodes for subsequent cellular events to be triggered (Liggett, 2011).

1.1.5. Internalization of G protein-coupled receptors

Another way to modulate GPCR signaling is a reduction of receptors available on the membrane by their internalization (endocytosis) (Mills, 2007) (**Fig. 2**). Internalization is usually triggered by ligand binding to the receptor. However, internalization can occur in the absence of ligand as well. Such internalization is called constitutive (McMahon and Boucrot, 2011).

By binding to the receptor, β-arrestin triggers a cascade of internalization events. Bound β-arrestin links the receptor to clathrin via adaptor protein 2 and thus facilitates its clathrin-mediated endocytosis (Hamdan et al., 2007; Luttrell and Gesty-Palmer, 2010). In the early stages of endocytosis, other adaptor proteins such as Fer/Cip4 homology domain only protein 1/2 (FCHO1/2) have an essential function initiating membrane invagination and promoting clathrin network formation around the endocytosed part of the membrane (Henne et al., 2010). Many endocytic proteins combine during this (nucleation) stage, both activators, and inhibitors. The protein studied in this thesis, SGIP1, acts as a negative regulator in CB1R endocytosis in HEK293 cells, maybe by shifting the equilibrium towards the endocytosis inhibition (Hajkova et al., 2016) (see chapters 1.7.1 and 1.8).

During later stages of endocytosis, clathrin-coated pits are scissioned by the GTPase dynamin, leading to intracellular vesicles' formation. Inside the cell, the clathrin coat is disassembled, and the vesicle fuses with an early endosome. In the endosome, receptors are dephosphorylated and further recycled back to the membrane or sent for degradation in a lysosome (McMahon and Boucrot, 2011).

In the endosome, β-arrestin may remain associated with the GPCR for some time, thus allowing further signaling. This signaling utilizes mainly extracellular signal-regulated kinases 1/2 (ERK1/2). It has been shown that even the G protein signaling can partially occur on intracellular membranes (Calebiro and Godbole, 2018).

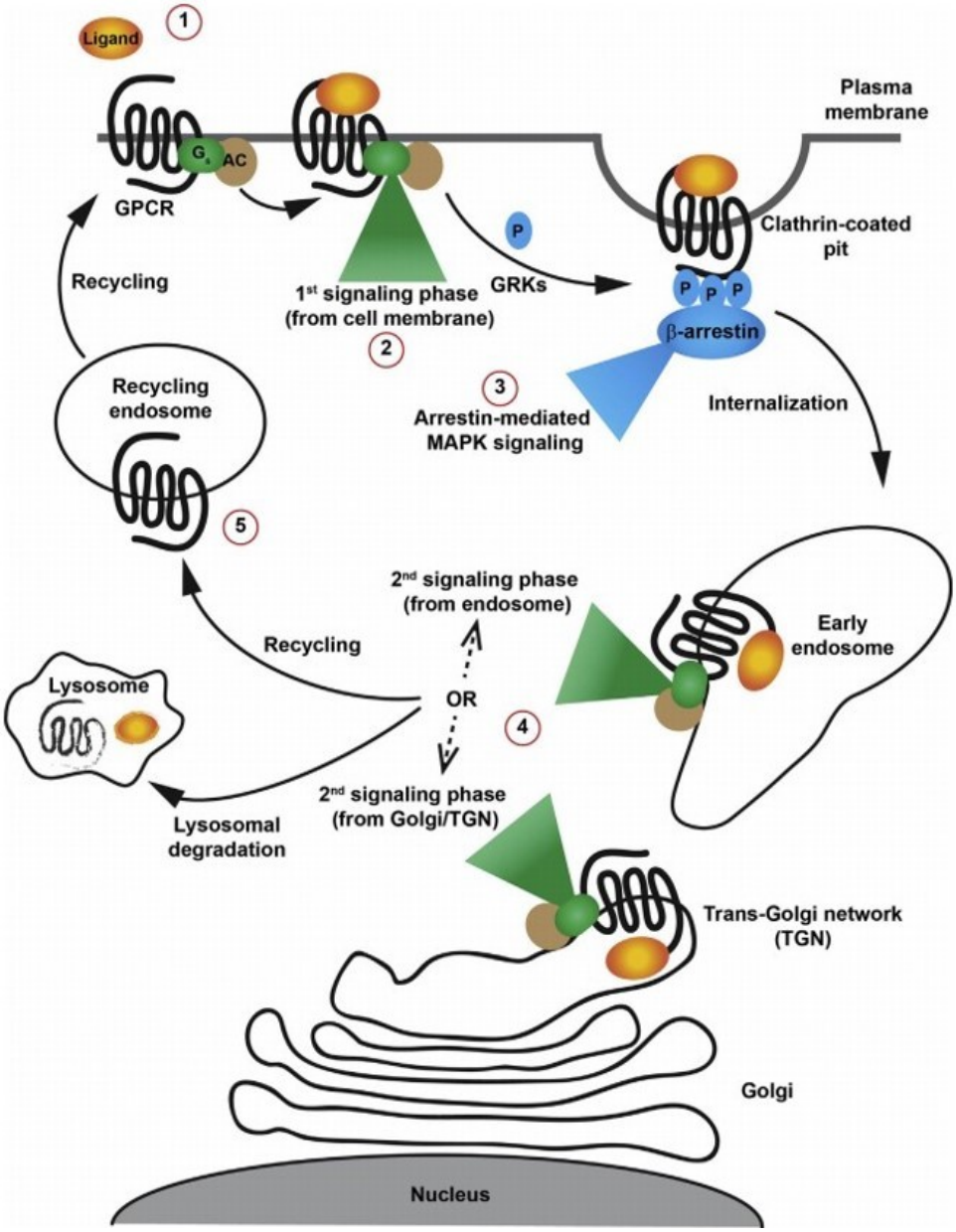

Fig. 2. Internalization of G protein-coupled receptors (GPCRs) in relation to their signaling. (**1**) Ligand binding triggers (**2**) the first wave of G protein signaling near the plasma membrane. Phosphorylation of an activated receptor by G protein-coupled receptor kinase (GRK) allows the binding of β-arrestin to the receptor and the subsequent receptor desensitization. (**3**) Signaling by mitogen-activated protein kinases (MAPK) or extracellular signal-regulated kinases 1/2 (ERK1/2) also occurs during this process. (**4**) β-arrestin further triggers internalization of the receptor, which may trigger the second phase of signaling via G proteins from the early endosome or trans-Golgi apparatus. (**5**) Finally, the receptor is degraded in the lysosome or recycled and transported back to the plasma membrane, where it can engage in the next round of signal transduction (Calebiro and Godbole, 2018).

1.1.6. Functional selectivity at G protein-coupled receptors

GPCRs can act in favor of the G-protein or β-arrestin signaling, depending on what ligand activates the receptor. This leads to functional selectivity of different agonists binding the same receptor, or in other words, to biased signaling (Berg and Clarke, 2018).

To describe the pharmacological properties of ligands as accurately as possible, it is necessary to examine all signaling pathways that may be affected by the activity of the GPCR they bind. One ligand can act on the receptor as an agonist, an inverse agonist, and an antagonist, depending on the observed signaling pathway (Berg and Clarke, 2018; Smith et al., 2018) (**Fig. 3**). Functional selectivity of GPCR ligands is a promising tool for the development of new therapeutics with comparable, or even better, efficacy and less negative properties than those of existing drugs. Several functionally selective GPCR ligands are already undergoing late phases of clinical testing (Wisler et al., 2018).

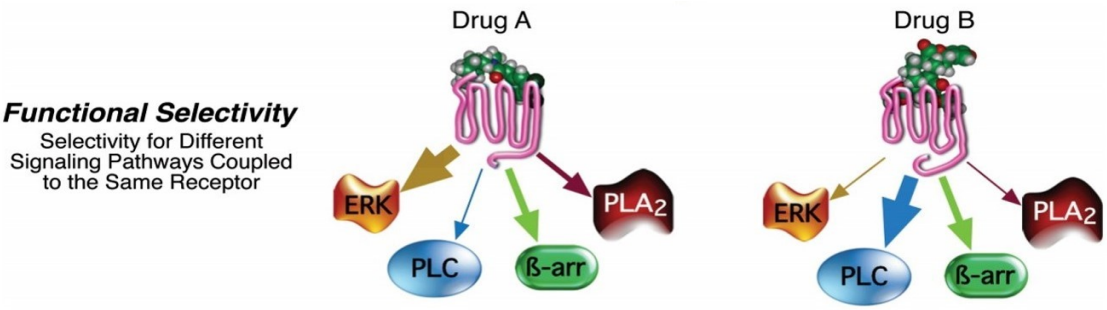

Fig. 3. Functional selectivity of G protein-coupled receptors. Functional selectivity is based on ligands' different abilities to activate signaling pathways within the cell via their binding to a receptor. The thickness of the arrow indicates the degree of functional selectivity towards a specific pathway. Extracellular signal-regulated kinases (ERKs), phospholipase C (PLC), β-arrestins (β-arr), and phospholipase A (PLA) can serve as effector proteins (Berg and Clarke, 2018).

1.2. Endocannabinoid system

The endocannabinoid system (ECS) is a neuromodulatory system that plays an important role in the development of the central nervous system (CNS) and the body's responses to the external environment (Lu and Mackie, 2016). The ECS consists of endogenous ECS ligands (endocannabinoids), enzymes involved in their synthesis and

degradation, and receptors recognizing these ligands (Piomelli, 2003). The major endocannabinoids are 2-arachidonoylglycerol (2-AG) (Sugiura et al., 1995) and N-arachidonoylethanolamine (anandamide, AEA) (Devane et al., 1992). These compounds with long polyunsaturated chains (**Fig. 4**) are synthesized from phospholipids of the postsynaptic membrane. 2-AG is synthesized from diacylglycerol by two isoforms of diacylglycerol lipase (DAGLα, β). The primary enzyme for AEA synthesis is N-acyl-phosphatidylethanolamine phospholipase D (NAPE-PLD). After the synthesis, the endocannabinoids are transported through the synaptic cleft and act on receptors located in the presynaptic membrane. Endocannabinoids that do not bind to receptors are removed from the synaptic cleft and degraded in the neuron's presynaptic part. 2-AG is degraded by monoacylglycerol lipase (MGL) and AEA by fatty acid amide hydrolase (FAAH) (Toczek and Malinowska, 2018).

Besides endogenous cannabinoids, exogenous substances of plant origin, such as Δ^9-tetrahydrocannabinol (THC) and cannabidiol (CBD), or synthetic cannabinoids, such as WIN 55, 212-2 mesylate (WIN), act as cannabinoid receptors ligands (**Fig. 4**) (Pertwee, 2009).

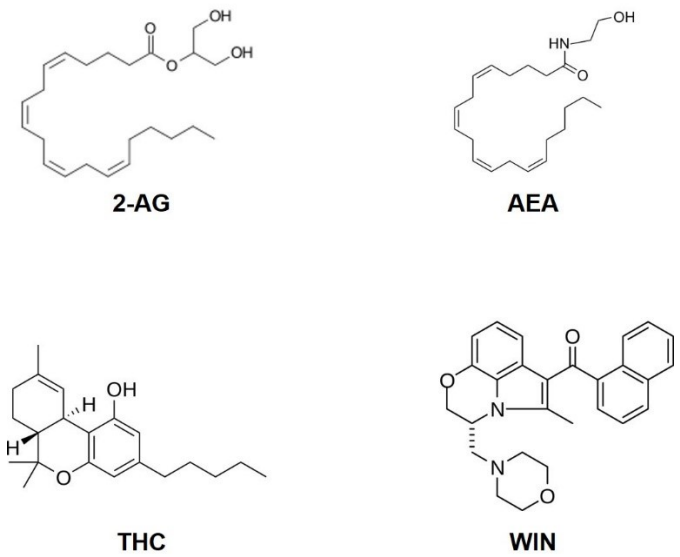

Fig. 4. Structures of major cannabinoid receptor 1 agonists. Major cannabinoid receptor 1 agonists include 2-arachidonoylglycerol (2-AG), N-arachidonoylethanolamine (AEA), Δ^9-tetrahydrocannabinol (THC), and WIN 55, 212-2 mesylate (WIN).

Cannabinoid-activated receptors include CB1R (Howlett et al., 1990), cannabinoid receptor 2 (CB2R) (Munro et al., 1993), and other, less numerous, receptors such as peroxisome proliferator-activated receptor (PPAR), transient receptor potential vanilloid subfamily member (TRPV1) or GPR55 (from G-protein coupled receptor 55) (Begg et al., 2005).

CB1R is the most abundant GPCR in the CNS (de Jesus et al., 2006). In the brain, CB1R is expressed primarily in the cortex, hippocampus, basal ganglia, and cerebellum (Freund et al., 2003) (**Fig. 5**). In neurons, CB1R is located on presynaptic membranes (Howlett et al., 2002).

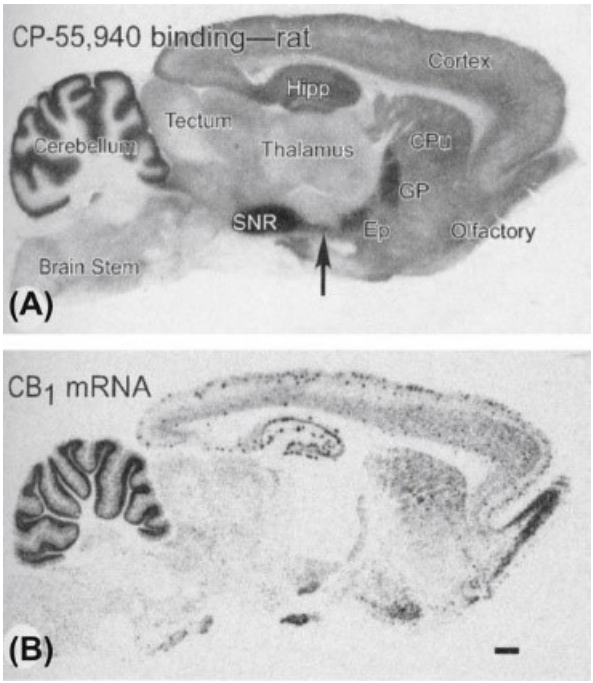

Fig. 5. Localization of cannabinoid receptor 1 in rat brain. Autoradiographic staining showing the localization of CB1R in the sagittal section of the rat brain. (**A**) Staining by the tritiated CB1R ligand CP-55, 940, and (**B**) specific oligonucleotide probes indicate CB1R localization at the protein and mediator ribonucleic acid (mRNA) level, respectively. High expression of CB1R is evident in the structures of the basal ganglia - globus pallidus (GP), entopeduncular nucleus (Ep), and substantia nigra pars reticulata (SNR). Furthermore, CB1R is abundantly localized in the cerebellum, hippocampus, cortex, and caudate putamen (Cpu). Low CB1R expression occurs in the brain stem, tectum, and thalamus (Freund et al., 2003).

1.3. Cannabinoid receptor 1 structure and signaling

CB1R transmits signals primarily through the $G\alpha_{i/0}$ family of G proteins (Childers and Deadwyler, 1996). $G\alpha_{i/0}$ proteins inhibit AC and block the flow of calcium ions through N and P/Q channels into the cell (Freund et al., 2003). $G\alpha_{i/0}$ proteins also affect type A and M potassium channels (Mu et al., 1999; Schweitzer, 2000). Via G proteins, CB1R regulates the release of neurotransmitters, such as the major excitatory and inhibitory neurotransmitters glutamate and γ-aminobutyric acid (GABA), opioids, acetylcholine, dopamine, noradrenaline, and cholecystokinin (Schlicker and Kathmann, 2001).

In addition to the signaling pathways of $G_{i/0}$ proteins, CB1R, to a lesser extent, activates G_s and G_q proteins and also G protein-independent pathways, e.g., the aforementioned β-arrestin signaling (Ligresti et al., 2016). CB1R affects several cellular signaling cascades, including the mammalian target of rapamycin (mTOR), ERK1/2, the c-Jun N-terminal kinase (JNK), and phosphatidylinositol-3 kinase (PI3K). The resulting CB1R response to ligands depends on the cell type and its available signaling pathways (Busquets-Garcia et al., 2015).

1.3.1. Electrophysiological characteristics of the cannabinoid receptor 1 signaling

Activated CB1R causes retrograde inhibition of the neurotransmitter release into the synaptic cleft (**Fig. 6**). This phenomenon is called synaptic plasticity (Di Marzo et al., 2004). Three basic forms of synaptic plasticity affected by CB1R are recognized and can be studied by electrophysiological methods - depolarization-induced suppression of neurotransmission, metabotropic suppression of neurotransmission, and long-term suppression of neurotransmission (Lu and Mackie, 2016; Mackie, 2008).

Depolarization-induced suppression of neurotransmission is a response to a strong synapse activation by repeated action potentials lasting several tens of seconds or brief membrane depolarization (Lu and Mackie, 2016). During this process, a short-term reduction of the neurotransmitter release into the synaptic cleft occurs. Depending on the type of synapse and the neurotransmitter that is primarily released at the given synapse,

two types of short-term synaptic plasticity are recognized - depolarization-induced suppression of excitation (DSE) and depolarization-induced suppression of inhibition (DSI). In the case of DSE, glutamate release is suppressed at excitatory synapses. During DSI, GABA release is suppressed at inhibitory synapses (Kreitzer and Regehr, 2001; Pitler and Alger, 1992).

Metabotropic suppression of neurotransmission is triggered upon activation of postsynaptically localized metabotropic receptors associated with $G_{q/11}$ proteins, including, for example, mGluR1 and mGluR5 (Kano et al., 2009). As with DSE/DSI, two types of synaptic plasticity are recognized - metabotropic suppression of excitation (MSE) with reduced glutamate release and metabotropic suppression of inhibition (MSI) in the case of the neurotransmitter GABA (Lu and Mackie, 2016).

Long-term depression (LTD) is typically induced by a persistent low-frequency stimulation and can occur homosynaptically or heterosynaptically. Homosynaptic LTD manifests at the same synapse that is stimulated. Heterosynaptic LTD occurs at the synapse adjacent to the stimulated neuron (Lu and Mackie, 2016).

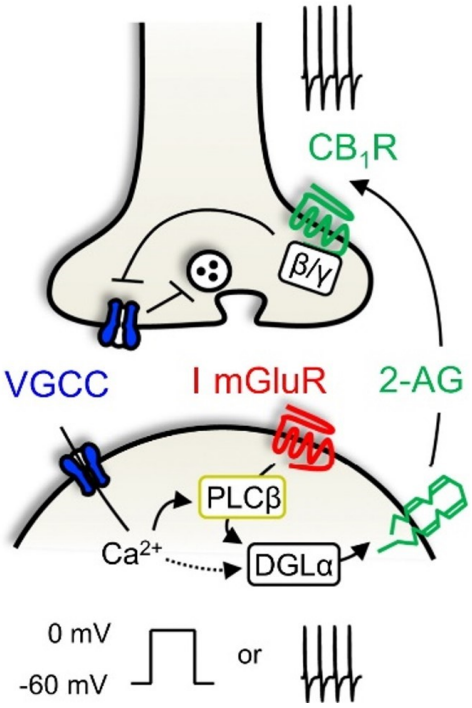

Fig. 6. Retrograde control of excitatory synaptic transmission by cannabinoid receptor 1. Postsynaptic activity triggers Ca^{2+} influx into the cell via voltage-gated Ca^{2+} channels (VGCCs). Increased Ca^{2+} level promotes the production of endocannabinoids by diacylglycerol lipase α (DGLα). The presynaptic activity can also lead to endocannabinoid production by activating postsynaptic group I metabotropic glutamate receptors (I mGluRs) and subsequently phospholipase C β (PLCβ). Synthesized endocannabinoids, mainly 2-arachidonoylglycerol (2-AG), retrogradely target presynaptic CB1Rs. The CB1R activated βγ subunits of G proteins couple to presynaptic VGCCs to reduce neurotransmitter release (Castillo et al., 2012).

1.4. Behavioral aspects of the cannabinoid receptor 1 signaling

All types of synaptic plasticity mentioned above are involved in the modulation of behavior. Areas of behavior physiologically affected by CB1R will be discussed in the following chapters.

Changes in cannabinoid signaling can have severe pathological effects on behavior. However, there are also positive effects of the modulation of cannabinoid signaling. The most common symptom of CB1R agonist (THC) intoxication in humans is a mild euphoric state. There are several other manifestations of THC intoxication, such as impaired linear thinking, impaired concentration, worsened memory and locomotor abilities, tachycardia, but also improved sensory perception, pain relief, nausea relief, and increased appetite (Hollister, 1986). In mice, CB1R agonists cause a characteristic

combination of four symptoms called the cannabinoid tetrad. The tetrad behavior consists of catalepsy (decreased ability to move), antinociception (decreased sensitivity to pain), hypothermia (decreased body temperature), and hypoactivity (decreased spontaneous horizontal activity) (Chaperon and Thiebot, 1999).

1.4.1. Motor functions

CB1R is also located in the basal ganglia and cerebellum, the parts of the brain that directly control motor function. Biochemical changes in the cannabinoid system are accompanied by etiological manifestations of several motor function diseases. Excessive ECS activity has been observed in patients with Parkinson's disease (Pisani et al., 2005), and, conversely, a decrease in CB1R signaling accompanies Huntington's disease (Glass et al., 1993).

Mice with genetic deletion of CB1R have impaired locomotor activity and tend to be more cataleptic compared to mice naturally expressing CB1R. Although the cerebellar cortex contains the highest amount of CB1R within the brain, ECS signaling changes are not profoundly manifested in motor skills. CB1R primarily affects discrete motor learning (Kishimoto and Kano, 2006).

1.4.2. Memory and cognitive functions

The function of CB1R is important in the process of memory formation (Marsicano and Lafenetre, 2009). Memory consists of acquiring, storing, and recalling any information about previous experiences (Milner et al., 1998). Several studies have shown that cannabinoid intoxication impairs cognitive function by altered activation of memory-associated brain regions (Bossong et al., 2014). The critical structure responsible for memory formation is the hippocampus (Squire, 2004), in which CB1R is highly expressed (Herkenham et al., 1990). The adverse effects of exogenous cannabinoids on memory are probably manifested mainly due to their function in the hippocampus. The effects of CB1R agonists topically injected directly into the hippocampus are consistent with the effects of systemically administered cannabinoids (Han et al., 2012; Lichtman et al., 1995; Suenaga and Ichitani, 2008).

γ-oscillations in the neural network are associated with forming memories (Nyhus and Curran, 2010). CB1R agonists reduce these oscillations and thus impair memory (Robbe et al., 2006). The molecular mechanism behind these changes is probably a decrease in synaptic activity and a consequent change in synaptic plasticity caused by CB1R in the CA3-CA1 region of the hippocampus (Hampson and Deadwyler, 2000).

1.4.3. Fear and anxiety

Fear and anxiety are manifested similarly. However, they differ in what evokes them. Fear is a response to a specific imminent danger, while anxiety is an emotion occurring without an immediate cause. ECS is involved in regulating fear and anxiety, but its mechanism of action has not yet been elucidated (Micale et al., 2013; Patel et al., 2017). CB1R agonists often have contradictory, so-called biphasic effects on anxiety in humans and experimental animals. At lower doses, they act as anxiolytics (i.e., relieving anxiety), at higher doses as anxiogenics (i.e., inducing anxiety) (Rey et al., 2012).

Similarly, administration of CB1R antagonists can cause (Navarro et al., 1997) but also alleviate anxiety (Haller et al., 2002). Marijuana intoxication in low doses is often accompanied by reduced anxiety in humans. However, at high doses, it can cause dysphoric reactions, panic, paranoia, and psychosis (Viveros et al., 2005). The molecular basis of the biphasic effect of CB1R ligands could be explained by the balance between glutamatergic and GABAergic signaling. Stimulation of CB1R with low doses of its agonists increases CB1R activation in glutamatergic synapses, which has anxiolytic effects. In contrast, after stimulation with high concentrations of agonists, increased CB1R signaling in GABAergic synapses is manifested by anxiogenic effects (Rey et al., 2012).

The principle of fear conditioning is pairing between an initially neutral stimulus (conditioned stimulus) and a stimulus evoking fear (unconditional stimulus, e.g., mild electric shock). To experimentally test fear conditioning, the sensation of fear is induced, for example, by a loud tone. After one such pairing, the observed subject pairs the two stimuli and responds to the conditioned stimulus with fear immediately upon the next encounter with it (LeDoux, 2000).

Acquiring and storing aversive memories is one of the essential functions of the CNS in animals (LeDoux, 2000). If an acquired memory is not strengthened, it gradually weakens until it disappears completely. However, the disappearance of an aversive memory can also be an active process. A reduction in the conditioned fear response occurs after repeated encounters with a conditioned stimulus that is not accompanied by an element causing fear (Myers and Davis, 2007). CB1R plays a vital role in the process of aversive memories forgetting. Mice with a genetic deletion of CB1R have more difficulties in forgetting traumatic experiences than mice that express CB1R normally (Marsicano et al., 2002).

Gender also plays an important role in the cannabinoid regulation of anxiety and fear (Cooper and Craft, 2018). Acute administration of cannabinoids causes stronger anxiogenesis in female rats than in males rats (Marco et al., 2006).

1.4.4. Pain

The antinociceptive effects, i.e., pain-reducing effects, of endocannabinoids have been described in several animal models of pain. Cannabinoids are considered promising agents for the treatment of pain, especially inflammatory and neuropathic pain. These kinds of pain do not respond well to conventional therapy available (Rice, 2001). The cannabinoid-related pain relief is manifested at distinct signaling levels; in the CNS, but also peripheral sensory neurons and the spinal cord (Pertwee, 2001). Cannabinoids inhibit synaptic transmission in neurons located in the periaqueductal gray (PAG) (Vaughan et al., 2000). These nuclei are part of descending nociceptive pathways that affect the transmission of painful stimuli at the spinal cord level (Fields et al., 1991). The antinociceptive effects of endogenous cannabinoids were demonstrated by electrical stimulation of PAG *in vivo* in the rat brain. Stimulation resulted in a local release of anandamide, and as a consequence, an increase of the thermal pain threshold was observed. When a selective CB1R antagonist was pre-administered to the tested rats, the antinociceptive effect of the electrical stimulation did not occur (Walker et al., 1999).

CB1R signaling is intertwined with the opioid system (Cichewicz, 2004). CB1R and the mu (μ) opioid receptor (MOR) form functional heterodimers (Hojo et al., 2008).

Spinal administration of various cannabinoids to mice combined with morphine has a more than additive antinociceptive effect (Welch and Stevens, 1992). However, the potentiation of morphine-induced antinociception by cannabinoids is not a universal phenomenon. Pain perception and treatment has two components - spinal and supraspinal. Some cannabinoids enhance the effect of morphine in the brain, others act in the spinal cord (Welch et al., 1995). Therefore, knowledge about the effect of one particular cannabinoid cannot be applied to other cannabinoids.

1.4.5. Energy homeostasis

Increased activity of the endocannabinoid system leads to weight gain, decreased insulin sensitivity, and glucose intolerance (Di Marzo and Matias, 2005). Cannabinoids stimulate food intake in fed animals (Hao et al., 2000; Williams and Kirkham, 1999; Williams et al., 1998). In contrast, blockade of the CB1R signaling by antagonist leads to weight loss due to increased secretion of anorexigenic signals and increased insulin sensitivity (Colombo et al., 1998; Rowland et al., 2001; Simiand et al., 1998).

ECS controls food intake by two mechanisms. On the one hand, ECS strengthens the motivation to consume food, probably through the mesolimbic pathways, which are part of the reward system in the brain. On the other hand, ECS can be triggered by a stimulus activation, such as brief starvation. Activated ECS transiently regulates the levels of other orexigenic and anorexigenic substances to increase appetite (Di Marzo and Matias, 2005).

Rimonabant (SR141716, Acomplia®), a selective CB1R antagonist, has been used in clinical practice in Europe as an obesity treatment drug (Scheen and Paquot, 2009). In obese people, rimonabant caused weight loss and accelerated lipid and glucose metabolism. However, for rimonabant, increased detection of depression and suicidal tendencies compared to other treatments was reported, and therefore its further use was stopped (Christopoulou and Kiortsis, 2011).

1.5. Cannabinoid receptor 1 signaling modulation

CB1R signaling is associated with a number of physiological as well as pathological manifestations. Modulation of cannabinoid signaling by exogenous ligands is an important area and may lead to the development of new drugs. CB1R ligands can act as full or partial agonists or antagonists. Synthetic THC (dronabinol), a partial CB1R agonist, is used in the United States as a drug for chemotherapy-related nausea and also to support appetite in cachectic patients (Badowski and Yanful, 2018). In contrast, CB1R antagonists act as food restriction agents (Black, 2004). One of them, rimonabant, was briefly marketed as an anti-obesity drug in Europe (see chapter 1.4.5).

Full CB1R agonists and antagonists cause many side effects that limit their medical use (Pertwee, 2012). Current research is focused on more subtle modulation of the CB1R signaling, e.g., by allosteric modulators that fine-tune the effects of orthosteric ligands. For example, CBD, the second most abundant substance in marijuana, acts on CB1R as a negative allosteric modulator (Laprairie et al., 2015; Straiker et al., 2018). These discoveries may well be a lead in the development of novel therapies.

The discovery of functionally selective or biased ligands provides another possibility for modulating the signaling of CB1R (Picone and Kendall, 2015). As of now, there are not many CB1R biased ligands described. One of them is PNR-4-20, an agonist that activates CB1R G protein signaling more than β-arrestin mediated signaling. So far, this substance has been studied only experimentally in mice but shows the yet unexplored potential of functionally selective CB1R ligand (Ford et al., 2019). Such ligands could be used for better-controled modulation of CB1R signaling, with less serious side effects.

CB1R signaling may be affected at the level of the receptor desensitization and internalization. These processes determine signaling properties, timing, and availability of the receptors on the plasma membrane to external stimuli. In this matter, CB1R interacting partners may play an important role.

1.6. Cannabinoid receptor 1-interacting partners

Proteins that interact intracellularly with CB1R influence cannabinoid signaling. So far, only a few proteins interacting with the C-terminus of CB1R have been described

(Fletcher-Jones et al., 2020). These include proteins that generally interact with GPCRs, such as β-arrestin 1 and 2, adaptor protein 3 (AP3), and G protein-associated sorting protein 1 (GASP1). Specific CB1R interaction partners are CB1R-interacting protein 1a (CRIP1a) and SGIP1, identified in our lab (Hajkova et al., 2016). The CB1R interaction sites for GASP1, CRIP1a, and SGIP1 are shown in **Fig. 7**.

β-arrestins are molecules that are generally responsible for the desensitization and internalization of GPCRs (see chapters 1.1.4 a 1.1.5). Desensitization or internalization is triggered depending on which part of the CB1R C-terminus the β-arrestin 2 binds. If β-arrestin 2 binds the proximal C-terminus, specifically phosphorylated serines S426 and S430, it mediates CB1R desensitization (Jin et al., 1999). The binding of β-arrestin 2 to phosphorylated serine and threonine residues in the distal CB1R C-tail leads to the receptor internalization (Daigle et al., 2008b).

β-arrestins affect CB1R signaling (Delgado-Peraza et al., 2016). The importance of β-arrestin 2 for endocannabinoid signaling and related behavior was demonstrated in experiments with mice in which the β-arrestin 2 gene was deleted. THC administration in the β-arrestin 2 knock out mice causes higher antinociception and hypothermia, and their tolerance to nociceptive effects of THC develops more slowly. In contrast, the tolerance to cataleptic effects of THC develops faster in β-arrestin 2 knockout mice than in wild-type (WT) mice. While THC induces a change in β-arrestin 2 knockout mice pain perception, other CB1R agonists (CP55940 or JWH-073) do not have this effect (Breivogel et al., 2008; Nguyen et al., 2012).

Adaptor protein 3 (AP-3) is involved in the sorting of internalized CB1Rs. AP-3 is associated with CB1R during its transport from the cell biosynthetic compartment to lysosomes (Rozenfeld and Devi, 2008). GASP1 also binds the C-terminus of CB1R, specifically in the region of the eighth intracellular helix (Simonin et al., 2004). GASP1 is involved in the sorting of endocytosed proteins and controls the lysosomal transport of CB1R and other GPCRs (Boeuf et al., 2009; Martini et al., 2007; Whistler et al., 2002).

CRIP1a is abundant in the brain, where it is localized presynaptically in both excitatory and inhibitory synapses, but can be found also in non-CB1R expressing cells (Guggenhuber et al., 2016). The interaction of CB1R and CRIP1a was demonstrated by

co-immunoprecipitation from the rat brain. CRIP1a binds to the distal C-terminus of CB1R and affects its signaling and agonist-induced internalization by competing with β-arrestin 2 for binding to the CB1R C-tail (Blume et al., 2016; Blume et al., 2017; Mascia et al., 2017; Niehaus et al., 2007). CRIP1a also negatively modulates constitutive endocytosis of CB1R (Mascia et al., 2017). In neurons, CRIP1a attenuates CB1R-mediated inhibition of voltage-gated calcium channels (Niehaus et al., 2007).

Accordingly, overexpression of CRIP1a attenuates CB1R G protein signaling in HEK293 cells, N18TG2 cells, and autaptic neuronal cultures, reducing the downstream inhibition of N-type VGCCs and activation of ERK (Niehaus et al., 2007; Blume et al., 2015, 2017; Smith et al., 2015).

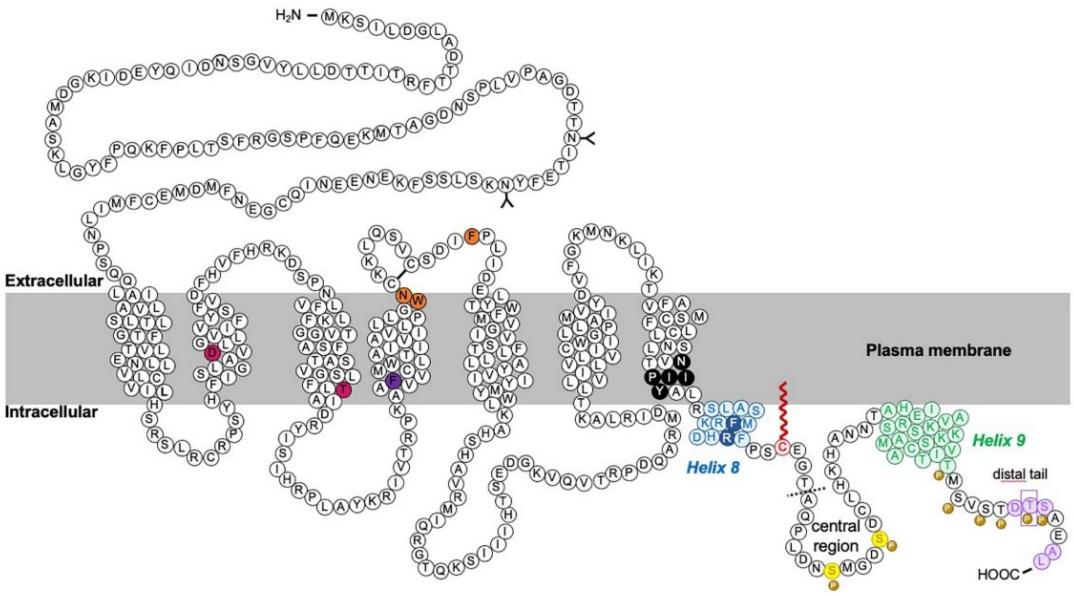

Fig. 7. Schematic CB1R structure with a depiction of protein interaction sites. Two residues located within the 2nd and 3rd transmembrane domains required for constitutive internalization are shown in pink. Two intracellular helices, helix 8 (H8) and helix 9 (H9), are highlighted in blue and green, respectively. Phosphorylation of two serine residues (yellow) in the intracellular C-terminus mediates desensitization. Phosphorylation of 6 serine/threonine residues in the distal tail (indicated by the "P" symbols) is required for internalization. GASP1 likely binds the H8 and distal C-tail. The motifs required for CRIP1a binding are shown in purple. Phosphorylation of T468 (purple rectangle) decreases affinity for CRIP1a and allows β-arrestin 2 binding. The exact binding site of SGIP1 is unknown, but it binds downstream of A420 (dotted line). (Fletcher-Jones et al., 2020)

1.7. SGIP1

SGIP1 was first described in the literature in a search for genes associated with the development of obesity. Israeli sand rat (*Psammomys obesus*), a polygenic animal model of obesity, insulin resistance, and type 2 diabetes, was used for this search (Trevaskis et al., 2005). Israeli sand rats live in the desert region, where these animals have food hard to get. With this regime, they are lean and have physiological blood glucose levels (Shafrir and Gutman, 1993). However, when sand rats are fed *ad libitum*, they become overweight and develop the metabolic syndrome (Walder et al., 2000).

The hypothalamus is a key area for the regulation of food intake. The expression of hypothalamic mediator ribonucleic acid (mRNA) in obese and lean gerbils in captivity was compared. SGIP1 mRNA transcript was significantly more expressed in obese gerbils. This gene, coding for SGIP1, has not been described until then. SGIP1 overexpression has been confirmed in another obesity and type 2 diabetes model - the lethal yellow agouti mouse (Trevaskis et al., 2005). Thus, SGIP1 protein can be perceived as a physiological stimulus for food intake.

1.7.1. SGIP1 structure and molecular function

The longest splice variant of SGIP1 (SGIP1a) contains 854 amino acids (in mouse) (Uezu et al., 2007). Together with endocytic adaptor proteins FCHO1/2, they belong to the muniscin family. SGIP1 and FCHO1/2 share several domains: adaptor protein 2 activating (APA) domain, polyproline domain, and μ homologous (μHD) domain (Henne et al., 2010; Hollopeter et al., 2014; Trevaskis et al., 2005). The domain arrangement of FCHO1/2 and SGIP1 is shown in **Fig. 8**. The main structural difference between FCHO1/2 and SGIP1 lies in the N-termini of these proteins. N-terminal F-BAR domain is present in FCHO1/2 and membrane phospholipid binding (MP) domain in SGIP1. Both F-BAR and MP domains were shown to bind membranes in the early stages of endocytosis (Frost et al., 2008; Uezu et al., 2007). However, FCHO1/2 and SGIP1 seem to have an opposite influence on endocytosis. While FCHO1/2 promote endocytosis, SGIP1 stalls it (Hajkova et al., 2016; Henne et al., 2010), and the difference in their N-termini may account for this.

The SGIP1 polyproline domain contains a large number of Src homology region 3 and WW (WWP repeating motif) domains and allows protein-protein interactions. The polyproline domain is also involved in the interaction of SGIP1 with endophilin-3 and 1, regulators of clathrin endocytosis (Schuske et al., 2003; Trevaskis et al., 2005).

SGIP1 is highly conserved among species and has a homolog Syp1 in yeast (Stimpson et al., 2009). This may point to the evolutional significance of SGIP1. Ultimately, both SGIP1 and FCHO1/2 might have emerged as Syp1p gene duplications and undergo specialization.

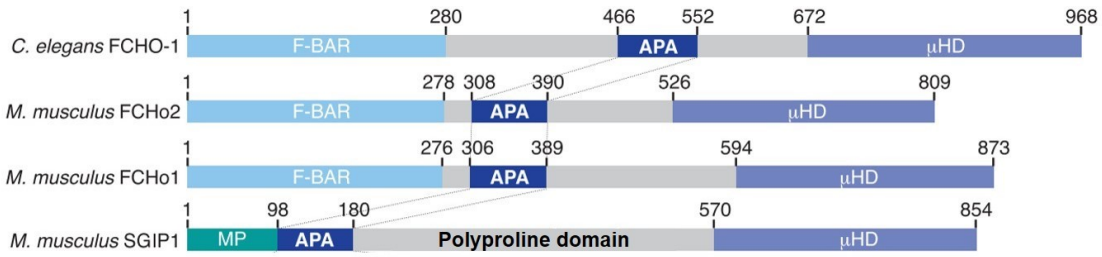

Fig. 8. Domain structure of FCHO1/2 and SGIP1. The figure schematically shows the domains of the FCHO1/2 proteins from the nematode (*C. elegans*) and house mice (*M. musculus*) and the SGIP1 domains. The FCHO1/2 proteins share a homologous N-terminal domain F-BAR. The N-terminus of SGIP1 forms a unique membrane phospholipid binding (MP) domain. All displayed proteins share in their structure the adaptor protein 2 activating domain (APA) and the µ homologous domain (µHD). A polyproline domain is indicated in the central part of the SGIP1 protein (Hollopeter et al., 2014).

1.8. SGIP1 influence on cannabinoid receptor 1 signaling

During a search for intracellular interacting partners of CB1R, SGIP1 was detected in our laboratory. The yeast two-hybrid system was employed for the search. As a bait, the C-terminal portion of CB1R (specifically amino acids 420-473, which follow the eighth intracellular helix) was used. The search was performed against a prey, a rat forebrain-derived cDNA library. One of the hits, the last 99 C-terminal amino acids of SGIP1, was marked as positive (Hajkova et al., 2016).

SGIP1, co-expressed with CB1R in a heterologous system, affects the function and signaling properties of this receptor in HEK293 cells. SGIP1 prevents the internalization

of activated CB1R (**Fig. 9**). SGIP1 stabilizes and prolongs the association of β-arrestin with the activated CB1R (**Fig. 10**). A study of SGIP1 in our laboratory revealed its effect on the signaling of activated CB1R (**Fig. 11**). While CB1R signaling via G proteins is not affected by SGIP1, ERK1/2 signaling is reduced in the presence of SGIP1 (Hajkova et al., 2016). Changes in CB1R signaling *in vitro* indicate that SGIP1 is a vital regulator of CB1R.

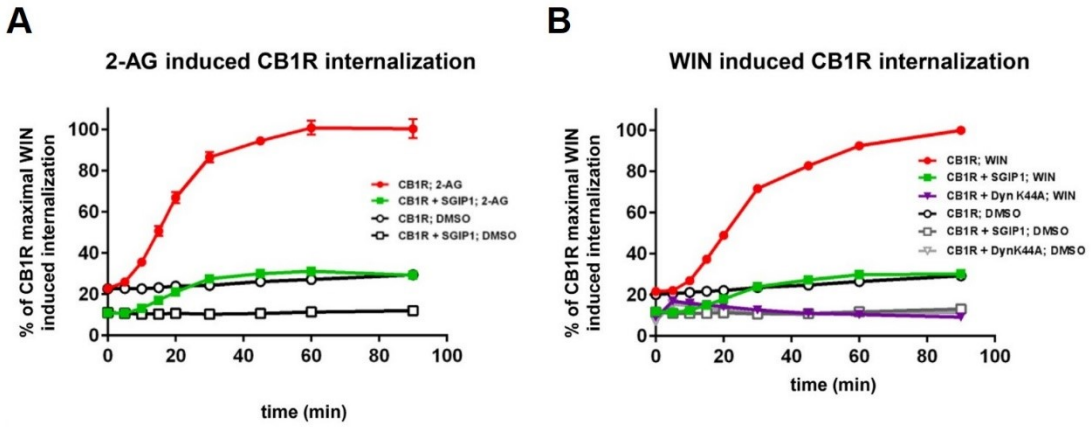

Fig. 9. Internalization of cannabinoid receptor 1 (CB1R) in transfected human embryonic kidney cells (HEK293). (**A**) CB1R activated with 2-arachidonoylglycerol (2 AG) is readily internalized into the cell in the absence of SGIP1. In cells expressing CB1R and SGIP1, CB1R internalization is suppressed. (**B**) Similarly, after activation of CB1R by WIN 55, 212-2 mesylate (WIN), CB1R only internalizes if SGIP1 is not expressed in the cells (Hajkova et al., 2016).

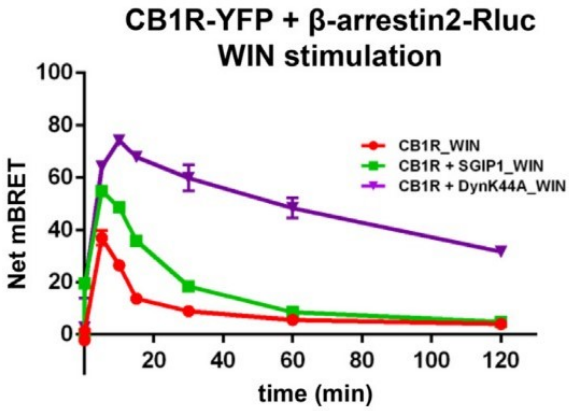

Fig. 10. SGIP1 increases and prolongs the β-arrestin 2 association with cannabinoid receptor 1 (CB1R). Stimulation with WIN 55, 212-2 mesylate (WIN) promotes increased and prolonged association of CB1R with β-arrestin 2 in the presence of SGIP1 compared to the association of these proteins in the absence of SGIP1. The association of the proteins of interest is more prolonged and increased in the presence of dynamin carrying a mutation that prevents internalization (DynK44A). Rluc - *renilla* luciferase, YFP - yellow fluorescent protein. (Hajkova et al., 2016)

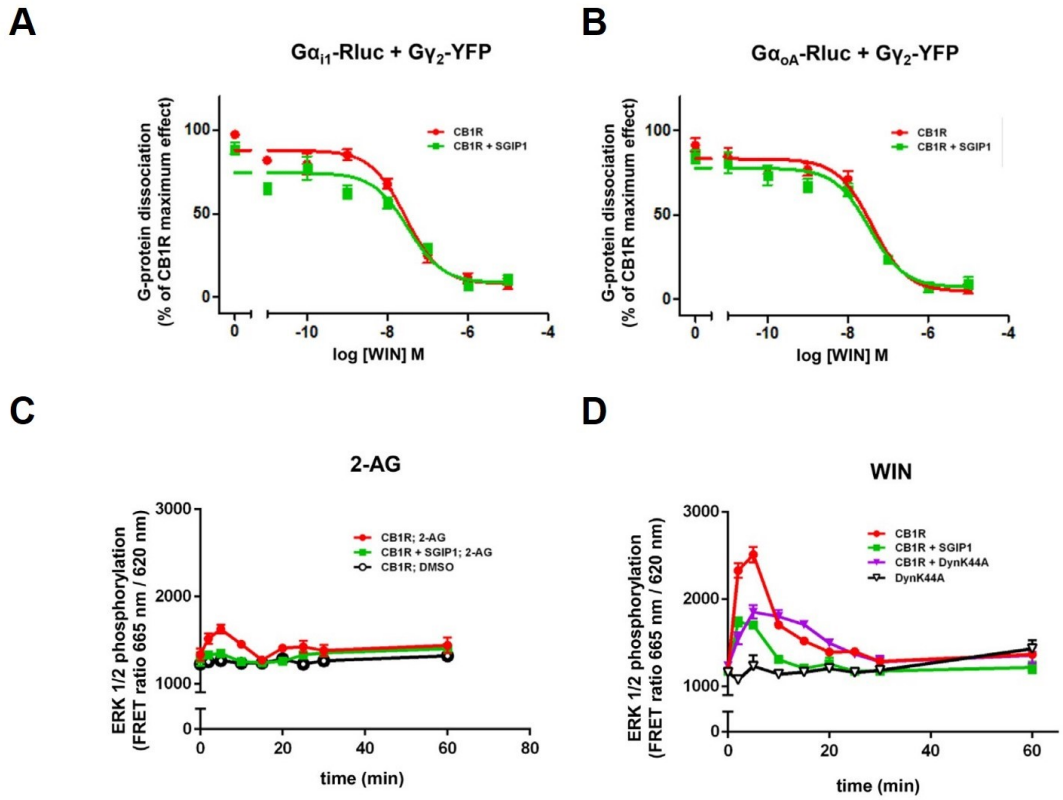

Fig. 11. SGIP1 selectively affects cannabinoid receptor 1 (CB1R) signaling. (**A, B**) CB1R-induced G protein dissociation is not affected by the presence of SGIP1. (**C**)

Phosphorylation of extracellular signal-regulated kinases 1 and 2 (ERK1/2) is very low after CB1R stimulation with 2-arachidonoylglycerol (2-AG). (**D**) WIN 55, 212-2 mesylate (WIN) stimulates CB1R mediated ERK1/2 phosphorylation in the absence of SGIP1. The ERK1/2 phosphorylation is reduced by the presence of SGIP1 or dynamin carrying a mutation that prevents internalization (DynK44A). Rluc - renilla luciferase, YFP - yellow fluorescent protein (Hajkova et al., 2016).

2. AIMS AND HYPOTHESES

CB1R signaling is very complex and can be modulated at different levels by interacting partners. An interacting partner's influence on the receptor signaling may be reflected in behavior.

We previously detected the protein-protein interaction of CB1R and SGIP1 and characterized it biochemically and pharmacologically using transfected mammalian cells. This thesis focuses on further characterization of CB1R-SGIP1 interaction and mapping its function in neuronal cultures and *in vivo* using a mouse model.

For this purpose, we used a reverse genetic approach. We prepared a mouse line with SGIP1 gene deletion ($SGIP1^{-/-}$).

This thesis's main aim was to study the phenotype of SGIP1 knockout ($SGIP1^{-/-}$) mice compared to the WT mice. The behavioral testing was focused on aspects of behavior that are known to be affected by the CB1R signaling.

3. MATERIAL AND METHODS

3.1. Chemicals and enzymes

Unless stated otherwise, chemicals were purchased from Sigma-Aldrich, USA. Tissue culture and transfection reagents were purchased from Invitrogen, USA.

Δ^9-tetrahydrocannabinol (THC)	kindly provided by Ing. Martin Kuchař, Ph.D. (Forensic Laboratory of Biologically Active Substances, UCT, Prague)
acrylamide	Serva, Germany
agarose	Serva, Germany
ammonium persulfate	Serva, Germany
dithiothreitol	Serva, Germany
ethanol	Penta, Czech Republic
ethidium bromide	Top Bio, Czech Republic
fetal bovine serum	Gibco, USA
Fluoromount-G™	Thermo Fisher Scientific, USA
horse serum	Gemini, Great Britain
hydrochloric acid	Penta, Czech Republic
isopropanol	Penta, Czech Republic
methanol	Penta, Czech Republic
N, N, N′, N′-tetramethylethylenediamine	Serva, Germany
N,N′methylenbisacrylamide	Amersham Pharmacia Biotech, USA
papain	Worthington Biochemical Corporation, USA
polymerase with GoTaq Master Mix buffer	Promega, USA
proteas inhibitors	Roche, Switzerland
protein A/G agarose beads	Thermo Fisher Scientific, USA
sodium chloride	Serva, Germany
Tris-HCl	Serva, Germany

Triton X-100	Serva, Germany
Tween 20	Serva, Germany

3.2. Solutions

Blocking buffer for immunohistochmistry	5% BSA, 0.5% Triton X-100 in PBS
extracellular solution for electrophysiology	119mM NaCl, 5mM KCl, 2.5mM $CaCl_2$, 1.5mM $MgCl_2$, 30mM glucose, 20mM HEPES
homogenization buffer	100mM NaCl, 20mM Tris, pH = 7
intracellular solution for electrophysiology	121.5mM potassium gluconate, 17.5mM KCl, 9mM NaCl, 1mM $MgCl_2$, 10mM HEPES, 0.2mM EGTA, 2mM MgATP, 0.5mM LiGTP
medium for HEK293 cultivation	Dulbecco's Modified Eagle's (DMEM) medium + 10% fetal bovine serum
medium for hippocampal neurons cultivation	DMEM, 20mM glucose, 10% horse serum
medium for HEK293 cells cultivation	Opti-MEM®
lysis buffer for DNA isolation	1M Tris-Cl, 1M NaCl, 0.5M EDTA, 10% SDS, 0.2 mg/ml proteinkinase K
Phosphate buffered saline (PBS)	137mM NaCl, 2.7mM KCl, 4.3mM Na_2HPO_4, 1.4mM KH_2PO_4; pH 7.3
co-immunoprecipitation solution	0.1% sodium dodecylsulphate (SDS), 0.1% deoxycholate, 0.1% Triton X-100
SDS-PAGE solution	25mM Tris, 192 mM glycine, 0.1% SDS, pH 8.3)
sample buffer for SDS-PAGE	250mMTris-HCl, 8 % SDS, 20 % w/v glycerole, 0.02 % bromophenol blue, 40mM DTT, pH 6.8

3.3. Antibodies

Anti-CB1R (a-CB1R), produced in rabbit (for Western blot and microscopy)	ImmunoGenes, Hungary
anti-CB1R (a-CB1R), produced in rabbit (for co-immunoprecipitation)	polyclonal antibodies produced in our laboratory, antigen: MKSILDGLADTTFRTITTDLLYVGS NDIQYEDIKGDMASKLGYFPQKFP LTSFRGSPFQEKMTAGD
anti-GP Alexa Fluor 488 nm, produced in donkey	Invitrogen, USA
anti-GP conjugated with horseradish peroxidase, produced in goat	Santa Cruz Biotechnology, USA
anti-M Alexa Fluor 594 nm, produced in donkey	Invitrogen, USA
anti-mGluR1, produced in mouse	Santa Cruz Biotechnology, USA
anti-Piccolo, produced in mouse	Synaptic Systems, Germany
anti-R Alexa Fluor 647 nm, produced in donkey	Invitrogen, USA
anti-SGIP1, produced in guinea pig	polyclonal antibodies produced in our lab, antigen: MMEGLKKRTRKAFGIRKKEKDTD STGSC

3.4. Recombinant DNA

prk5_Flag_SGIP1 (DNA for mouse SGIP1 with Flag tag inserted in plasmid prk5, the protein expressed from this plasmid will be referred to as Flag-SGIP1)

prk5_GFP (DNA for green fluorescent protein (GFP) inserted in plasmid prk5)

3.5. Human embryonal kidney cells

HEK293T/17 cell line (from now on referred to as HEK293, human embryonic kidney cell line with inserted SV40 T-antigen, clone 17; ATTC, Rockefeller University)

3.6. Mouse embryonic stem cells

Embryonic stem cells carrying DNA with a deletion of the second exon in the SGIP1 gene (Sgip1$^{tm1a(EUCOMM)Hmgu}$; GeneBank identification: NM_001285852). These cells were derived from mice with the genetic background C57N1 / NCrl.

3.7. Animals

Mouse strains expressing Flp flippase (Gt(ROSA)26Sor$^{tm2(CAG-flpo,-EYFP)lcs}$) and Cre recombinase (Gt(ROSA)26Sor$^{tm1(ACTB-cre,\ EGFP)lc}$ were used for a crossing leading to SGIP1 gene deletion. The mice underwent more than 10 backcrossings, which led to the exclusion of the Flp and Cre recombinase coding sequences and homogenization to C57Bl/NCrl background.

Mice were housed in animal facilities that complied with laboratory animal handling rules. Mice were bred and group-housed in a pathogen-free facility with temperature 22±2°C, 45% humidity, 12:12 hour light/dark cycle, food, and water *ad libitum*. The mice were acclimated to the facility for two weeks before the experiments. Testing was performed during the light phase of the circadian cycle. For all testings, mice aged 8-12 weeks were used.

All procedures used in this study followed applicable laws and obeyed the Guidelines of the National Institutes of Health on the Care and Use of Animals and Directive 2010/63/EU. All animal models and experiments in this study were ethically reviewed and approved by the Institutional Animal Care and Use Committee of Indiana University or the Institute of Molecular Genetics, depending on where the experiments were conducted.

3.8. Instruments

Fear conditioning apparatus	Ugo Basile, Gemonio, Italy
centrifuge Mikro 120 (Rotor 1212)	Hettich Zentrifugen, Germany
water bath TW12	Julabo, USA
fluorescence microscope TCS SP5 AOBS Tandem	Leica, Germany
incubator 4000 series	Contherm Scientific, New Zealand
microscope Axioskop 2, FS Plus	ZEISS, Germany
Flaming/Brown Pipette Puller P-97	Sutter, USA
RotaRod	TSE Systems, Germany
acquisition system LIH 8+8	HEKA Elektronik, Germany
thermocycler PTC-200	Marshall Scientific, USA
amplifier triple patch-clamp EPC 10	HEKA Elektronik, Germany

3.9. Software

EthoVision	Noldus, USA
GraphPad Prism, versions 7.03 and 8.0.1 for OS Windows	GraphPad Software, USA
ImageJ	NIH, USA
PatchMaster	HEKA Elektronik, Germany
PPI software	Med Associates Inc., USA
Viewer	Biobserve GmbH, Germany

3.10. SDS-PAGE and immunoblotting

The sodium dodecyl sulfate-polyacrylamide gel electrophoresis (SDS-PAGE) method was adapted according to the Hoefer laboratory manual (Hoefer, 1994). Samples corresponding to 5 µg of total protein from mouse brain homogenate were electrophoretically separated on a 10% tris-glycine gel (SDS-PAGE). The separated proteins were further transferred onto a nitrocellulose membrane, which was blocked overnight in 5% milk in PBST (PBS + 0.1% Tween® 20) at 4 ° C. Between each step, the membrane was always rinsed with PBST 3x for 10 min. Specific primary antibodies

(anti-SGIP1 antibodies developed in our laboratory (Hajkova et al., 2016), dilution 1: 5000) and secondary antibodies conjugated to horseradish peroxidase recognizing antigens of the animal in which the primary antibodies were produced (for anti-SGIP1 antibody - guinea pig, dilution 1:5000) were used for labeling. Proteins were visualized with SuperSignal® West Femto chemiluminescent substrate. Chemiluminescence was detected digitally with LAS-300.

3.11. Co-immunoprecipitation

The experiment was performed as described previously (Techlovská et al., 2014), only minor changes were made in the procedure. The mouse forebrain was homogenized in homogenization buffer with protease inhibitors. Samples were diluted to a total protein concentration of 5 µg/ml. Subsequently, 3 - [(3-cholamidopropyl) dimethylammonio] -1-propanesulfonate hydrate (CHAPS) (total concentration 1%) was added to the samples, and the samples were incubated at 37 ° C for 1 h. The samples were centrifuged for 1 h at 100,000 x g and 4 ° C. The supernatant was diluted 10x with homogenization buffer, which additionally contained 0.1% Triton X-100. Next, 20 µl of agarose beads with immobilized protein A/G and bound anti-CB1R antibody (rabbit antibody produced in our laboratory (Hajkova et al., 2016) were added to the sample, and the mixture was incubated for 4 h, at 4 ° C with slow tube rotation. The samples were centrifuged for 1 min at 2000 x g. The beads were washed three times by centrifugation with 0.1% Triton X-100 homogenization buffer. The bead pellet contained a fraction of bound proteins, the supernatant contained the remaining unbound proteins. All samples were dissolved in 50 µl of SDS-PAGE sample buffer, heated to 70 ° C for 10 min. 10 µl of each sample was loaded onto a gel and analyzed by immunoblotting.

3.12. Cell culture and transfection of HEK293 cells

HEK293 human embryonic kidney cells were cultured in DMEM medium with glucose and L-glutamine and added 10% fetal bovine serum (FBS). Cells were cultured at 37 ° C in an atmosphere of 5% CO 2 and 95% humidity. The cells were split every two days in the ratio

of 1: 4. Cells were incubated for 5 min in trypsin solution, which was subsequently diluted with culturing medium in the ratio of 1: 1.

For transfection, cells were plated in 10 cm diameter culture dishes at least 24 h before transfection. A mixture of plasmid DNA (total 10 µg/ml) and CaCl 2 (0.26 mol/l) in 1 ml cell culture grade H_2O was pipetted into 1 ml of transfection buffer (total DNA concentration 5 µg/ml) and immediately dripped onto the cells. The transfected cells were incubated for 24 h at 37 ° C and 5% CO 2.

3.13. Immunohistochemistry

Cells plated on microscope slides were fixed with pre-cooled 4% paraformaldehyde for 20 min. Slides were washed 3 times in PBS. Next, slides were blocked in blocking buffer for immunohistochemistry for 1 h at room temperature. Blocking buffer was aspirated, and slides were incubated with primary antibody solution (1: 300 dilution in blocking buffer) for 3 h at room temperature. This was again followed by three rinses in PBS. Slides were incubated in secondary antibody solutions (1: 500 dilution in blocking buffer) for 2 h at room temperature. Slides were washed 3x in PBS, 1x in distilled water, and left on the table to dry. Dry slides were attached to the slide with Fluoromount-G mounting medium.

3.14. Microscopy and image processing

Microscopy slides were visualized with Leica TCS SP5 inverted fluorescence confocal microscope with HC PL APO 40x / 1.30 OIL and HC PL APO 63x / 1.40 OIL objectives. Image processing was performed in the ImageJ program. Z-stack images were maximal intensity projected, and brightness and contrast were adjusted for the entire image.

3.15. Generation of SGIP1$^{-/-}$ mice

SGIP1$^{-/-}$ mice were generated in cooperation with the Czech Center for Phenogenomics led by doc. Dr. Radislav Sedláček, Ph.D. The embryonic stem cells of

C57Bl/NCrl background were obtained from the European Conditional Mouse Mutagenesis Program (EUCOMM) (Dickinson et al., 2016). The embryonic stem cells ($Sgip1^{tm1a(EUCOMM)Hmgu}$) carried the SGIP1 gene (GeneBank Accession: NM_001285852) modified by homologous recombination. The FRT sites flanked exon 2 of the SGIP1 gene, and the LoxP sites bordered additional sequences. Using a laser-assisted technique, embryonic stem cells were injected into 8-cell stage embryos to generate chimeric mice. $Sgip1^{tm1a+/-}$ mice were crossed. Selected offspring were bred with Flp-expressing $Gt(ROSA)26Sor^{tm2(CAG-flpo,-EYFP)Ics}$, to delete aberrant sequences, and their offspring were further crossed with a strain expressing Cre recombinase $Gt(ROSA)26Sor^{tm1(ACTB-cre,-EGFP)Ics}$ to excise the Exon 2. Used mouse lines were from the same source (Birling et al., 2012).

3.16. Isolation of genomic DNA

Tissue samples from mouse tails were dissolved in lysis buffer at 55 ° C overnight. Subsequently, the samples were centrifuged briefly. 0.5 ml of the mixture of phenol, chloroform, and isoamyl alcohol was added to the samples, and the solution was stirred by inverting the tubes. The samples were centrifuged in a tabletop centrifuge for 5 min. The upper aqueous phase was removed, and 0.5 ml of chilled (-20 ° C) 96% ethanol was added to it in a new tube. The samples were again mixed by inverting and centrifuged for 5 min. The supernatant was poured from the tube, and 0.5 ml of 75% ethanol was added to the remaining pellet. The samples were centrifuged for 5 min. The supernatant was poured out again, and the pellets were vented in a fume hood for 2 h. Finally, 100 µl of water was added, and the pellets were dissolved at 4 ° C overnight.

3.17. Mouse genotyping

Mice were genotyped by polymerase chain reaction (PCR). The following primers were used for the reaction:

SGIP1 5´arm AGGCACAGCATCCTTAGGCACAGC

SGIP1 3´arm GAATGTATCAGGGAAGGTTCAGCC

LoxP reverse CACAACGGGTTCTTCTGTTAGTCC.

The composition of the PCR reaction mixture was as follows:

polymerase with GoTaq Master Mix buffer	12,5 µL
SGIP1 5´arm	1 µL
SGIP1 3´arm	1 µL
LoxP reversne	1 µL
isolated genomic DNA	1 µL
PCR grade H_2O	8,5 µL.

The reaction mixture was placed in a thermocycler in which PCR was performed according to the following protocol:

95 °C	1 min	
95 °C	30 s	30 cycle repeats
60 °C	30 s	
72 °C	2 min	
72 °C	10 min	
4 °C	until the end of the procedure.	

The PCR products were visualized with ethidium bromide (1 µl into 5 µl of a sample) on an agarose gel.

3.18. Autaptic hippocampal neurons cultivation

Autaptic hippocampal neurons were cultured as described previously (Bekkers and Stevens, 1991; Furshpan et al., 1976). Neurons were isolated from CA1-CA3 regions of

mouse hippocampi (postnatal day 0-2) and plated on a previously prepared feeder layer of astrocytes (Levison and McCarthy, 1991). Neuronal cultures were kept in high glucose (20mM) DMEM containing 10% horse serum and used for recording after 8 days in culture. Neurons were used only up to 14 days after isolation.

3.19. Whole-cell patch-clamp electrophysiology

All experiments were performed on isolated autaptic neurons. The cells were kept at room temperature for the whole time of the recording, and they were not used for longer than three hours after removal from culture media. Whole-cell patch-clamp recordings were performed using HEKA Triple Patch Clamp EPC10 amplifier (HEKA Elektronik, Lambrecht/Pfalz, Germany) and recording electrode filled with intracellular solution. The extracellular solution was used to fill the chamber. The flow rate of the solution through the chamber was ~3ml/min.

Only the cells with stable access resistance and holding current were included in the dataset. DSE was induced after establishing a 10-20 s 0.5 Hz baseline. For DSE dose-response experiments, depolarization to 0 mV for 50 ms, 100 ms, 300 ms, 500 ms, 1 s, 3 s, 10 s. Values before depolarization were normalized to 1, and the DSE values are presented as fractions of 1.

For 2-AG dose-response experiments, the membrane potential was held at -70 mV, and the excitatory postsynaptic currents (EPSCs) were triggered every 20 s with a 1 ms depolarizing step. After establishing a 5 min baseline without the drug, 2-AG was added to the cells in subsequently higher concentrations (1nM, 10nM, 100nM, 1uM, 5uM), and the EPSC was continuously recorded. The solution's flow rate through the chamber was ~3ml/min, and the cells were treated with each drug concentration for 5 min. Relative EPSC charge data are normalized to baseline EPSC.

For desensitization experiments neurons were incubated in 100 nM WIN55,212-2 (WIN) in 0.001% DMSO overnight. After the overnight treatment, cells were washed for at least 20 min before they were used to record DSE dose-response (as described above).

3.20. Spontaneous alteration

Assessment of spontaneous alteration (SA) was performed in the Y maze (Hughes, 2004). In this test, the short-term memory of subjects is examined. The mouse is left to freely explore the maze and filmed with a camera from above for 5 minutes. The software calculates how many arm alterations (in percent) the mouse has made in a given time. The equation for calculating the spontaneous alteration was as follows: %SA = (TA * 100) / (TE-2), where %SA - the percentage of spontaneous alteration, TA - total number of alterations performed by the mouse, TE - total number of maze arm entries.

3.21. Prepulse inhibition of the startle response

Sensorimotor gating was monitored by the pre-pulse inhibition (PPI) (Yeomans and Frankland, 1995). Testing took place in soundproof boxes, to which the animals were accustomed 10 minutes before the testing session. Tones of different volumes (70, 77, 82, 85 dB) were presented to the animal either alone or followed by a tone of volume 110 dB, which should frighten the animal. The aversive tone always followed 120 ms after the prepulse tone. Each animal was tested six times, and each of these tests consisted of 10 prepulse tone pairings with an aversive tone or a non-tone delay. Prepulse intensities and their pairing with sound or silent delay were alternated. The response is presented in the graphs as a decrease in the startle response amplitude in the presence of prepulse (% PPI).

3.22. Open field test

The open field test (OF) was used to monitor the anxiety of mice and their overall activity (Choleris et al., 2001). The mouse is placed in an arena, which is virtually divided into center and periphery by software that is connected to the camera recording. The mouse is filmed on video, and the time spent in the middle of the arena and the distance traveled is evaluated by software.

3.23. Elevated plus maze

Elevated plus maze (EPM) assesses mice's anxious behavior and works on a similar principle as OF (Lister, 1987). The maze consists of four elevated arms, which are crossed into the shape of a plus. Two of the arms are open, and two are protected with walls. Each animal was allowed to explore the maze for 5 minutes. Each animal was filmed with a camera from the top. The record was automatically evaluated by software that calculated the time each mouse spent in the open and closed arms and the center. The total distance that each mouse traveled was also analyzed.

3.24. Tail suspension test

To investigate depression-like behavior, the tail suspension test (TST) was used (Porsolt et al., 1977). In the TST, the tested mouse is secured with adhesive tape to the hook by its tail. The mouse is hung by its tail for 6 minutes and recorded with a camera. From the record, the software calculates the time the mouse spent motionless.

3.25. Fear conditioning

Fear conditioning (FC) is based on the pairing of an electric shock with a context or a conditioned stimulus (cue) such as a specific tone (Stiedl et al., 1999). Each mouse was placed in an experimental box where it was acclimated for 4 minutes. After this time, a conditioned stimulus (tone of 77 dB and 9kHz), which lasted 20 s, was triggered in the box. With the last second of the conditioned stimulus, a weak electric current / unconditional stimulus (0.6 mA for 1 s) was released into the box floor. Contextual fear conditioning was tested 24 hours later. The environment of the test box was the same as during the learning of fear conditioning. Mice were videotaped for 6 min, and their freezing was recorded. After 3 h, the mice were monitored for response to a conditioned stimulus. The mice were placed in a box with a changed pattern on the walls, the box floor was replaced with another material, and also, a pulp with a novel essential oil was placed next to the box. After adaptation to the new environment (2 min), the mice were presented with the conditioned stimulus, and their freezing was recorded for 2 min.

In the extinction experiment, mice were taught fear conditioning in the same manner as in the above-mentioned experiment. The following days, the mice were placed in a box, allowed to become familiar with the environment for 1 min, and after acclimatization, presented with a conditioned stimulus (tone) for 3 min. Their immobility was recorded during these 3 minutes. The experiment was terminated when the extinction trend stopped developing in mice (males - 11 days, females - 5 days).

3.26. Tail immersion test

Nociception was tested by the tail immersion test (TIT). Mice were gently immobilized in a cotton cloth. They were acclimated to this procedure the day before the experiment. During the experiment, 1 cm of the tip of the mouse's tail was immersed in a water bath with a 52 ° C temperature. The time to tail flick was measured. The experiment was repeated 3 times with a 30-minute inter-interval between each measurement.

3.27. Cannabinoid tetrad

Male mice were used for the cannabinoid tetrad that describes the four manifestations of THC intoxication (Li et al., 2017). Their behavior was tested on days 1, 4, and 8 of the experiment, always 1 h after intraperitoneal administration of THC (10 mg/kg/day). The control group of mice was injected with VEH in the same manner. Baseline values were measured on day 1 of the experiment before the first THC administration.

The individual tests were performed in the order in which they are mentioned herein. The catalepsy test was performed by placing the mouse on a 6.35 cm diameter steel ring mounted 16 cm above the base. Mice were monitored for 5 min and the duration of catalepsy, i.e., immobility, was recorded. The results are presented as a percentage of the maximum possible effect (% MPE) according to the equation %MPE = [(immobility after the injection - immobility before injection) / (300 - immobility before injection)] x 100. The TIT was used to determine the nociception (see chapter 3.26). Results are reported as %MPE according to the equation %MPE = [(latency after injection - latency before injection) / (10 - latency before injection)] x 100. Mice body temperature was

measured with a rectal thermometer. Results are presented as percent change in body temperature (%ΔBT) according to the equation %ΔBT = [(pre-injection temperature) - (post-injection temperature)] / [pre-injection temperature] x 100. For the rotarod test, mice were trained two days before the experiment. Mice were placed on an accelerating rotating cylinder (4-40 rpm) and the time spent on the cylinder before falling was recorded as latency.

3.28. THC withdrawal

Subjects from the previous experiment were used to test the THC withdrawal. On day 9 of the experiment, mice were injected intraperitoneally with THC or VEH. After 30 minutes, the mice received another injection with VEH only, and after another 30 minutes, the mice were injected with 10 mg/kg of rimonabant (**Fig. 12**). Mice were videotaped throughout the experiment, and a blinded observer analyzed behaviors. The incidence of withdrawal behaviors (headshakes, paw shakes, scratching and grooming, and jumping) was manually calculated.

Fig. 12. Schematic representation of the order of intraperitoneal injections for THC withdrawal. The mice were treated with intraperitoneal injections of Δ^9-tetrahydrocannabinol (THC) (10 mg/kg) for 9 consecutive days. The mice were injected with a vehicle (VEH) 30 minutes after the last drug deliveries, and after another 30 minutes, CB1R inverse agonist rimonabant (10 mg/kg) was intraperitoneally injected.

3.29. Testing of antinociception induced by CB1R ligands and morphine

The effect of ligands on nociception in mice was investigated by TIT (see chapter 3.26). First, the baseline latency in TIT was measured, and the test was repeated 1 h after intraperitoneal injection of each dose of the drugs. The individual doses were always injected starting with the lowest and ending with the highest. The cut off of 10 s was used

in the experiment with THC and WIN, 15 s was used for the morphine experiment. Data are presented as %MPE = [(latency after injection - latency before injection) / (10 (15 for morphine) - latency before injection)] x 100.

3.30. Order of behavioral tests and statistical analysis of behavioral data

In the case of tests in which both sexes of mice were tested, each sex was tested separately. The order of tests was as follows: OF, SA, EPM, TST, PPI, TIT. New cohorts of mice were used to test FC, extinction of aversive memories, the nociceptive effect of THC, WIN, and morphine. A new cohort consisted of males only was used for cannabinoid tetrad and THC withdrawal. Finally, a new cohort of males was used to test the nociceptive effect of rimonabant.

The experimental procedures and data analysis were blinded to the experimenter, in cases of video analyses blinded to the observer.

The F test was used to analyze the homogeneity of sample variances in the R program (stats library). No violations of normality or sphericity were detected using the R program (library moments) (Komsta and Novomestsky, 2015) in our data except the incidence of jumping in THC withdrawal. Here the analysis was done using a general linear model using the Poisson link in the R program (library stats) (R Core Team, 2020).

Qq plots were used to inspect the normal distribution of residuals and to calculate the correlation coefficient between observed residuals and theoretical residuals, R library olsrr (Hebbali, 2020). Log transformation for data that showed an abnormality in the qq plot was used. Bonferroni post hoc test was applied when F in ANOVA achieved $P < 0.05$ only, and there was no significant variance inhomogeneity.

To analyze the ligand dose needed for 50% effect (ED_{50}), the curves were fitted as nonlinear regressions with variable slope (four parameters). The curves were constrained to 0 at the bottom and 100 at the top. The ED_{50} values, the 95% confidence intervals, and Hill slopes were determined from the fit.

T-tests, ANOVA, and nonlinear regression analyses were performed using GraphPad Prism version 8.0.1. for Windows (GraphPad Software, USA). The remaining experiment analysis was performed by the general linear model in the R program (version 4), library stats. $P < 0.05$ was considered significant.

4. RESULTS

The co-localization and interaction of CB1R and SGIP1 *in vitro* were previously verified by microscopic, biochemical, and pharmacological methods (Hajkova et al., 2016). The interaction of CB1R and SGIP1 was confirmed by co-immunoprecipitation. A mouse line with the SGIP1 gene deletion was developed to study the effect of SGIP1 on CB1R signaling further. Modulation of CB1R-SGIP1 signaling was studied by whole-cell patch-clamp electrophysiology in neurons derived from SGIP1$^{-/-}$ and WT mice. Finally, changes in the phenotype of SGIP1$^{-/-}$ mice were monitored.

4.1. Characterization of SGIP1 antibodies

Anti-SGIP1 antibodies were produced in our laboratory (Hajkova et al., 2016), and their specificity was verified by immunoblotting of samples from SGIP1-transfected HEK293 cells (**Fig. 13**). Protein samples from non-transfected cells did not show any specific labeling with the anti-SGIP1 antibody.

To test antibody selectivity, cells were transfected with a plasmid encoding Flag-SGIP1. Labeling was also performed with an antibody against the Flag tag protein. The bands visualized by both antibodies showed similar mobility. The mobility of the detected bands corresponded to the molecular weight of the Flag-SGIP1 fusion protein.

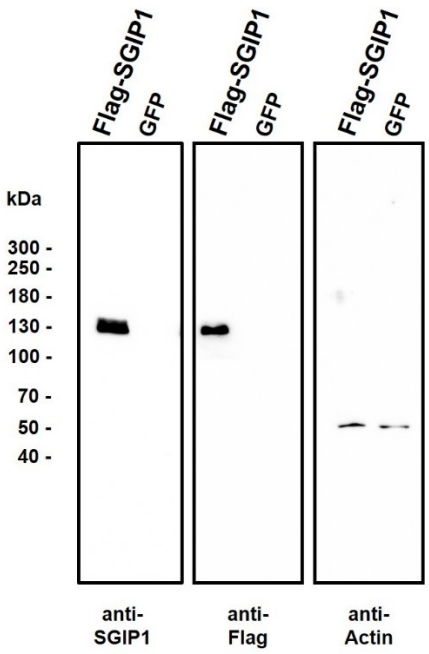

Fig. 13. Characterization of SGIP1 antibodies. Human embryonic kidney cells (HEK293) were transfected with plasmid encoding Flag-SGIP1 or green fluorescent protein (GFP), which served as a negative control. Protein samples obtained from transfected cells were electrophoretically separated and visualized by immunoblotting. Antibodies against SGIP1 (anti-SGIP1), peptide Flag tag (anti-Flag), and actin (anti-Actin) were used. The anti-SGIP1 and anti-Flag antibodies recognize an identical ~ 130 kDa band that corresponds to the Flag-SGIP1 fusion protein. The comparable intensity of the anti-Actin antibody-labeled bands (~ 50 kDa) confirms comparable protein loading in both samples.

4.2. SGIP1 interacts with cannabinoid receptor 1

The protein-protein interaction of SGIP1 and CB1R was confirmed by co-immunoprecipitation from a detergent soluble fraction prepared from the mouse brain (**Fig. 14**). Anti-CB1R antibodies generated in our laboratory were used for this experiment (Hajkova et al., 2016). SGIP1 was detected by immunoblotting in samples precipitated with the anti-CB1R antibody. The control experiment consisted of using an irrelevant antibody (anti-mGluR1) to precipitate from the same tissue samples.

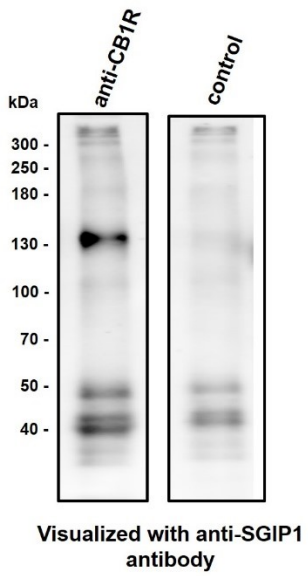

Fig. 14. Co-immunoprecipitation of SGIP1 and CB1R. Cannabinoid receptor 1 (CB1R) was precipitated from the detergent solution-soluble fraction prepared from mouse brain homogenate by anti-CB1R antibody, and anti-metabotropic glutamate receptor 1 antibody was used as a negative control. The precipitated proteins were then electrophoretically separated and visualized by immunoblotting. The anti-SGIP1 antibody was used for visualization, which detected SGIP1 bound to precipitated CB1R (~ 130 kDa).

4.3. SGIP1 partially co-localizes with cannabinoid receptor 1 in neurons

To determine whether SGIP1 is located in neurons in the same subcellular compartments as CB1R, immunohistochemical antibody labeling of both proteins was performed in mouse primary hippocampal neuronal cultures (**Fig. 15**).

The partial co-localization of CB1R and SGIP1 was detected in the microscopic images, especially in the synaptic areas labeled with the Piccolo marker.

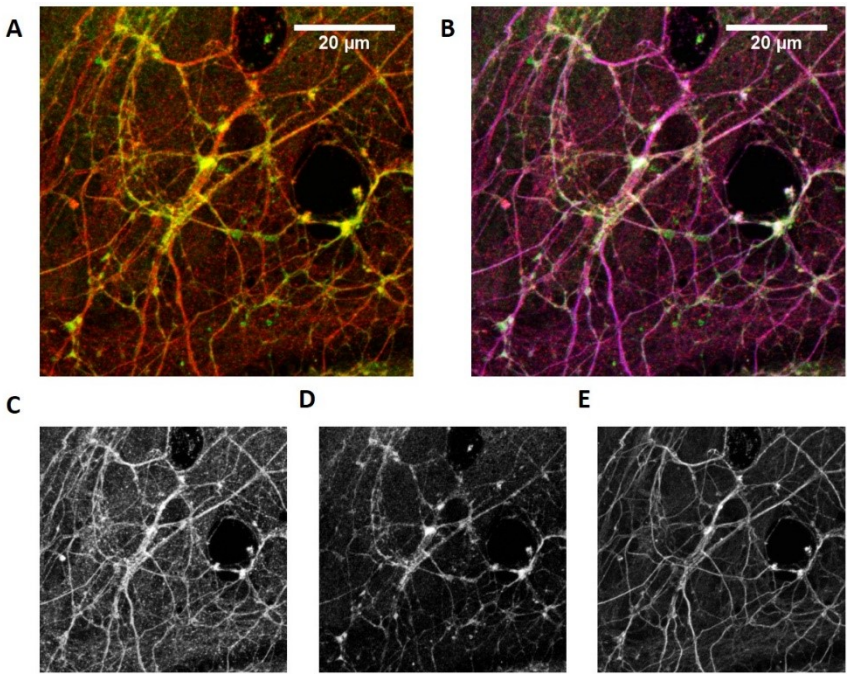

Fig. 15. Localization of cannabinoid receptor 1 (CB1R) and SGIP1 in hippocampal neurons. Neurons were labeled with anti-CB1R (red) and anti-SGIP1 (green) antibodies. Panel (**A**) demonstrates the overlap (yellow) of these two stainings at the synapses. Also, the synaptic marker Piccolo labeling (blue) is added in panel (**B**). The bottom row of the figures shows the individual stainings in grayscale: (**C**) anti-CB1R, (**D**) anti-SGIP1, (**E**) anti-Piccolo. The scale bar in the upper right corner shows 20 µm.

4.4. Preparation of a genetically modified mouse line lacking SGIP1

The embryonic stem cells Sgip1$^{tm1a(EUCOMM)Hmgu}$ for the preparation of SGIP1 knockout mice were obtained from the European Conditional Mouse Mutagenesis Program (EUCOMM) (Dickinson et al., 2016). In these cells, the second exon of the SGIP1 gene is flanked by FRT and LoxP sequences (**Fig. 16**). The cells were used to prepare a mouse line with a developmental deletion of the gene for SGIP1. Embryonic cells were introduced into eight-cell embryos. The resulting chimeric SGIP1$^{tm1a\ +/-}$ mice were crossed in between themselves. Progeny from this crossing were bred with mice expressing flippase (Flp) (Gt(ROSA)26Sor$^{tm2(CAG-flpo,-EYFP)lcs}$) and subsequently with mice expressing Cre recombinase Cre (Gt(ROSA)26Sor$^{tm1(ACTB-cre,\ EGFP)lcs}$.

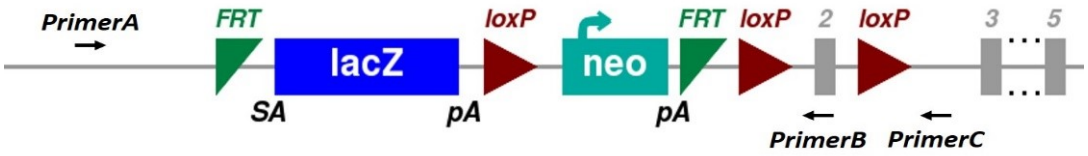

Fig. 16. Schematic depiction of the mutated gene for the development of the SGIP1 knockout mice. The second exon of the gene encoding SGIP1 is flanked by FRT and LoxP sequences. By crossing mice carrying this gene with mice expressing Flp and subsequently crossing the offspring with mise expressing Cre recombinase, the second exon of the SGIP1 gene is excised in the offspring mice.

This crossing causes a frameshift with stop codon insertion in the gene and a consequent loss of expression of the respective protein. The SGIP1$^{-/-}$ mice were fertile, and no apparent abnormalities in their physiology were observed. Deletion of the SGIP1 was verified by PCR in all mice undergoing behavioral testings (**Fig. 17**).

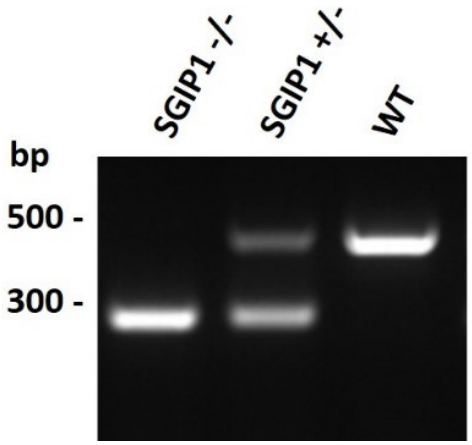

Fig. 17. Verification of SGIP1 PCR gene deletion. The genotype of the mice was analyzed by a polymerase chain reaction. The allele carrying the uncleaved exon 2 in the SGIP1 produced a band of the size 456 bp, the allele with the cleaved exon 2 then produced a band of the size 245 bp. The figure representative figure of the genotyping of homozygous mice with a deletion of SGIP1 (SGIP1$^{-/-}$), heterozygous mice (SGIP1$^{+/-}$), and mice with unchanged genotype (WT).

4.5. Deletion of the second exon of the SGIP1 gene results in loss of SGIP1 expression in mice

To verify the loss of SGIP1 at the protein level, homogenates from mouse brains were analyzed by immunoblotting. Specific antibodies recognizing the N-terminal portion of SGIP1 (sequence: MMEGLKKRTRKAFGIRKKEKDTDSTGSC) were used to visualize SGIP1. A representative immunoblot from mouse brains (**Fig. 18**) shows that homozygous SGIP1$^{-/-}$ mice do not express SGIP1. SGIP1 expression is maintained in heterozygous and WT mice.

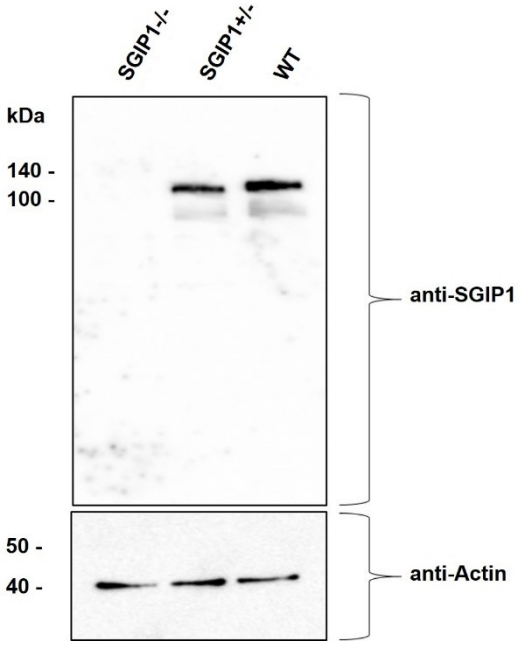

Fig. 18. Characterization of protein expression in mouse brain. Homogenates from brains of homozygous mice with a deletion of SGIP1 (SGIP1$^{-/-}$), heterozygous mice (SGIP1$^{+/-}$), and mice with unchanged genotype (WT) were electrophoretically separated and analyzed by immunoblotting. Samples were visualized with antibodies to SGIP1 (and SGIP1) and actin (anti-Actin). In SGIP1$^{-/-}$ mice, a complete loss of SGIP1 (~ 130 kDa) was confirmed, while SGIP1$^{+/-}$ and WT mice still express SGIP1. A comparable protein loading in all samples is visible when labeled with an anti-Actin antibody.

4.6. Cannabinoid receptor 1 signaling is affected by SGIP1 in autaptic hippocampal neurons

To study the effect of SGIP1 on CB1R function in autaptic hippocampal neurons, DSE measurements by the whole-cell patch-clamp electrophysiology were performed. DSE is a form of synaptic plasticity solely dependent on ECS (Kreitzer and Regehr, 2001) and can therefore be considered as a representation of CB1R signaling.

DSE can be quantified in a dose-response manner by generating successively longer depolarizations. First, the effect of SGIP1 deletion on the DSE responses over a range of depolarizations (50 ms, 100 ms, 300 ms, 500 ms, 1 s, 3 s, 10 s) was tested. In WT mice, longer depolarizations yielded a successively greater inhibition of neurotransmitter release, measured as a smaller excitatory postsynaptic current (EPSC). Compared to WT, the DSE depolarization-response curve is shifted to the right in SGIP1$^{-/-}$ neurons (**Fig. 19A,** tab. 1 in appendix). Therefore, the DSE response to a given depolarization is weaker in the absence of SGIP1. This was particularly evident for longer depolarizations.

2-AG activates CB1R to mediate DSE in autaptic neurons (Straiker and Mackie, 2005). Therefore, if SGIP1 modulates CB1R signaling presynaptically, the application of increasing concentrations of 2-AG should mimic changes in DSE similar to those induced by depolarization. WT and SGIP1$^{-/-}$ derived neurons were treated with increasing concentrations of 2-AG (1nM-5µM), and EPSCs were evoked every 20 s with 0mV depolarization lasting 1 ms. In WT mice, 2-AG decreased the EPSCs in a concentration-dependent manner as expected. Importantly, 2-AG was less effective in neurons lacking SGIP1, reminiscent of the impaired DSE observed in SGIP1$^{-/-}$ neurons (**Fig. 19B,** tab. 1 in appendix).

Next, we asked whether the chronic application of agonist will lead to differential desensitization of CB1R in WT compared to SGIP1$^{-/-}$ neurons. The neurons were treated with 100nM WIN55,212-2 (WIN) overnight and washed WIN for at least 20 minutes before measuring DSE responses. The SGIP1$^{-/-}$ neurons, similar to the WT neurons, were almost completely desensitized by this treatment (**Fig. 19C,** tab. 1 in appendix).

The results of electrophysiological measurements in SGIP1$^{-/-}$ neurons have not yet been published.

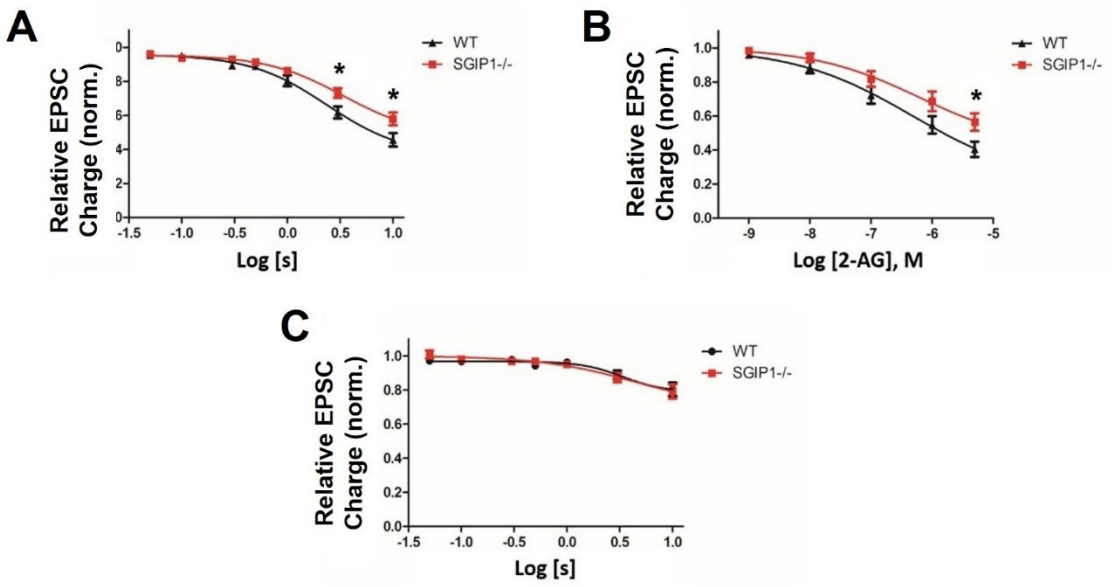

Fig. 19. Depolarization-induced suppression of excitation (DSE) is modulated by SGIP1 protein. Autaptic neurons were depolarized for progressively longer intervals to induce DSE **(A)**. SGIP1$^{-/-}$ neurons are significantly less responsive to depolarization compared to wild-type neurons. (WT: 2.358 s; ED50 SGIP1$^{-/-}$: 3.344 s). (**B**) SGIP1$^{-/-}$ neurons are also less sensitive to 2-AG (ED50 WT: 475.5nM, ED50 SGIP1$^{-/-}$: 639.4nM). Suppression of EPSC charge by increasing concentration of 2-AG was evaluated in autaptic neurons. (**C**) SGIP1$^{-/-}$ neurons desensitize at the same rate and extent as WT neurons. Cells were treated overnight with the CB1R agonist WIN 55,212-2 (100 nM), washed for 20 minutes, and DSE was evaluated. Both SGIP1$^{-/-}$ and WT neurons were almost completely desensitized by treatment with WIN 55,212-2. Baseline response was normalized to 1, and DSE is plotted as fractions of 1. Data are expressed as mean ± SEM. (n = 9-24 per group). * $p < 0.05$.

4.7. Study of SGIP1 function *in vivo*

In vivo experiments examined how SGIP1 deletion affects the phenotype of mice in aspects associated with CB1R signaling. Selected phenotyping tests were assessed separately in males and females, as some studies are pointing to differences in the ECS functioning in male and female mice (Fattore and Fratta, 2010).

4.7.1. SGIP1$^{-/-}$ mice have an intact working memory, exploration levels, and sensorimotor gating

Working memory and exploration in WT and SGIP1$^{-/-}$ mice were assessed in the Y maze. Rodents in this maze spontaneously alternate both arms while exploring the maze. From the alternations between the arms, it is possible to assess short-term memory. Furthermore, the overall activity and the exploration levels of the mice can be monitored in this assay. Both groups of mice examined were comparably active during testing (**Fig. 20C-D**), and no change in the number of alterations (arm rotation) was observed when examining SGIP1$^{-/-}$ mice compared to WT mice (**Fig. 20A-B**). SGIP1$^{-/-}$ mice have a comparable level of exploration and intact working memory when compared with WT mice.

Sensorimotor learning was assessed by determination of prepulse inhibition of the startle response (PPI). No significant changes in startle response were observed between SGIP1$^{-/-}$ and WT mice (**Fig. 20E-F**).

The statistical analysis of working memory and PPI tests is shown in the appendix in the tab. 2.

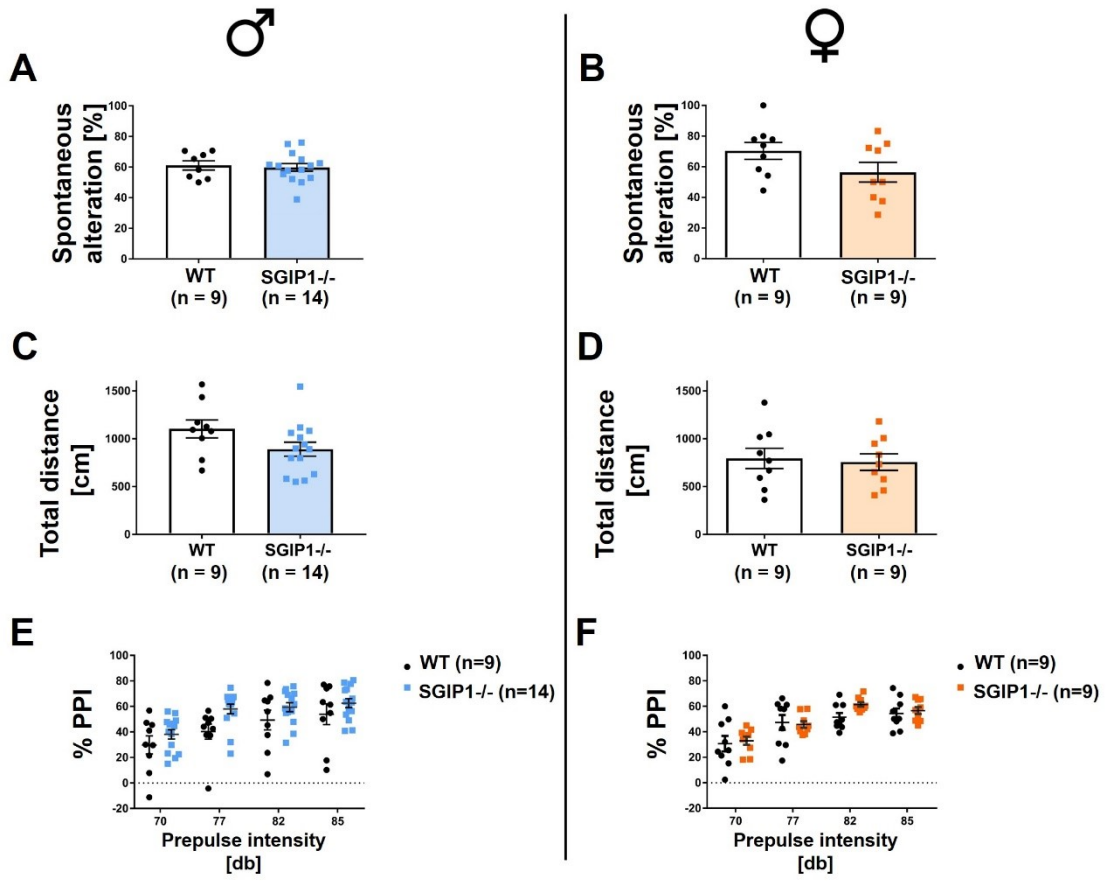

Fig. 20. SGIP1$^{-/-}$ mice have intact short-term memory, environmental exploration, and sensorimotor learning. (**A, B**) No significant changes in spontaneous alterations or (**C, D**) distance traveled in the Ypsilon maze were detected in the compared cohorts of males and females. (**E, F**) Similarly, no significant changes were detected in the SGIP1$^{-/-}$ and WT mice in prepulse inhibition of the startle response (PPI). Data are presented as mean ± SEM.

4.7.2. SGIP1$^{-/-}$ mice show signs of anxiolytic-like phenotype

Several behavioral tests were used to analyze anxiety-like behavior and depressive-like behavior in tested cohorts of mice.

Open field test and elevated plus maze were used to test for anxiety-like behavior. These tests take advantage of the conflict between the urge to explore a new environment and the fear of open and lighted space. The animals are placed in an unknown environment that they should explore. At the same time, animals are expected to avoid brightly lit open areas that are highly aversive for nocturnal animals such as mice.

The time spent in the center of the OF serves as an indicator of anxiolysis. Less anxious mice spend more time in the middle of an open field. SGIP1$^{-/-}$ males spent significantly more time at the center than the control group (**Fig. 21A**), while traveling a comparable distance across the arena as male WTs (**Fig. 21C**). Comparable distance traveled was also recorded in females (**Fig. 21D**), but unlike males, SGIP1$^{-/-}$ females did not spend longer time in the middle of the OF (**Fig. 21B**). During the test, other manifestations, e.g., episodes of freezing indicating fear, were observed. There were no significant differences in the number of these episodes in females and SGIP1$^{-/-}$ males compared to controls (**Fig. 21E-F**). Furthermore, the number of rearings, which are manifestations of active exploration of the environment, was analyzed. SGIP1$^{-/-}$ males had a higher incidence of this behavior than WT males (**Fig. 21G**). In females, the frequency was similar in both compared groups (**Fig. 21H**). Based on the longer time spent in the center of the open arena and the increased number of exploratory behaviors, we can conclude that SGIP1$^{-/-}$ males are less anxious in the new environment than WT males. In females, this difference was not detected in the OF test.

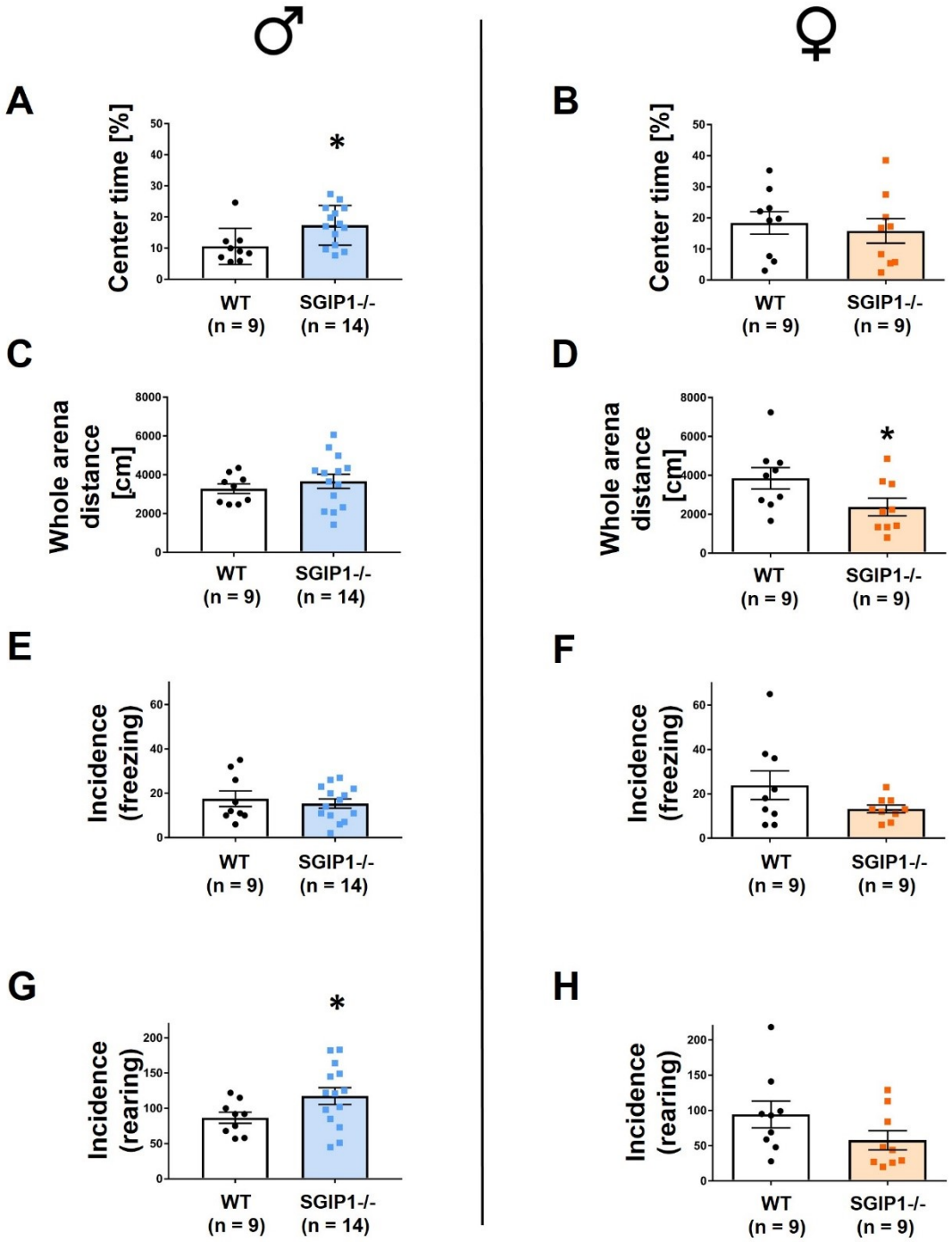

Fig. 21. SGIP1$^{-/-}$ males showed an anxiolytic phenotype in the open field test. (**A**) SGIP1$^{-/-}$ males spent significantly more time in the center of the open field than WT males. (**B**) This difference was not observed in females. (**C**) Both groups of males walked a comparable distance in the arena. (**D**) SGIP1$^{-/-}$ females traveled significantly shorter distances than WT females. (**E-F**) The incidence of freezing was comparable between the studied groups in both males and females. (**G**) The incidence of rearing was higher in SGIP1$^{-/-}$ males than in WT males. (**H**) The difference in rearing incidence was not significant in females. Data are presented as mean ± SEM; * $p < 0.05$.

The elevated plus maze uses the same principle as the OF test. The two open arms of the maze serve as anxiogenic zones, the two arms protected by the walls then serve as zones where the mice feel safe. (**Fig. 22A-B**) Both SGIP1$^{-/-}$ males and females spent significantly more time in the open arms and (**Fig. 22C-D**) traveled a greater distance in the entire maze than the WT control mice. SGIP1$^{-/-}$ mice were less anxious and generally more active. (**Fig. 22E-F**) When comparing the number of open and closed arm visits, the differences between SGIP1$^{-/-}$ and WT mice were not significant. (**Fig. 22G-H**) Similarly, no significant difference was observed in the experimental groups of mice in the number of rearings in the maze.

The statistical analysis of tests for anxiolytic-like behavior is shown in the appendix in the tab. 3.

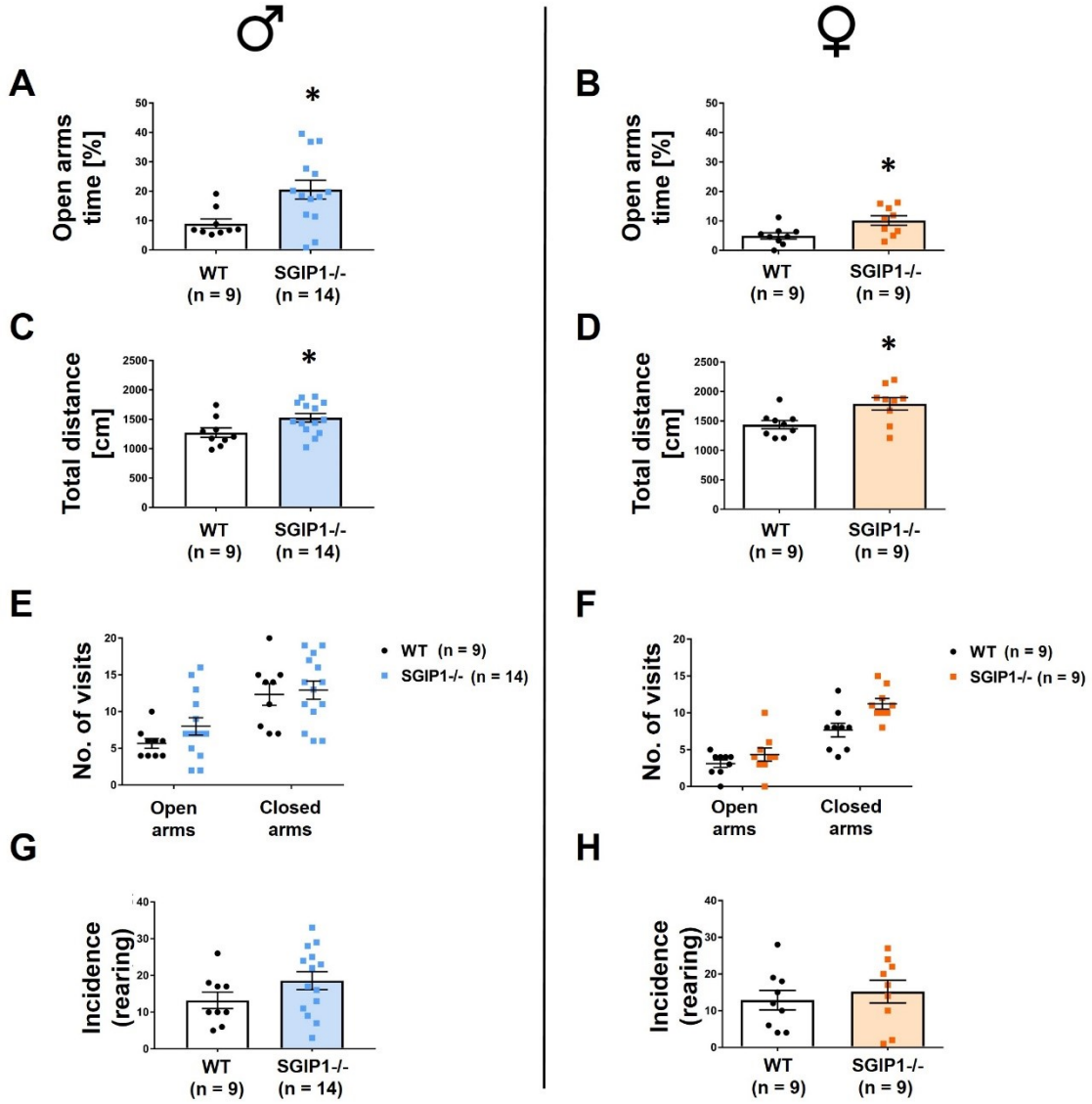

Fig. 22. SGIP1$^{-/-}$ males and females showed an anxiolytic phenotype in the elevated plus maze. (**A-B**) Both SGIP1$^{-/-}$ males and females spent more time in the open arms of the maze than the WT control groups, and also (**C-D**) traveled longer distances in the maze. (**E-F**) No significant changes in the number of open and closed arm visits were observed between the groups. (**G- H**) Also, the incidence of rearings in both SGIP1$^{-/-}$ males and females were comparable to the incidence of rearings in WT mice. Data are presented as mean ± SEM; * p <0.05.

4.7.3. SGIP1$^{-/-}$ mice have a more vigorous response to an unescapable situation

Depressive-like behavior was observed in the tail suspension test. The animals were exposed to a situation from which it was impossible to escape and were expected to try

to escape from it nevertheless. Depressive-like animals generally give up their escape efforts earlier. SGIP1$^{-/-}$ mice spent more time active, trying to escape, and demonstrated greater resilience in the hopeless situation (**Fig. 23A-B**).

The statistical analysis of tail suspension tests is shown in the appendix in the tab. 3.

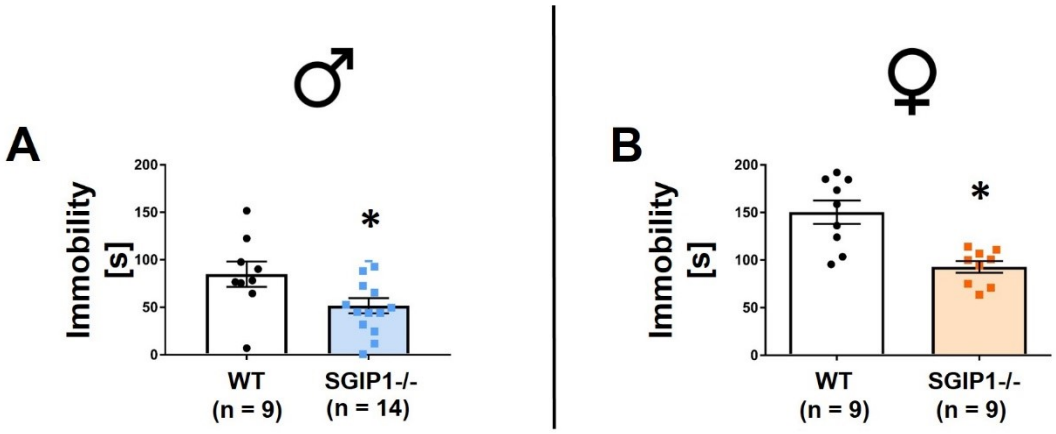

Fig. 23. SGIP1$^{-/-}$ mice cope better with an unescapable situation. The time the mice spent motionless in the tail hinge was significantly lower in both (**A**) male and (**B**) female SGIP1$^{-/-}$ than WT mice. Data are presented as mean ± SEM; * p <0.05.

4.7.4. Fear conditioning is intact in SGIP1$^{-/-}$ mice; the fear extinction is reinforced in SGIP1$^{-/-}$ females

The fear conditioning of the aversive memory connected with context and a cue was examined. Male and female SGIP1$^{-/-}$ mice spent comparable time freezing as their WT littermates (**Fig. 24A-B**). Extinction of the cued aversive memory occurred at a similar pace for SGIP1$^{-/-}$ and WT male mice (**Fig. 24C**). However, in female SGIP1$^{-/-}$ mice, the extinction to tone was facilitated compared to WT female mice (**Fig. 24D**). The data are presented as the percent of time spent freezing.

The statistical analysis of fear conditioning and fear extinction is shown in the appendix in the tab. 3.

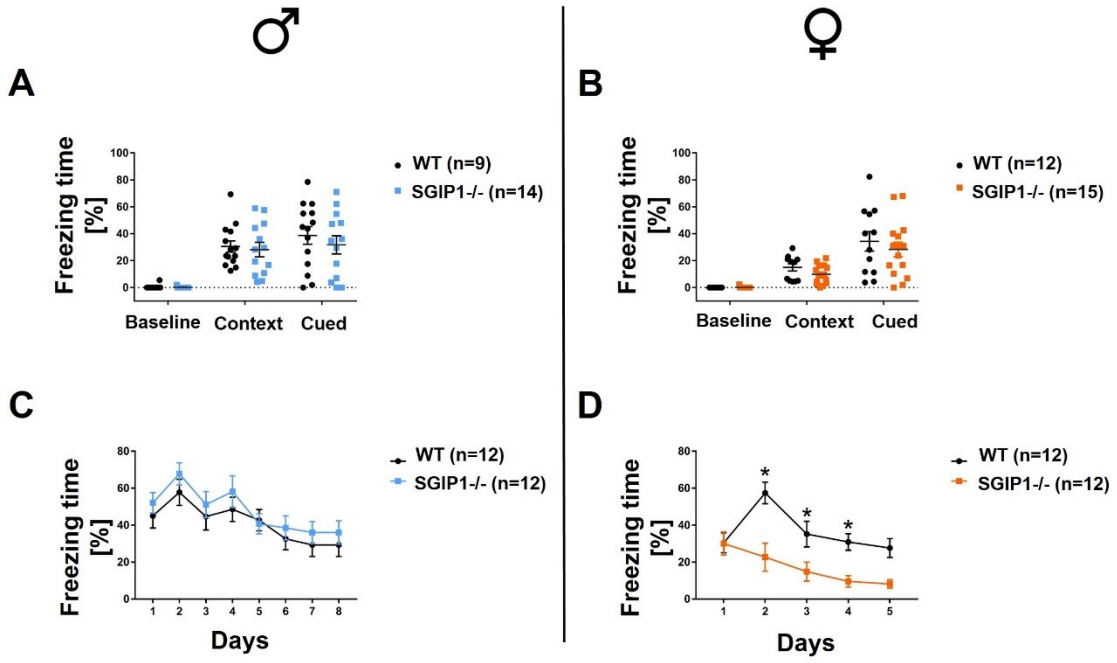

Fig. 24. Fear conditioning was intact in SGIP1$^{-/-}$ mice, SGIP1$^{-/-}$ females showed a faster extinction of aversive memories. Fear conditioning in response to context and cue was comparable in (**A**) males and (**B**) females of SGIP1$^{-/-}$ and WT genotype. (**C**) SGIP1$^{-/-}$ males exerted similar fear extinction as WT males. (**D**) SGIP1$^{-/-}$ females showed accelerated fear extinction. Data are presented as a percentage of the time the mice spent freezing, relative to the total time spent in the test chamber. Data are presented as mean ± SEM; * $p < 0.05$.

4.7.5. Cannabinoid tetrad tests revealed alterations in SGIP1$^{-/-}$ mice

The behavior of male SGIP1$^{-/-}$ and WT was compared in a set of tests referred to as the cannabinoid tetrad. These tests evaluate four manifestations of CB1R agonist intoxication - catalepsy, antinociception, hypothermia, and impaired motor skills. The acute response to THC was evaluated as well as the development of tolerance with daily administration of 10 mg/kg THC intraperitoneally for 8 days. Control groups of mice injected with VEH only for the whole time of the experiment were also included in the testing.

Mice were not cataleptic before the first injection of THC. The first injection of THC induced comparable catalepsy in both SGIP1$^{-/-}$ and WT mice. On days 4 and 8 of testing, SGIP1$^{-/-}$ mice were significantly more cataleptic than control WT mice (**Fig. 25A**). Control groups that did not receive THC did not develop catalepsy. On the first day of testing, SGIP1$^{-/-}$ mice had an increased latency to tail flick after the THC administration compared to WT mice (**Fig. 25B**). On day one, the hypothermia evoked by acute THC treatment was more profound in SGIP1$^{-/-}$ mice than in WT mice. On days 4 and 8 of testing, this change was no longer observable (**Fig. 25C**). In the Rotarod test, the genotype effect between SGIP1$^{-/-}$ and WT mice was not significant before and after the treatments. (**Fig. 25D**).

The statistical analysis of the cannabinoid tetrad is shown in the appendix in the tab. 4.

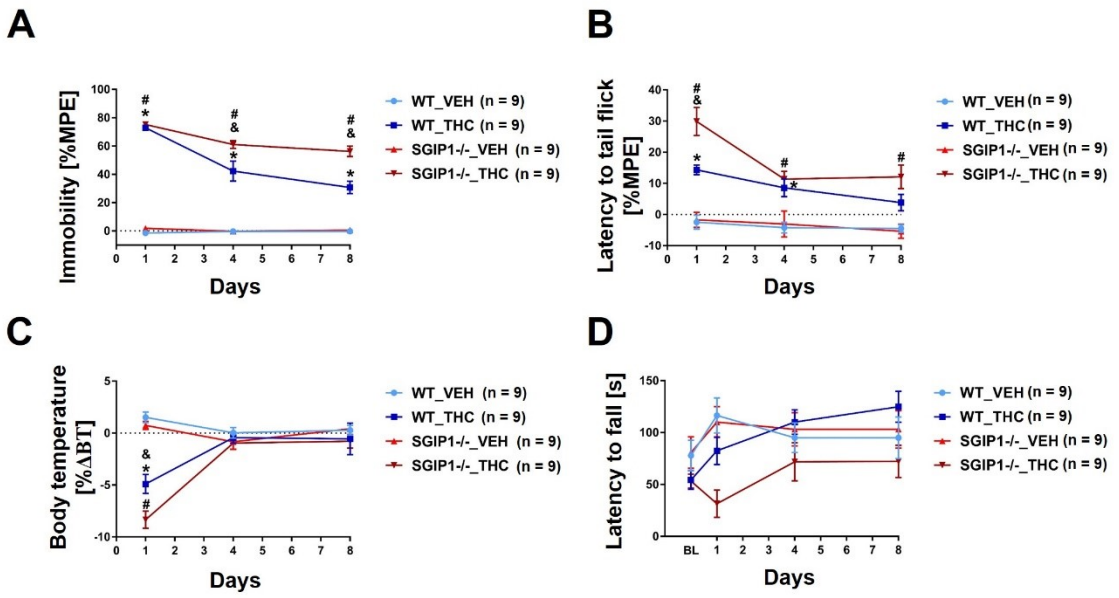

Fig. 25. The cannabinoid tetrad behavior is altered in SGIP1$^{-/-}$ males. The cannabinoid tetrad behavior was observed for 8 days, during which time the tested males received daily intraperitoneal doses of 10 mg/kg Δ^9-tetrahydrocannabinol (THC). Control groups of mice received only vehicle without active substance (VEH). Cannabinoid tetrad was performed 1 h after injection on days 1, 4, and 8 of the experiment. (**A**) In the ring test, THC induced comparable immobility in SGIP1$^{-/-}$ and WT mice. On days 4 and 8, SGIP1 $^{-/-}$ mice were more cataleptic after THC than WT mice. (**B**) In the tail flick test, prolonged tail-flick latencies were detected in SGIP1$^{-/-}$ mice versus WT mice before THC injection. On day 1 of testing, THC injection doubled the latency in SGIP1$^{-/-}$ mice

compared to WT mice. This difference was no longer observed on days 4 and 8. (**C**) THC caused a significant decrease in body temperature in WT and SGIP1$^{-/-}$ mice on day 1. Both groups of mice receiving THC became tolerant to THC in this aspect as early as day 4. (**D**) The rotarod test detected a significant effect of genotype and administered drug in the tested groups of mice, but the post hoc test did not reveal significance in individual days. Data are presented as mean ± SEM; *, #, & $p < 0.05$. The group comparison is shown by different symbols: * WT_THC vs. WT_VEH, # SGIP1$^{-/-}$_ THC vs. SGIP1$^{-/-}$_ VEH, & SGIP1$^{-/-}$_ THC vs. WT_THC.

4.7.6. THC withdrawal symptoms in SGIP1$^{-/-}$ mice

Symptoms of the THC withdrawal were observed in males that were given 10 mg/kg/day of THC for 9 days. The control group of mice received VEH instead of THC during this time. On the 9th day, the mice were injected with 10 mg/kg THC, followed by VEH injection 30 minutes later, and another 30 minutes later, 10 mg/kg rimonabant was applied. Headshakes, paw shakes, and scratching and grooming were monitored as the withdrawal symptoms. No increased incidence of headshakes or scratching/grooming after the rimonabant injection in THC pretreated WT and SGIP1$^{-/-}$ mice was observed (**Fig. 26A-B**). A higher incidence of paw shakes in THC pretreated WT and SGIP1$^{-/-}$ mice after the rimonabant injection was observed. However, there was no significant difference between the two monitored genotypes (**Fig. 26C**). In SGIP1$^{-/-}$ mice, the withdrawal was expressed as intense jumping manifested as straight leaps in the air with a strong charging from all four paws (**Fig. 26D**).

The statistical analysis of the THC withdrawal is shown in the appendix in the tab. 5.

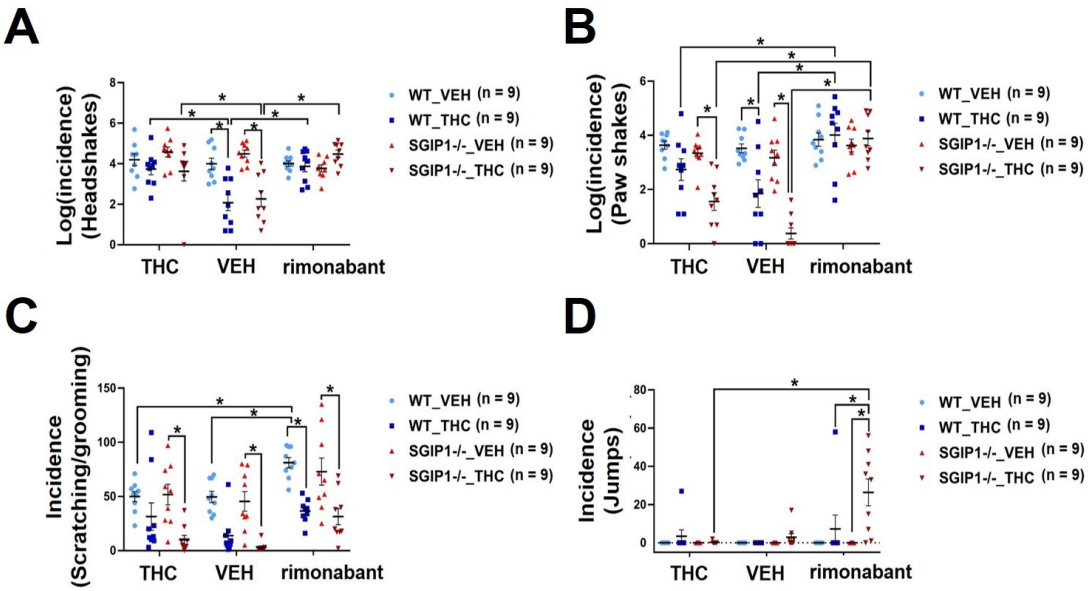

Fig. 26. Jumping as an unusual symptom of Δ^9-tetrahydrocannabinol (THC) withdrawal in SGIP1$^{-/-}$ mice. After 8 days of daily administration of 10 mg/kg THC or vehicle (VEH), withdrawal symptoms were precipitated with the cannabinoid receptor antagonist 1 rimonabant. On the 9th day of the experiment, mice were injected with THC, then VEH, and finally rimonabant, and their behavior was recorded on video.
The incidence of THC withdrawal signs: headshakes (**A**), paw shakes (**B**), scratching/grooming (**C**) was observed. There were no relevant differences between WT and SGIP1$^{-/-}$ mice in the manifestations of headshakes, paw shakes, and scratching/grooming. However, after rimonabant application, SGIP1$^{-/-}$ mice jumped more frequently (**D**). Data are presented as mean ± SEM; * p <0.05.

4.7.7. Decreased reactivity to acute pain and increased sensitivity to cannabinoid receptor agonists in SGIP1$^{-/-}$ mice

As shown in the cannabinoid tetrad, SGIP1$^{-/-}$ mice have an increased acute pain threshold compared to WT mice. The tail flick latency was significantly longer in both males and females (**Fig. 27A-B**). Nociception was measured three times with a 30-minute interval between single tests to exclude the effect of repeating the experiment on the resulting latencies. Latencies did not change significantly with the repetition of the experiment (**Fig. 27C-D**).

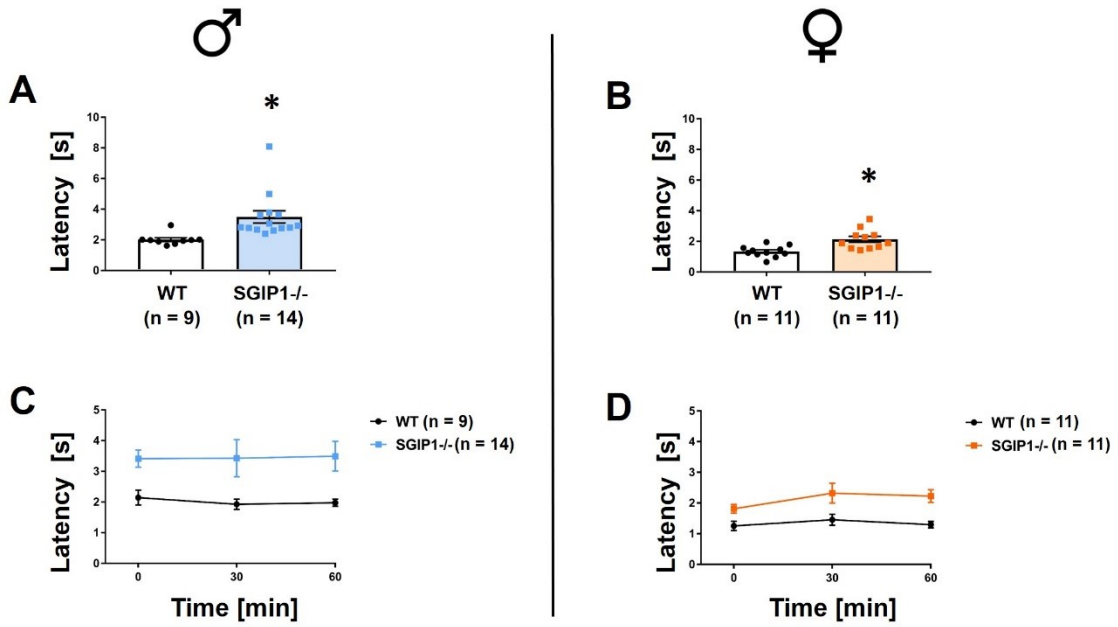

Fig. 27. Decreased reactivity to acute pain in SGIP1$^{-/-}$ mice. The tail flick latency from the water bath (52 ° C) was measured in triplicate with a 30-minute interval between measurements. (**A-B**) The mean latency of the three replicates is significantly higher in both male and female SGIP1$^{-/-}$ than in male and female WTs. (**C-D**) When comparing individual replicates, there was no significant difference between the individual trials. Data are presented as mean ± SEM; * p <0.05.

THC-induced antinociception was assessed in SGIP1$^{-/-}$ and WT mice. In this experiment, mice were injected with increasing doses of THC (0, 1, 3, 10, 30, 50 mg/kg, intraperitoneally), and after each dose, the latency to tail flick was measured. The latency dose-response curve was shifted to the left in SGIP1$^{-/-}$ males when compared to WTs (**Fig. 28A**), but not in females (**Fig. 28B**). The ED50s with the 95% confidence interval in parentheses were for males 28.24 (21.67 - 37.91) mg/kg (WT), 10.77 (9.09 - 15.58) mg/kg (SGIP1$^{-/-}$) and for females 31.20 (24.63 - 40.13) mg/kg (WT), 30.67 (23.31 - 37.23) mg/kg (SGIP1$^{-/-}$).

The antinociceptive effect of WIN was also observed in the compared groups of mice that received increasing doses of this drug (0, 0.3, 1, 3, 10 mg/kg, intraperitoneally). The antinociceptive effect of WIN is enhanced in both SGIP1$^{-/-}$ males and females (**Fig. 28C-D**). The ED50s with the 95% confidence interval in parentheses were for males 4.73 (3.74 - 5.86) mg/kg (WT), 1.70 (1.48 - 1.96) mg/kg (SGIP1$^{-/-}$) and for females 18.11 (13.63 - 38.23) mg/kg (WT), 3.20 (2.71 - 3.83) mg/kg (SGIP1$^{-/-}$).

The statistical analysis of the tail flick test and the reactivity to acute pain is shown in the appendix in the tab. 6.

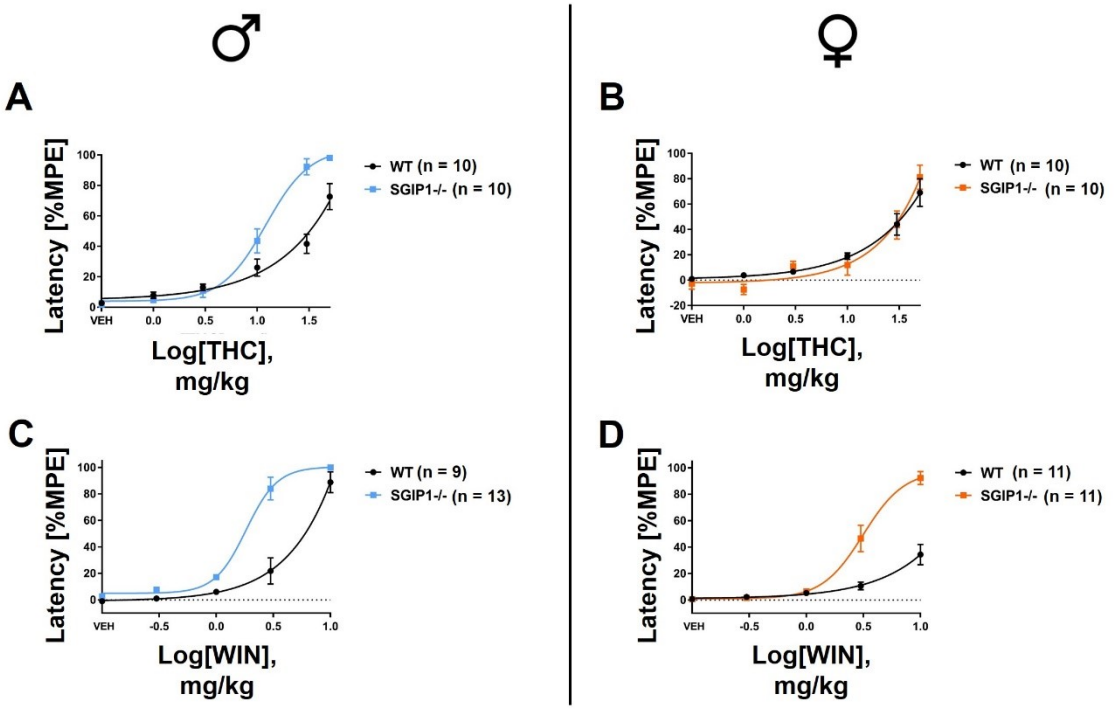

Fig. 28. Effect of cannabinoid receptor 1 (CB1R) agonists on pain perception in mice. Mice were injected with CB1R agonists Δ^9-tetrahydrocannabinol (THC; 0, 1, 3, 10, 30 and 50 mg/kg) or WIN 55, 212-2 (WIN; 0, 0.3, 1, 3, 10 mg/kg) intraperitoneally in gradually increasing doses. VEH on the axis x depicts an administration of a carrier without an active substance. The tail flick latency from the water bath (52 ° C) was measured 1 h after each dose. (**A**) In SGIP1$^{-/-}$ males, the THC dose-response latency curve was shifted to the left compared to the curve measured in WT males, (**C**) the leftward shift in SGIP1$^{-/-}$ males was also observed after WIN administration. (**B**) SGIP1$^{-/-}$ females responded to THC in a comparable way to WT females. (**D**) When WIN was administered, the dose-response latency curve of WIN was shifted to the left from the curve measured in female WTs. Data are presented as mean ± SEM; * $p < 0.05$.

4.7.8. Enhanced antinociceptive effects of morphine in SGIP1$^{-/-}$ mice

The effect of morphine on acute pain was also studied in our mice. Mice were injected intraperitoneally with morphine in increasing doses (0, 0.3, 1, 3, 10, 30 mg/kg), and their latency to tail flick was monitored. The morphine dose-response curve was shifted to the left in both SGIP1$^{-/-}$ males and females compared to the curves obtained in WTs (**Fig. 29A-B**). The ED50s with the 95% confidence interval in parentheses were for

males 4.86 (3.88 - 6.14) mg/kg (WT), 2.18 (1.70 - 2.76) mg/kg (SGIP1$^{-/-}$) and for females 5.71 (4.58 - 7.12) mg/kg (WT), 3.20 (2.23 - 4.61) mg kg (SGIP1$^{-/-}$).

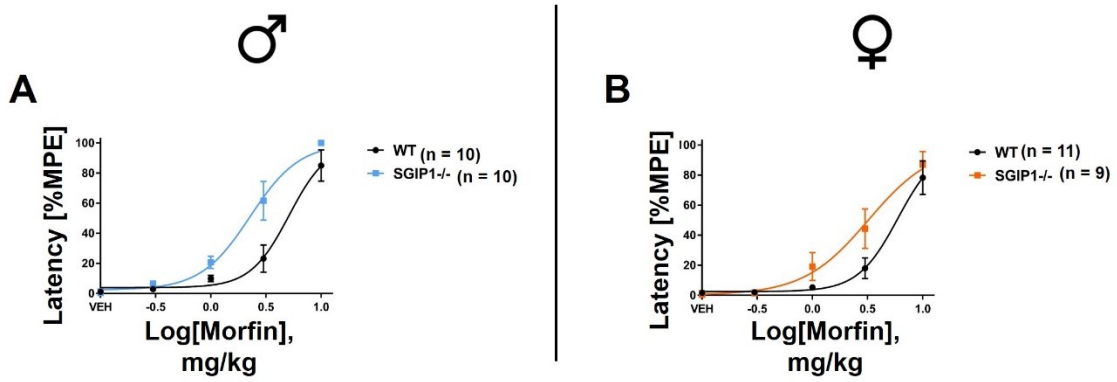

Fig. 29. The reaction to morphine is stronger in SGIP1$^{-/-}$ males than in WT males. Mice were injected with morphine intraperitoneally in gradually increasing doses (0, 0.3, 1, 3, 10 mg/kg). The tail flick latency from the water bath (52 ° C) was measured 1 h after each dose. (**A-B**) In both SGIP1$^{-/-}$ males and females, the morphine dose-response curve was shifted to the left from the WT curve. Data are presented as mean ± SEM; * p <0.05.

4.7.9. Short-term effect of a CB1R antagonist on nociception in SGIP1$^{-/-}$ mice

To demonstrate that the effect of SGIP1 deletion on nociception in mice is associated with CB1R activity, the effect of the CB1R inverse agonist, rimonabant, on pain sensation was studied. In SGIP1$^{-/-}$ and WT male mice, the effects of rimonabant administration on acute nociception and the nociception after daily administration for three days were studied. Rimonabant induced a reduced tail flick latency on the first day of administration in SGIP1$^{-/-}$ mice compared to mice of the same genotype injected with VEH (**Fig. 30A**). Compared to the respective group of WT mice, the changes are not significant. The difference in SGIP1$^{-/-}$ mice does not persist until the third day of dosing, in which the differences are no longer significant (**Fig. 30B**).

The statistical analysis of the tail flick test after the injection of the CB1R antagonist is shown in the appendix in the tab. 7.

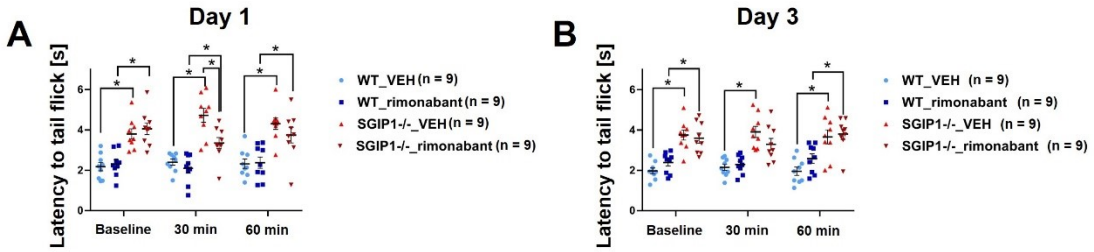

Fig. 30. Rimonabant has a transient effect on nociception in SGIP1$^{-/-}$ male mice. Male mice were injected intraperitoneally with 10 mg/kg of the cannabinoid receptor 1 inverse agonist (CB1R) rimonabant. The control group was injected with vehicle (VEH). Mice were injected daily for 3 days, and their latency to tail flick from a warm bath was measured on days 1 and 3 of experiment 30 and 60 minutes after injection. (**A**) Baseline latency was increased in SGIP1$^{-/-}$ mice compared to WT mice. At 30 min after injection, a significant decrease in latency was observed in SGIP1$^{-/-}$ mice that received rimonabant compared to SGIP1$^{-/-}$ mice that were injected with VEH. (**B**) On day 3 of the experiment, this difference was no longer observed, and only increased latency remained in SGIP1$^{-/-}$ mice compared to WTs. Data are presented as mean ± SEM; * p <0.05.

4.7.10. SGIP1$^{-/-}$ mice have normal body weight

Bodyweight was measured continuously during behavioral experiments over 6 weeks. No significant difference in weight was detected in SGIP1$^{-/-}$ males or females compared to WT mice (**Fig. 31**).

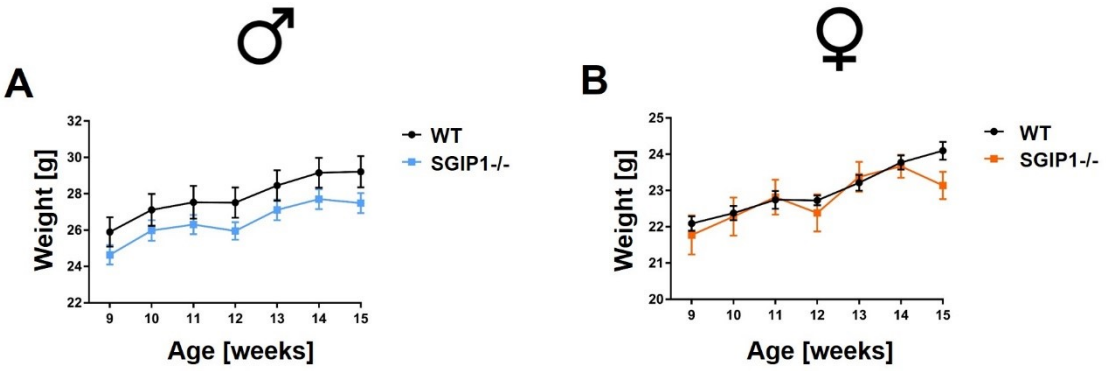

Fig. 31. The bodyweight of SGIP1$^{-/-}$ mice is comparable to that of WT mice. No significant differences in the weights of the SGIP1$^{-/-}$ and WT mice were observed when the mice were weighed for 6 weeks period during which they were phenotyped. Data are presented as mean ± SEM.

5. DISCUSSION

5.1. SGIP1 interacts with cannabinoid receptor 1, and together, they are localized in synaptic compartments

During the search for CB1R interaction partners by the yeast two-hybrid system, SGIP1 was detected as a positive hit (Hajkova et al., 2016). In rodents, SGIP1 is localized mainly in the CNS (Trevaskis et al., 2005) as well as CB1R (Freund et al., 2003). Both SGIP1 and CB1R are associated with energy homeostasis and body weight regulation (Di Marzo and Matias, 2005; Walder et al., 2000). Therefore, it was likely that their mechanism of action could be linked. SGIP1 was selected as a suitable candidate for studying intracellular modulation of CB1R signaling.

The protein-protein interaction of SGIP1 with CB1R in the mouse brain was confirmed by co-immunoprecipitation from the detergent soluble fraction. Both proteins are co-localized in the synaptic compartments of murine neurons. SGIP1 accounts for more than 0.4 % of the protein content in synaptic terminals (Wilhelm et al., 2014) and could play a role in the CB1R membrane stability. The ninth intracellular helix of CB1R, laying within the SGIP1 interaction part, is essential for maintaining CB1R surface stability in the axonal membrane. When CB1R lacks the ninth helix, it is readily internalized and transported into dendrites (Fletcher-Jones et al., 2019). Thus, by interacting with this CB1R helix, SGIP1 could help stabilize CB1R in the axonal membrane. In dendrites where SGIP1 is less expressed, CB1R is profoundly internalized (Leterrier et al., 2006).

The movement of CB1R in the membrane is very dynamic. Receptors are transported between synaptic and extrasynaptic compartments. CB1R desensitization prevents such movement; receptor diffusion is slowed during desensitization up to a point when CB1R remains immobile in the extrasynaptic compartments. This causes a reduction in the number of available CB1Rs in synaptic regions (Mikasova et al., 2008). Ultimately, regulation of CB1R by internalization or transport may impact signaling and behavioral manifestations associated with CB1R's activity. The SGIP1 modulation of CB1R signaling may be may play a role in the CB1R internalization and transport.

For the study of SGIP1 function in neurons and *in vivo*, a line of genetically modified mice carrying a deletion of the SGIP1 gene was prepared. Deletion of the SGIP1 gene is achieved by removing the second exon of the SGIP1 from genomic DNA, which results in a frameshift and loss of SGIP1 expression. The absence of SGIP1 in the brain of $SGIP1^{-/-}$ mice was confirmed by immunoblotting.

5.2. Cannabinoid receptor signaling in autaptic hippocampal neurons is affected by the absence of SGIP1

Continuous activation of CB1R leads to its desensitization, internalization (Howlett et al., 2004; Martini et al., 2007), and development of tolerance (Gainetdinov et al., 2004). The underlying basis of CB1R desensitization is the phosphorylation of serines S426 and S430 by GRKs. When these two serines at positions 426 and 430 are mutated to alanines (S426A/S430A), the phosphorylation site is removed, and CB1R desensitization can not occur (Daigle et al., 2008a; Jin et al., 1999).

CB1R internalization is mediated by β-arrestins, which interact with the phosphorylated C-terminus of CB1R (DeWire et al., 2007; Moore et al., 2007). SGIP1 enhances β-arrestins association with activated CB1R and prevents CB1R endocytosis, which causes changes in the signaling of this receptor in transfected HEK293 cells (Hajkova et al., 2016). Because HEK293 cells do not endogenously express CB1R, we wondered how SGIP1 affects signaling in neurons.

For the study of the SGIP1 and CB1R interaction, autaptic hippocampal neurons were used. In this model system, SGIP1 and CB1R are endogenously expressed, and CB1R mediates DSE as a form of retrograde signaling upon 2-AG binding. DSE serves as a measure of CB1R signaling in these neurons and can be triggered by either neuronal depolarization or exogenous 2-AG application. DSE can be measured electrophysiologically by a whole-cell patch-clamp method (Straiker and Mackie, 2005)

In neurons derived from mice carrying the S426A/S430A mutation, short-term DSE enhancement and decreased desensitization were observed (Morgan et al., 2014). In neurons carrying CB1R truncated by 13 C terminal amino acids or with a mutation of the last 6 C-terminal serines and threonines to alanines, the DSE is still present, although not

in the same magnitude as in WTs; however, the desensitization does not occur in these neurons (Straiker et al., 2012). We expected that changes in CB1R signaling would also be recorded using electrophysiology in neurons from SGIP1$^{-/-}$ mice due to the results from studies in neurons carrying mutations affecting desensitization and internalization.

To determine whether CB1R signaling at the neuronal level is altered in SGIP1$^{-/-}$ mice, the system's responses to stimulation of neurons isolated from SGIP1$^{-/-}$ and WT mice were compared. In SGIP1$^{-/-}$ neurons, decreased DSE was observed as a consequence of both depolarization and exogenous administration of 2-AG.

In the absence of SGIP1, the activated CB1R can be rapidly internalized, leading to a reduced number of available receptors on the membrane. Such a situation would result in a reduced DSE. In contrast, in mice with mutated serines 426 and 430, CB1R is not desensitized, signaling is still ongoing, and DSE is elevated. The presence of SGIP1 in neurons causes a similar shift in the DSE curves as the serine 426 and 430 mutations (Morgan et al., 2014). However, the effect is only temporary because, after 16 hours of incubation with WIN, neurons of both genotypes show almost total desensitization, which is typical for CB1R (Straiker and Mackie, 2005).

5.3. The absence of SGIP1 caused changes in the anxiety-like and depressive-like behavior, fear conditioning, and nociception and reinforced responses to CB1R agonists and morphine

A reverse genetic approach was used to determine the effect of SGIP1 on mouse behavior. By comparing SGIP1$^{-/-}$ and WT mice in behavioral assays, it is possible to monitor which aspects of behavior are affected by the SGIP1 deletion. Our testing was focused on cannabinoid-related behavior.

In the experiments, the behaviors of SGIP1$^{-/-}$ and WT mice were compared within the same sex. According to the literature, female rodents may be more sensitive to the administration of cannabinoids in tests of nociception and motor skills (Craft and Leitl, 2008). This would suggest an increase in basal ECS function in females. Similarly, women are more prone to developing cannabinoid dependence and suffer from more severe withdrawal symptoms than men (Craft et al., 2013). ECS function in females is

affected by the estrous cycle. Estradiol increases the antinociceptive effect of THC but does not affect motor skills. Reinforced effects of THC were observed in rats when females were in the estrous phase of their cycle (Craft and Leitl, 2008). In some areas of the brain, endocannabinoid levels (Bradshaw et al., 2006) and the number and affinity of CB1R (Rodriguez de Fonseca et al., 1994) vary depending on gender and phase of the hormonal cycle. For these reasons, it is crucial to characterize endocannabinoid signaling not only in males but also in females. For the highest accuracy of the results, it would also be appropriate to synchronize the estrous cycle of the tested females. For this work, such synchronization was not performed.

SGIP1$^{-/-}$ mice have an intact working memory, exploration levels, and sensorimotor gating

Environmental exploration, working memory, and sensorimotor gating are CB1R-influenced functions that ensure the survival of animals in the wild. When observing mice with a deletion of the CB1R gene (CB1R$^{-/-}$) in the Morris water maze, it was found that CB1R$^{-/-}$ mice learn comparably to WT mice. However, CB1R$^{-/-}$ mice perform worse in the Morris water maze if the learned situation changes and the animals need to adapt to the new situation. This phenomenon is probably related to the activity of CB1R in memory extinction. CB1R$^{-/-}$ mice have a more significant problem to actively reshape learned schemes (Varvel and Lichtman, 2002).

CB1R$^{-/-}$ mice in which the gene deletion is developmental do not show changes in sensorimotor learning. When CB1R expression is reduced by the use of conditional mouse knockout during adulthood, sensorimotor learning is impaired (Marongiu et al., 2012). In developmental knockout, this phenotype is probably suppressed by an unknown compensation mechanism.

In our cohorts of mice, working memory was observed in the Y-maze. The levels of exploration of the new environment, mobility, and working memory were comparable in SGIP1$^{-/-}$ mice and WT mice.

Sensorimotor learning was examined by the PPI test, which measures the transmission of afferent sensory perception and the motor response following signaling

through efferent fibers. Similar to working memory, sensorimotor gating is not impaired in SGIP1$^{-/-}$ mice.

Since SGIP1$^{-/-}$ mice performances in the Y-maze and PPI tasks were normal, altered exploratory drives or impaired working memory or sensorimotor gating was excluded as causative for the observed differences in further behavioral examinations.

SGIP1$^{-/-}$ mice show signs of anxiolysis and cope better with an unescapable situation

ECS affects mood, fear, and adaptive coping with stress situations (Lutz et al., 2015; Mechoulam and Parker, 2013; Micale et al., 2013; Morena et al., 2016). Behavior similar to human manifestations of anxiety can be studied in mice using OF and EPM tests, which exploit the conflict between the drive to explore a new environment and avoidance of open, lighted spaces. The longer time spent in the center of the OF arena or the open arms of the EPM indicates increased anxiolysis (reduced anxiety).

SGIP1$^{-/-}$ males spent more time in the OF center than WT males, while this difference was not observed in females. In the case of EPM, both SGIP1$^{-/-}$ males and females spent more time in anxiogenic zones and also traveled a greater total distance than the WT control groups. In males, SGIP1$^{-/-}$ both tests used indicate an anxiolytic phenotype; in females, this observation was confirmed only in the EPM test.

Differences in anxiety-like behavior in male and female mice have been described previously. In a study comparing emotionality, cannabinoids reduced environmental exploration levels and anxiety-like behavior in female rats, but not in males (Biscaia et al., 2003). In our experiments, the anxiolytic effect of SGIP1 deletion was more pronounced in males than in females. The behavioral testing of females must take into account the possibility of the estrous cycle influencing their behavior. However, when anxiety-like behavior was studied in male rats and female rats at various stages of the cycle, gender differences were described, but no significant differences between groups of females at different stages of the cycle were found (Scholl et al., 2019).

By comparing the phenotype of SGIP1$^{-/-}$ mice with the results of observations of mice that underwent genetic or pharmacological manipulation of ECS, conclusions about the activity of SGIP1 can be drawn. The CB1R$^{-/-}$ mice are less active in OF and more anxious than WTs (Zimmer et al., 1999). Lately, enzymes that degrade or synthesize endocannabinoids are studied extensively. By their genetic or pharmacological manipulation, changes in behavior can also be achieved. Decreased FAAH activity by pharmacological inhibition (Kathuria et al., 2003) or total deletion (Moreira et al., 2008) leads to an increase in AEA levels in the brain, increased ECS stimulation, and anxiolysis. Reducing endogenous 2-AG levels by total deletion of DAGLα, on the other hand, leads to increased manifestations of anxiety-like behavior (Jenniches et al., 2016; Shonesy et al., 2014). Due to the biphasic effect of cannabinoids on CB1R (see chapter 1.4.3) (Rey et al., 2012), we hypothesize that in SGIP1$^{-/-}$ mice, ECS activity is only slightly increased and therefore acts anxiolytically, especially in males.

Anxiety and depressive behavior are often closely related. Further testing has been focused on how SGIP1$^{-/-}$ mice cope with an unescapable situation. In the TST, the observed mouse is hung by the tail and cannot escape, which creates a stressful situation. Mice showing signs of depressive-like behavior give up their effort to escape easily and remain motionless. SGIP1$^{-/-}$ mice were more active in their attempts to free themselves than WT mice, suggesting their greater ability to cope with an unescapable situation. As with anxiety-like behavior, depressive-like behavior is alleviated with increased ECS activity (Bortolato et al., 2007; Danandeh et al., 2018), confirming our hypothesis that SGIP1 deletion increases ECS activity, especially in males.

Fear conditioning is intact in SGIP1$^{-/-}$ mice, SGIP1$^{-/-}$ have an increased extinction of aversive memories

CB1R signaling is closely connected with acquiring and forgetting memories with a strong emotional subtext (often fear). Mice with a deletion of the CB1R gene are a valuable model for studying post-traumatic stress disorder. Extinction of aversive memories is facilitated in CB1R$^{-/-}$ mice, while other memory attributes are not impaired (Marsicano et al., 2002).

In our study, the response to the context or cue associated with electric shock was comparable in both SGIP1$^{-/-}$ male and female compared to WT mice. Sexual dimorphism has been reported in the extinction of aversive memories (Velasco et al., 2019). While SGIP1$^{-/-}$ males forgot aversive memories as fast as WT males, SGIP1$^{-/-}$ females had a faster extinction than WT females.

Some components of fear conditioning are dependent on the sex of the test animals. In a recent study, the response to the conditioned stimulus, which is associated with danger, was greater in males than in females. However, males also have a faster extinction of aversive memories (Clark et al., 2019).

Altered cannabinoid tetrad behavior and unusual THC withdrawal symptoms in SGIP1$^{-/-}$ mice

Acute THC intoxication is typically manifested by a combination of four symptoms: catalepsy, antinociception, hypothermia, and hypoactivity (Chaperon and Thiebot, 1999). In the characterization of behavior affected by the ECS signaling, the cannabinoid tetrad is a fundamental tool. Therefore, cannabinoid tetrad was used to characterize SGIP1$^{-/-}$ mice.

Catalepsy, nociception, and body temperature were influenced by the mouse genotype in our experiments. In the case of catalepsy, THC tolerance developed more slowly in SGIP1$^{-/-}$ mice than in WT mice. In the case of nociception, a difference was found in the baseline values of the latency to tail flick. SGIP1$^{-/-}$ mice had a significantly increased tail flick latency compared to WT mice and maintained this difference throughout the 8-day dosing period. On the first day of the test, THC caused significantly higher antinociception in SGIP1$^{-/-}$ mice than in WTs. THC induced hypothermia was more profound in SGIP1$^{-/-}$ mice than in WT mice, but all subjects became tolerant to THC in this aspect as early as day 4. Motor functions were not significantly affected by genotype and drug administration.

During the THC withdrawal experiment, numerous jumps were observed in SGIP1$^{-/-}$ mice that were injected with THC during the previous 8 days. Such behavior is not typical in THC-induced withdrawal but has been described in mice with a CB1R

mutation (S426A, S430A) that prevents its desensitization (Morgan et al., 2014). Similar to SGIP1$^{-/-}$ mice, these mice have increased sensitivity to THC and slower development of tolerance.

In GASP1 knockout mice, the development of tolerance in nociception caused by a CB1R agonist is also slowed down. Mice with a genetic deletion of β-arrestin 2 show increased sensitivity to THC and decreased tolerance to the antinociceptive effects of THC. In contrast, in THC-induced catalepsy, tolerance develops faster in β-arrestin 2 knockout mice than in control mice. These mice also have prolonged opioid-induced antinociception and reduced morphine tolerance (Bohn et al., 1999), suggesting synergistic mechanisms of action of the endocannabinoid and opioid systems. The ERK1/2 signaling pathway is probably also important for the development of tolerance to THC. In mice with a deletion of the Ras-specific guanine nucleotide exchange factor, the development of tolerance to the sedative and antinociceptive effects of THC is impaired (Rubino et al., 2006). These observations point to the importance of knowing the precise receptor signaling mechanisms as changes at different levels of signaling have different effects (Martini et al., 2010).

The unusual THC withdrawal indicates possible involvement of other signaling pathways. Jumping is also a common manifestation of morphine withdrawal in rodents (Francis and Schneider, 1971). It is possible that the interaction of ECS and the opioid system, which has been described several times in the literature, is responsible for the phenotype observed in SGIP1$^{-/-}$ mice (Ledent et al., 1999; Robledo et al., 2008). If ECS activity is enhanced in SGIP1$^{-/-}$ mice, this enhancement may be reflected in other CB1R-interacting systems.

Decreased nociception and increased sensitivity to cannabinoid receptor agonists and morphine in SGIP1$^{-/-}$ mice

CB1R activation is known to relieve pain (Hasanein et al., 2007; Mascarenhas et al., 2017; Woodhams et al., 2017). Cannabinoid tetrad revealed reduced nociception in SGIP1$^{-/-}$ mice, so we focused on a detailed examination of nociception in mice. Nociception was decreased in SGIP1$^{-/-}$ mice compared to WT mice. Both SGIP1$^{-/-}$ males

and females responded more strongly to the CB1R full agonist (WIN) antinociceptive effects. However, when THC, which is only a partial CB1R agonist, was administered, this enhancement of antinociception was only observed in SGIP1$^{-/-}$ males.

The very strong antinociception caused by WIN administration in SGIP1$^{-/-}$ mice suggests more than an additive effect of the WIN effect and the altered genotype. A study from our laboratory showed that WIN causes a more increased β-arrestin 2 association with CB1R and more profound CB1R-mediated inhibition of ERK1/2 than 2-AG in CB1R and SGIP1 expressing cells (Hajkova et al., 2016). Therefore, we hypothesize that when the CB1R stimulation is mild, the effect of SGIP1 on this receptor is only slight; however, it increases when CB1R is strongly activated.

Co-administration of THC and morphine enhances the antinociceptive effects of morphine, even when THC is administered at a dose that itself does not provide a measurable effect (Cichewicz, 2004; Smith et al., 1998). Jumping, as a manifestation of THC withdrawal in SGIP1$^{-/-}$ mice, suggested a possible involvement of SGIP1 in the regulation of opioid signaling. The antinociceptive effects of morphine were therefore tested in mice. SGIP1$^{-/-}$ mice responded more strongly to administered morphine, supporting our hypothesis of an enhanced endocannabinoid signaling in these mice. This observation also supports findings of the cooperation of cannabinoid and opioid systems.

Short-term effect of a CB1R antagonist on nociception in SGIP1$^{-/-}$ mice

The CB1R inverse agonist (rimonabant) effect on nociception was tested in SGIP1$^{-/-}$ and WT mice to confirm the SGIP1 modulation of CB1R. Some studies show that administration of rimonabant to mice or rats causes increased nociception (Costa and Colleoni, 1999; Meng et al., 1998; Richardson et al., 1998). Other studies have shown no effect of rimonabant on nociception (Compton et al., 1996; Rinaldi-Carmona et al., 1994).

In our experiments, no effect of rimonabant on nociception in WT mice was observed. However, increased nociception was observed in SGIP1$^{-/-}$ mice 30 min after rimonabant administration compared to mice injected with vehicle alone. This change was no longer observable 60 minutes after rimonabant injection or on the third day of rimonabant administration. Based on our study results in HEK293 cells (Hajkova et al.,

2016), we conclude that SGIP1 acts in the early stages of endocytosis of activated CB1R. Therefore, it is possible that the inverse agonist effect is manifested only within a short time after its administration.

SGIP1$^{-/-}$ mice have normal body weight

Elevated SGIP1 mRNA levels have been described in gerbils with increased body weight (Trevaskis et al., 2005; Walder et al., 2000). A correlation between specific single nucleotide polymorphic mutations in the SGIP1 gene and an increased percentage of body fat has also been described in humans, more specifically in Mauritius's population (Cummings et al., 2012). Experimental reductions in SGIP1 mRNA levels in gerbils and rats reduce food intake and weight in these animals (Trevaskis et al., 2005). We expected that deletion of the SGIP1 gene could lead to a decrease in the weight of SGIP1$^{-/-}$ mice. This hypothesis was not confirmed; SGIP1$^{-/-}$ mice had body weight comparable to that of WT mice. Since SGIP1$^{-/-}$ mice are developmental knockouts, i.e., the gene for SGIP1 is deleted in the embryonic stage of their development, compensatory mechanisms may occur, replacing the action of SGIP1 on energy homeostasis.

6. CONCLUSIONS

CB1R and SGIP1 partially colocalize in the synaptic parts of neurons. Their protein-protein interaction was demonstrated in this work by immunoprecipitation from mouse brains. We have shown that SGIP1 interferes with the internalization of activated CB1R and modulates its downstream signaling in mammalian cell tissue cultures (Hajkova et al., 2016).

The effect of SGIP1 on CB1R signaling is also demonstrated in neurons here. We described the SGIP1 modulation of CB1R signaling in autaptic hippocampal neurons by electrophysiological approach. We used cultured neurons from mice with deleted SGIP1 and compared their signaling properties to WT neurons. The absence of SGIP1 causes a reduction in CB1R-mediated DSE.

Changes in CB1R signaling affect mouse behavior. We investigated the effect of SGIP1 deletion on mouse behavior experimentally by comparing SGIP1$^{-/-}$ mice with WT mice. Cognitive functions, such as short-term memory and sensorimotor learning, were not impaired by SGIP1 deletion. However, SGIP1$^{-/-}$ mice showed decreased anxiety-like behavior and coped better with an unescapable situation, while their fear conditioning remained intact. In SGIP1$^{-/-}$ females, an accelerated extinction of aversive memory occurred compared to WT females. Also, we observed changes in cannabinoid tetrad in SGIP1$^{-/-}$ mice, also stronger withdrawal symptoms were particularly noticeable in these mice. This phenotype may result from increased ECS activity or deregulation of CB1R signaling. Contrary to expectations, mouse body weight was not affected by SGIP1 deletion.

Both males and females SGIP1$^{-/-}$ had a significantly increased pain threshold and were more responsive to cannabinoids and morphine's antinociceptive effects.

Our results suggest that behavior in WT mice is affected by SGIP1 through its action on CB1R. CB1R signaling and its modulation by SGIP1 likely differ in various brain regions and different types of neurons. In the future, it would therefore be appropriate to focus on the study of SGIP1 function in specific parts of the brain and individual types of neurons. Due to the high-level SGIP1 expression in the brain, we

cannot rule out that SGIP1 also affects other proteins and receptors. This possibility should also be explored.

This work contributes to the understanding of the SGIP1 function. Our results point out the critical role of SGIP1 in the regulation of CB1R-mediated signaling. Our studies may be of importance in the development of drugs that act on CB1R, especially in pain management.

SUMMARY

The signaling of cannabinoid receptor 1 (CB1R) is influenced by its interaction with Src homology 3-domain growth factor receptor-bound 2-like (endophilin) interacting protein 1 (SGIP1). Both proteins are highly expressed in the brain, especially in neuronal synaptic terminals. SGIP1 hinders the endocytosis of activated CB1R. As a consequence of which the influence of SGIP1 leads to biased signaling of CB1R. The deletion of SGIP1 enhances the association of CB1R with arrestin, decreases the phosphorylation of extracellular signal-regulated kinases 1 and 2 (ERK1/2), whereas G-protein signaling is not influenced by the presence of SGIP1.

The deletion of SGIP1 has an effect on CB1R signaling in neurons. The lack of SGIP1 leads to changes in CB1R mediated synaptic plasticity in hippocampal neurons.

The changes in endocannabinoid signaling also influence physiological processes controlled by this signaling system. Mice with constitutive deletion of SGIP1 ($SGIP1^{-/-}$) were used to study the influence of SGIP1 on CB1R related behavior. The exploratory levels, working memory and sensorimotor gating was not altered in these mice. However, $SGIP1^{-/-}$ mice have decreased anxiety-like behaviors, and they cope better with despair situations than WT mice. The reactions to Δ^9-tetrahydrocannabinol (THC) were enhanced in $SGIP1^{-/-}$ mice and also jumping was detected as an unusual THC withdrawal symptom in these mice. Last but not least, SGIP1 deletion leads to decreased acute nociception and higher sensitivity to analgesics administration.

Observing the changes in the behavior of $SGIP1^{-/-}$ mice brings a piece of information about the effect of SGIP1 on cannabinoid signaling and its impact *in vivo*. This knowledge can serve as a basis for the development of new kinds of drugs acting on CB1R. The application of our data for the research in pain treatment seems very promising.

SOUHRN

Signalizace kanabinoidního receptoru 1 (CB1R) je ovlivněna interakcí se Src homology 3-domain growth factor receptor-bound 2-like (endophilin) interacting protein 1 (SGIP1). Oba proteiny jsou exprimovány v mozku v relativně velkých množstvích, a jsou lokalizovány především v presynaptických částech neuronů. SGIP1 zabraňuje endocytose aktivovaného CB1R. V důsledku toho dochází vlivem působení SGIP1 k odlišné funkčně selektivní signalizaci CB1R. V přítomnosti SGIP1 dochází ke zvýšení asociace s arrestinem, fosforylace extraculárním signálem regulovaných kinas 1 a 2 (ERK1/2) je snížena, zatímco G-proteinová signalizace je v přítomnosti SGIP1 nezměněna.

Delece SGIP1 mění signalizaci CB1R v synapsích. Nepřítomnost SGIP1 způsobuje v hipokampálních neuronech změny v synaptické plasticitě kontrolované CB1R.

Změny v endokanabinoidní signalizaci mají vliv na fyziologické procesy kontrolované tímto signalizačním systémem. Myši s konstitutivní delecí SGIP1 (SGIP1$^{-/-}$) byly využity ke studiu vlivu SGIP1 na chování spojené s CB1R. Míra zkoumání prostředí, krátkodobá paměť a senzomotorické učení nejsou u těchto myší pozměněny. Myši SGIP1$^{-/-}$ jsou méně úzkostlivé a lépe se vyrovnávají s bezvýchodnou situací než myši bez genetické modifikace (WT). Reakce na Δ^9-tetrahydrokanabinol (THC) byly u myší SGIP1$^{-/-}$ posíleny a také u nich bylo zaznamenáno neobvyklé skákání jako projev závislosti na THC. V neposlední řadě delece SGIP1 způsobuje snížení akutní nocicepce a větší citlivost na podávání látek s analgetickými účinky.

Pozorování změn v chování u myší SGIP1$^{-/-}$ nám umožnilo pozorovat důsledky ovlivnění CB1R proteinem SGIP1 a jeho vliv na endokanabinoidní signalizaci *in vivo*. Tyto poznatky mohou sloužit jako výchozí informace pro nové postupy ve vývoji léků působících na CB1R. Velmi slibnou může být například aplikace námi získaných poznatků při vývoji nových postupů pro zvládání bolestivých stavů.

REFERENCES

1. Alberts, B., Bray, D., Hopkin, K., Johnson, A., Lewis, J., Raff, M., Roberts, K., Walter, P., 2014. Essential Cell Biology, 4th ed. Garland Science.
2. Arensdorf, A.M., Marada, S., Ogden, S.K., 2016. Smoothened Regulation: A Tale of Two Signals. Trends. Pharmacol. Sci. 37, 62-72.
3. Badowski, M.E., Yanful, P.K., 2018. Dronabinol oral solution in the management of anorexia and weight loss in AIDS and cancer. Ther. Clin. Risk Manag. 14, 643-651.
4. Begg, M., Pacher, P., Batkai, S., Osei-Hyiaman, D., Offertaler, L., Mo, F.M., Liu, H., Kunos, G., 2005. Evidence for novel cannabinoid receptors. Pharmacol. Therapeut. 106, 133-145.
5. Bekkers, J.M., Stevens, C.F., 1991. Excitatory and inhibitory autaptic currents in isolated hippocampal neurons maintained in cell culture. Proc. Natl. Acad. Sci. U. S. A. 88, 7834-7838.
6. Berg, K.A., Clarke, W.P., 2018. Making Sense of Pharmacology: Inverse Agonism and Functional Selectivity. Int. J. Neuropsychoph. 21, 962-977.
7. Birling, M.C., Dierich, A., Jacquot, S., Herault, Y., Pavlovic, G., 2012. Highly-efficient, fluorescent, locus directed cre and FlpO deleter mice on a pure C57BL/6N genetic background. Genesis 50, 482-489.
8. Biscaia, M., Marin, S., Fernandez, B., Marco, E.M., Rubio, M., Guaza, C., Ambrosio, E., Viveros, M.P., 2003. Chronic treatment with CP 55,940 during the peri-adolescent period differentially affects the behavioural responses of male and female rats in adulthood. Psychopharmacology (Berl) 170, 301-308.
9. Black, S.C., 2004. Cannabinoid receptor antagonists and obesity. Curr. Opin. Investig. Drugs 5, 389-394.
10. Blume, L.C., Leone-Kabler, S., Luessen, D.J., Marrs, G.S., Lyons, E., Bass, C.E., Chen, R., Selley, D.E., Howlett, A.C., 2016. Cannabinoid receptor interacting protein suppresses agonist-driven CB1 receptor internalization and regulates receptor replenishment in an agonist-biased manner. J. Neurochem. 139, 396-407.
11. Blume, L.C., Patten, T., Eldeeb, K., Leone-Kabler, S., Ilyasov, A.A., Keegan, B.M., O'Neal, J.E., Bass, C.E., Hantgan, R.R., Lowther, W.T., Selley, D.E., Howlett, A.C., 2017. Cannabinoid Receptor Interacting Protein 1a Competition with beta-Arrestin for CB1 Receptor Binding Sites. Mol. Pharmacol. 91, 75-86.
12. Boeuf, J., Trigo, J.M., Moreau, P.H., Lecourtier, L., Vogel, E., Cassel, J.C., Mathis, C., Klosen, P., Maldonado, R., Simonin, F., 2009. Attenuated behavioural responses to acute and chronic cocaine in GASP-1-deficient mice. Eur. J. Neurosci. 30, 860-868.
13. Bohn, L.M., Lefkowitz, R.J., Gainetdinov, R.R., Peppel, K., Caron, M.G., Lin, F.T., 1999. Enhanced morphine analgesia in mice lacking beta-arrestin 2. Science 286, 2495-2498.
14. Bortolato, M., Mangieri, R.A., Fu, J., Kim, J.H., Arguello, O., Duranti, A., Tontini, A., Mor, M., Tarzia, G., Piomelli, D., 2007. Antidepressant-like activity of the fatty acid amide hydrolase inhibitor URB597 in a rat model of chronic mild stress. Biol. Psychiatry 62, 1103-1110.
15. Bossong, M.G., Jager, G., Bhattacharyya, S., Allen, P., 2014. Acute and Non-acute Effects of Cannabis on Human Memory Function: A Critical Review of Neuroimaging Studies. Curr. Pharm. Design 20, 2114-2125.

16. Bradshaw, H.B., Rimmerman, N., Krey, J.F., Walker, J.M., 2006. Sex and hormonal cycle differences in rat brain levels of pain-related cannabimimetic lipid mediators. Am. J. Physiol. Regul. Integr. Comp. Physiol. 291, R349-358.
17. Breivogel, C.S., Lambert, J.M., Gerfin, S., Huffman, J.W., Razdan, R.K., 2008. Sensitivity to delta9-tetrahydrocannabinol is selectively enhanced in beta-arrestin2 -/- mice. Behavioural pharmacology 19, 298-307.
18. Burack, W.R., Shaw, A.S., 2000. Signal transduction: hanging on a scaffold. Curr. Opin. Cell Biol. 12, 211-216.
19. Busquets-Garcia, A., Desprez, T., Metna-Laurent, M., Bellocchio, L., Marsicano, G., Soria-Gomez, E., 2015. Dissecting the cannabinergic control of behavior: The where matters. Bioessays 37, 1215-1225.
20. Calebiro, D., Godbole, A., 2018. Internalization of G-protein-coupled receptors: Implication in receptor function, physiology and diseases. Best. Pract. Res. Cl. En. 32, 83-91.
21. Castillo, P.E., Younts, T.J., Chavez, A.E., Hashimotodani, Y., 2012. Endocannabinoid Signaling and Synaptic Function. Neuron 76, 70-81.
22. Cichewicz, D.L., 2004. Synergistic interactions between cannabinoid and opioid analgesics. Life Sci. 74, 1317-1324.
23. Clark, J.W., Drummond, S.P.A., Hoyer, D., Jacobson, L.H., 2019. Sex differences in mouse models of fear inhibition: Fear extinction, safety learning, and fear-safety discrimination. Br. J. Pharmacol.
24. Colombo, G., Agabio, R., Diaz, G., Lobina, C., Reali, R., Gessa, G.L., 1998. Appetite suppression and weight loss after the cannabinoid antagonist SR 141716. Life sciences 63, PL113-117.
25. Compton, D.R., Aceto, M.D., Lowe, J., Martin, B.R., 1996. In vivo characterization of a specific cannabinoid receptor antagonist (SR141716A): inhibition of delta 9-tetrahydrocannabinol-induced responses and apparent agonist activity. J. Pharmacol. Exp. Ther. 277, 586-594.
26. Cooper, Z.D., Craft, R.M., 2018. Sex-Dependent Effects of Cannabis and Cannabinoids: A Translational Perspective. Neuropsychopharmacology 43, 34-51.
27. Costa, B., Colleoni, M., 1999. SR141716A induces in rats a behavioral pattern opposite to that of CB1 receptor agonists. Zhongguo Yao Li Xue Bao 20, 1103-1108.
28. Craft, R.M., Leitl, M.D., 2008. Gonadal hormone modulation of the behavioral effects of Delta9-tetrahydrocannabinol in male and female rats. Eur. J. Pharmacol. 578, 37-42.
29. Craft, R.M., Marusich, J.A., Wiley, J.L., 2013. Sex differences in cannabinoid pharmacology: a reflection of differences in the endocannabinoid system? Life Sci. 92, 476-481.
30. Cummings, N., Shields, K.A., Curran, J.E., Bozaoglu, K., Trevaskis, J., Gluschenko, K., Cai, G., Comuzzie, A.G., Dyer, T.D., Walder, K.R., Zimmet, P., Collier, G.R., Blangero, J., Jowett, J.B., 2012. Genetic variation in SH3-domain GRB2-like (endophilin)-interacting protein 1 has a major impact on fat mass. Int. J. Obes. (Lond) 36, 201-206.
31. Daigle, T.L., Kearn, C.S., Mackie, K., 2008a. Rapid CB1 cannabinoid receptor desensitization defines the time course of ERK1/2 MAP kinase signaling. Neuropharmacology 54, 36-44.

32. Daigle, T.L., Kwok, M.L., Mackie, K., 2008b. Regulation of CB1 cannabinoid receptor internalization by a promiscuous phosphorylation-dependent mechanism. J. Neurochem. 106, 70-82.
33. Danandeh, A., Vozella, V., Lim, J., Oveisi, F., Ramirez, G.L., Mears, D., Wynn, G., Piomelli, D., 2018. Effects of fatty acid amide hydrolase inhibitor URB597 in a rat model of trauma-induced long-term anxiety. Psychopharmacology (Berl) 235, 3211-3221.
34. de Jesus, M.L., Salles, J., Meana, J.J., Callado, L.F., 2006. Characterization of CB1 cannabinoid receptor immunoreactivity in postmortem human brain homogenates. Neuroscience 140, 635-643.
35. de Oliveira, P.G., Ramos, M.L.S., Amaro, A.J., Dias, R.A., Vieira, S.I., 2019. Gi/o-Protein Coupled Receptors in the Aging Brain. Front. Aging. Neurosci. 11, 89.
36. Delgado-Peraza, F., Ahn, K.H., Nogueras-Ortiz, C., Mungrue, I.N., Mackie, K., Kendall, D.A., Yudowski, G.A., 2016. Mechanisms of Biased beta-Arrestin-Mediated Signaling Downstream from the Cannabinoid 1 Receptor. Mol. Pharmacol. 89, 618-629.
37. Delom, F., Fessart, D., 2011. Role of Phosphorylation in the Control of Clathrin-Mediated Internalization of GPCR. Int. J. Cell. Biol. 2011, 246954.
38. Devane, W.A., Hanus, L., Breuer, A., Pertwee, R.G., Stevenson, L.A., Griffin, G., Gibson, D., Mandelbaum, A., Etinger, A., Mechoulam, R., 1992. Isolation and Structure of a Brain Constituent That Binds to the Cannabinoid Receptor. Science 258, 1946-1949.
39. DeWire, S.M., Ahn, S., Lefkowitz, R.J., Shenoy, S.K., 2007. Beta-arrestins and cell signaling. Annu. Rev. Physiol. 69, 483-510.
40. Di Marzo, V., Bifulco, M., De Petrocellis, L., 2004. The endocannabinoid system and its therapeutic exploitation. Nat. Rev. Drug Discov. 3, 771-784.
41. Di Marzo, V., Matias, I., 2005. Endocannabinoid control of food intake and energy balance. Nat. Neurosci. 8, 585-589.
42. Dickinson, M.E., Flenniken, A.M., Ji, X., Teboul, L., Wong, M.D., White, J.K., Meehan, T.F., Weninger, W.J., Westerberg, H., Adissu, H., Baker, C.N., Bower, L., Brown, J.M., Caddle, L.B., Chiani, F., Clary, D., Cleak, J., Daly, M.J., Denegre, J.M., Doe, B., Dolan, M.E., Edie, S.M., Fuchs, H., Gailus-Durner, V., Galli, A., Gambadoro, A., Gallegos, J., Guo, S., Horner, N.R., Hsu, C.W., Johnson, S.J., Kalaga, S., Keith, L.C., Lanoue, L., Lawson, T.N., Lek, M., Mark, M., Marschall, S., Mason, J., McElwee, M.L., Newbigging, S., Nutter, L.M., Peterson, K.A., Ramirez-Solis, R., Rowland, D.J., Ryder, E., Samocha, K.E., Seavitt, J.R., Selloum, M., Szoke-Kovacs, Z., Tamura, M., Trainor, A.G., Tudose, I., Wakana, S., Warren, J., Wendling, O., West, D.B., Wong, L., Yoshiki, A., International Mouse Phenotyping, C., Jackson, L., Infrastructure Nationale Phenomin, I.C.d.l.S., Charles River, L., Harwell, M.R.C., Toronto Centre for, P., Wellcome Trust Sanger, I., Center, R.B., MacArthur, D.G., Tocchini-Valentini, G.P., Gao, X., Flicek, P., Bradley, A., Skarnes, W.C., Justice, M.J., Parkinson, H.E., Moore, M., Wells, S., Braun, R.E., Svenson, K.L., de Angelis, M.H., Herault, Y., Mohun, T., Mallon, A.M., Henkelman, R.M., Brown, S.D., Adams, D.J., Lloyd, K.C., McKerlie, C., Beaudet, A.L., Bucan, M., Murray, S.A., 2016. High-throughput discovery of novel developmental phenotypes. Nature 537, 508-514.

43. Farrens, D.L., Altenbach, C., Yang, K., Hubbell, W.L., Khorana, H.G., 1996. Requirement of rigid-body motion of transmembrane helices for light activation of rhodopsin. Science 274, 768-770.
44. Fattore, L., Fratta, W., 2010. How important are sex differences in cannabinoid action? Br. J. Pharmacol. 160, 544-548.
45. Fields, H.L., Heinricher, M.M., Mason, P., 1991. Neurotransmitters in Nociceptive Modulatory Circuits. Annu. Rev. Neurosci. 14, 219-245.
46. Fletcher-Jones, A., Hildick, K.L., Evans, A.J., Nakamura, Y., Henley, J.M., Wilkinson, K.A., 2020. Protein Interactors and Trafficking Pathways That Regulate the Cannabinoid Type 1 Receptor (CB1R). Front. Mol. Neurosci. 13, 108.
47. Fletcher-Jones, A., Hildick, K.L., Evans, A.J., Nakamura, Y., Wilkinson, K.A., Henley, J.M., 2019. The C-terminal helix 9 motif in rat cannabinoid receptor type 1 regulates axonal trafficking and surface expression. Elife 8.
48. Ford, B.M., Cabanlong, C.V., Tai, S., Franks, L.N., Penthala, N.R., Crooks, P.A., Prather, P.L., Fantegrossi, W.E., 2019. Reduced Tolerance and Asymmetrical Crosstolerance to Effects of the Indole Quinuclidinone Analog PNR-4-20, a G Protein-Biased Cannabinoid 1 Receptor Agonist in Mice: Comparisons with Delta(9)-Tetrahydrocannabinol and JWH-018. J. Pharmacol. Exp. Ther. 369, 259-269.
49. Francis, D.L., Schneider, C., 1971. Jumping after Naloxone Precipitated Withdrawal of Chronic Morphine in Rat. Br. J. Pharmacol. 41, P424-+.
50. Fredriksson, R., Lagerstrom, M.C., Lundin, L.G., Schioth, H.B., 2003. The G-protein-coupled receptors in the human genome form five main families. Phylogenetic analysis, paralogon groups, and fingerprints. Mol. Pharmacol. 63, 1256-1272.
51. Freund, T.F., Katona, I., Piomelli, D., 2003. Role of endogenous cannabinoids in synaptic signaling. Physiol. Rev. 83, 1017-1066.
52. Frost, A., Perera, R., Roux, A., Spasov, K., Destaing, O., Egelman, E.H., De Camilli, P., Unger, V.M., 2008. Structural basis of membrane invagination by F-BAR domains. Cell 132, 807-817.
53. Furshpan, E.J., MacLeish, P.R., O'Lague, P.H., Potter, D.D., 1976. Chemical transmission between rat sympathetic neurons and cardiac myocytes developing in microcultures: evidence for cholinergic, adrenergic, and dual-function neurons. Proc. Natl. Acad. Sci. U. S. A. 73, 4225-4229.
54. Gainetdinov, R.R., Premont, R.T., Bohn, L.M., Lefkowitz, R.J., Caron, M.G., 2004. Desensitization of G protein-coupled receptors and neuronal functions. Annu. Rev. Neurosci. 27, 107-144.
55. Gether, U., Kobilka, B.K., 1998. G protein-coupled receptors - II. Mechanism of agonist activation. J. Biol. Chem. 273, 17979-17982.
56. Glass, M., Faull, R.L.M., Dragunow, M., 1993. Loss of Cannabinoid Receptors in the Substantia-Nigra in Huntingtons-Disease. Neuroscience 56, 523-527.
57. Guggenhuber, S., Alpar, A., Chen, R.Q., Schmitz, N., Wickert, M., Mattheus, T., Harasta, A.E., Purrio, M., Kaiser, N., Elphick, M.R., Monory, K., Kilb, W., Luhmann, H.J., Harkany, T., Lutz, B., Klugmann, M., 2016. Cannabinoid receptor-interacting protein Crip1a modulates CB1 receptor signaling in mouse hippocampus. Brain Struct. Funct. 221, 2061-2074.
58. Hajkova, A., Techlovska, S., Dvorakova, M., Chambers, J.N., Kumpost, J., Hubalkova, P., Prezeau, L., Blahos, J., 2016. SGIP1 alters internalization and

modulates signaling of activated cannabinoid receptor 1 in a biased manner. Neuropharmacology 107, 201-214.
59. Haller, J., Bakos, N., Szirmay, M., Ledent, C., Freund, T.F., 2002. The effects of genetic and pharmacological blockade of the CB1 cannabinoid receptor on anxiety. Eur. J. Neurosci. 16, 1395-1398.
60. Hamdan, F.F., Rochdi, M.D., Breton, B., Fessart, D., Michaud, D.E., Charest, P.G., Laporte, S.A., Bouvier, M., 2007. Unraveling G protein-coupled receptor endocytosis pathways using real-time monitoring of agonist-promoted interaction between beta-arrestins and AP-2. J. Biol. Chem. 282, 29089-29100.
61. Hampson, R.E., Deadwyler, S.A., 2000. Cannabinoids reveal the necessity of hippocampal neural encoding for short-term memory in rats. J. Neurosci. 20, 8932-8942.
62. Han, J., Kesner, P., Metna-Laurent, M., Duan, T.T., Xu, L., Georges, F., Koehl, M., Abrous, D.N., Mendizabal-Zubiaga, J., Grandes, P., Liu, Q.S., Bai, G., Wang, W., Xiong, L.Z., Ren, W., Marsicano, G., Zhang, X., 2012. Acute Cannabinoids Impair Working Memory through Astroglial CB1 Receptor Modulation of Hippocampal LTD. Cell 148, 1039-1050.
63. Hao, S., Avraham, Y., Mechoulam, R., Berry, E.M., 2000. Low dose anandamide affects food intake, cognitive function, neurotransmitter and corticosterone levels in diet-restricted mice. Eur. J. Pharmacol. 392, 147-156.
64. Hasanein, P., Parviz, M., Keshavarz, M., Javanmardi, K., 2007. CB1 receptor activation in the basolateral amygdala produces antinociception in animal models of acute and tonic nociception. Clinical and experimental pharmacology & physiology 34, 439-449.
65. Hebbali, A., 2020. Olsrr: Tools for Building OLS Regression Models. R package version 0.5.3. https://CRAN.R-project.org/package=olsrr.
66. Henne, W.M., Boucrot, E., Meinecke, M., Evergren, E., Vallis, Y., Mittal, R., McMahon, H.T., 2010. FCHo Proteins Are Nucleators of Clathrin-Mediated Endocytosis. Science 328, 1281-1284.
67. Herkenham, M., Lynn, A.B., Little, M.D., Johnson, M.R., Melvin, L.S., Decosta, B.R., Rice, K.C., 1990. Cannabinoid Receptor Localization in Brain. Proc. Natl. Acad. Sci. U. S. A. 87, 1932-1936.
68. Hoefer, S.I., 1994. Protein electrophoresis applications guide.
69. Hojo, M., Sudo, Y., Ando, Y., Minami, K., Takada, M., Matsubara, T., Kanaide, M., Taniyama, K., Sumikawa, K., Uezono, Y., 2008. mu-Opioid receptor forms a functional heterodimer with cannabinoid CB1 receptor: electrophysiological and FRET assay analysis. J. Pharmacol. Sci. 108, 308-319.
70. Hollister, L.E., 1986. Health-Aspects of Cannabis. Pharmacological reviews 38, 1-20.
71. Hollopeter, G., Lange, J.J., Zhang, Y., Vu, T.N., Gu, M.Y., Ailion, M., Lambie, E.J., Slaughter, B.D., Unruh, J.R., Florens, L., Jorgensen, E.M., 2014. The Membrane-Associated Proteins FCHo and SGIP Are Allosteric Activators of the AP2 Clathrin Adaptor Complex. Elife 3, 65.
72. Howlett, A.C., Barth, F., Bonner, T.I., Cabral, G., Casellas, P., Devane, W.A., Felder, C.C., Herkenham, M., Mackie, K., Martin, B.R., Mechoulam, R., Pertwee, R.G., 2002. International Union of Pharmacology. XXVII. Classification of cannabinoid receptors. Pharmacological reviews 54, 161-202.

73. Howlett, A.C., Breivogel, C.S., Childers, S.R., Deadwyler, S.A., Hampson, R.E., Porrino, L.J., 2004. Cannabinoid physiology and pharmacology: 30 years of progress. Neuropharmacology 47 Suppl 1, 345-358.
74. Howlett, A.C., Champion, T.M., Wilken, G.H., Mechoulam, R., 1990. Stereochemical effects of 11-OH-delta 8-tetrahydrocannabinol-dimethylheptyl to inhibit adenylate cyclase and bind to the cannabinoid receptor. Neuropharmacology 29, 161-165.
75. Hughes, R.N., 2004. The value of spontaneous alternation behavior (SAB) as a test of retention in pharmacological investigations of memory. Neuroscience and biobehavioral reviews 28, 497-505.
76. Chaperon, F., Thiebot, M.H., 1999. Behavioral effects of cannabinoid agents in animals. Crit. Rev. Neurobiol. 13, 243-281.
77. Childers, S.R., Deadwyler, S.A., 1996. Role of cyclic AMP in the actions of cannabinoid receptors. Biochem. Pharmacol. 52, 819-827.
78. Choleris, E., Thomas, A.W., Kavaliers, M., Prato, F.S., 2001. A detailed ethological analysis of the mouse open field test: effects of diazepam, chlordiazepoxide and an extremely low frequency pulsed magnetic field. Neuroscience and Biobehavioral Reviews 25, 235-260.
79. Christopoulou, F.D., Kiortsis, D.N., 2011. An overview of the metabolic effects of rimonabant in randomized controlled trials: potential for other cannabinoid 1 receptor blockers in obesity. J. Clin. Pharm. Ther. 36, 10-18.
80. Jenniches, I., Ternes, S., Albayram, O., Otte, D.M., Bach, K., Bindila, L., Michel, K., Lutz, B., Bilkei-Gorzo, A., Zimmer, A., 2016. Anxiety, Stress, and Fear Response in Mice With Reduced Endocannabinoid Levels. Biol. Psychiatry 79, 858-868.
81. Jin, W., Brown, S., Roche, J.P., Hsieh, C., Celver, J.P., Kovoor, A., Chavkin, C., Mackie, K., 1999. Distinct domains of the CB1 cannabinoid receptor mediate desensitization and internalization. J. Neurosci. 19, 3773-3780.
82. Kano, M., Ohno-Shosaku, T., Hashimotodani, Y., Uchigashima, M., Watanabe, M., 2009. Endocannabinoid-Mediated Control of Synaptic Transmission. Physiol. Rev. 89, 309-380.
83. Kathuria, S., Gaetani, S., Fegley, D., Valino, F., Duranti, A., Tontini, A., Mor, M., Tarzia, G., La Rana, G., Calignano, A., Giustino, A., Tattoli, M., Palmery, M., Cuomo, V., Piomelli, D., 2003. Modulation of anxiety through blockade of anandamide hydrolysis. Nat. Med. 9, 76-81.
84. Kelly, E., Bailey, C.P., Henderson, G., 2008. Agonist-selective mechanisms of GPCR desensitization. Br. J. Pharmacol. 153 Suppl 1, S379-388.
85. Kishimoto, Y., Kano, M., 2006. Endogenous cannabinoid signaling through the CB1 receptor is essential for cerebellum-dependent discrete motor learning. J. Neurosci. 26, 8829-8837.
86. Kolakowski, L.F., 1994. Gcrdb - a G-Protein-Coupled Receptor Database. Receptor Channel 2, 1-7.
87. Komsta, L., Novomestsky, F., 2015. Moments: Moments, cumulants, skewness, kurtosis and related tests. R package version 0.14. https://CRAN.R-project.org/package=moments.
88. Kreitzer, A.C., Regehr, W.G., 2001. Retrograde inhibition of presynaptic calcium influx by endogenous cannabinoids at excitatory synapses onto Purkinje cells. Neuron 29, 717-727.

89. Laprairie, R.B., Bagher, A.M., Kelly, M.E., Denovan-Wright, E.M., 2015. Cannabidiol is a negative allosteric modulator of the cannabinoid CB1 receptor. Br. J. Pharmacol. 172, 4790-4805.
90. Ledent, C., Valverde, O., Cossu, C., Petitet, F., Aubert, L.F., Beslot, F., Bohme, G.A., Imperato, A., Pedrazzini, T., Roques, B.P., Vassart, G., Fratta, W., Parmentier, M., 1999. Unresponsiveness to cannabinoids and reduced addictive effects of opiates in CB1 receptor knockout mice. Science 283, 401-404.
91. LeDoux, J.E., 2000. Emotion circuits in the brain. Ann. Rev. Neurosci. 23, 155-184.
92. Leterrier, C., Laine, J., Darmon, M., Boudin, H., Rossier, J., Lenkei, Z., 2006. Constitutive activation drives compartment-selective endocytosis and axonal targeting of type 1 cannabinoid receptors. J. Neurosci. 26, 3141-3153.
93. Levison, S.W., McCarthy, K.D., 1991. Characterization and partial purification of AIM: a plasma protein that induces rat cerebral type 2 astroglia from bipotential glial progenitors. J. Neurochem. 57, 782-794.
94. Li, A.L., Carey, L.M., Mackie, K., Hohmann, A.G., 2017. Cannabinoid CB2 Agonist GW405833 Suppresses Inflammatory and Neuropathic Pain through a CB1 Mechanism that is Independent of CB2 Receptors in Mice. Journal of Pharmacology and Experimental Therapeutics 362, 296-305.
95. Liggett, S.B., 2011. Phosphorylation barcoding as a mechanism of directing GPCR signaling. Sci. Signal. 4, pe36.
96. Ligresti, A., De Petrocellis, L., Di Marzo, V., 2016. From Phytocannabinoids to Cannabinoid Receptors and Endocannabinoids: Pleiotropic Physiological and Pathological Roles through Complex Pharmacology. Physiol. Rev. 96, 1593-1659.
97. Lichtman, A.H., Dimen, K.R., Martin, B.R., 1995. Systemic or Intrahippocampal Cannabinoid Administration Impairs Spatial Memory in Rats. Psychopharmacology 119, 282-290.
98. Lister, R.G., 1987. The Use of a Plus-Maze to Measure Anxiety in the Mouse. Psychopharmacology 92, 180-185.
99. Lu, H.C., Mackie, K., 2016. An Introduction to the Endogenous Cannabinoid System. Biol. Psychiatry 79, 516-525.
100. Luttrell, L.M., 2008. Reviews in molecular biology and biotechnology: Transmembrane signaling by G protein-coupled receptors. Mol. Biotechnol. 39, 239-264.
101. Luttrell, L.M., Gesty-Palmer, D., 2010. Beyond Desensitization: Physiological Relevance of Arrestin-Dependent Signaling. Pharmacological reviews 62, 305-330.
102. Lutz, B., Marsicano, G., Maldonado, R., Hillard, C.J., 2015. The endocannabinoid system in guarding against fear, anxiety and stress. Nat. Rev. Neurosci. 16, 705-718.
103. MacDonald, B.T., He, X., 2012. Frizzled and LRP5/6 Receptors for Wnt/ -Catenin Signaling. Cold Spring Harbor Perspectives in Biology 4, a007880-a007880.
104. Mackie, K., 2008. Signaling via CNS cannabinoid receptors. Mol. Cell. Endocrinol. 286, S60-S65.
105. Marco, E.M., Llorente, R., Moreno, E., Biscaia, J.M., Guaza, C., Viveros, M.P., 2006. Adolescent exposure to nicotine modifies acute functional responses to cannabinoid agonists in rats. Behav. Brain Res. 172, 46-53.
106. Marongiu, M.F., Poddie, D., Porcu, S., Manchinu, M.F., Castelli, M.P., Sogos, V., Bini, V., Frau, R., Caredda, E., Collu, M., Ristaldi, M.S., 2012. Reversible

disruption of pre-pulse inhibition in hypomorphic-inducible and reversible CB1-/- mice. Plos One 7, e35013.
107. Marsicano, G., Lafenetre, P., 2009. Roles of the Endocannabinoid System in Learning and Memory. Curr. Top. Behav. Neuro. 1, 201-230.
108. Marsicano, G., Wotjak, C.T., Azad, S.C., Bisogno, T., Rammes, G., Cascio, M.G., Hermann, H., Tang, J.R., Hofmann, C., Zieglgansberger, W., Di Marzo, V., Lutz, B., 2002. The endogenous cannabinoid system controls extinction of aversive memories. Nature 418, 530-534.
109. Martini, L., Thompson, D., Kharazia, V., Whistler, J.L., 2010. Differential Regulation of Behavioral Tolerance to WIN55,212-2 by GASP1. Neuropsychopharmacology 35, 1363-1373.
110. Martini, L., Waldhoer, M., Pusch, M., Kharazia, V., Fong, J., Lee, J.H., Freissmuth, C., Whistler, J.L., 2007. Ligand-induced down-regulation of the cannabinoid 1 receptor is mediated by the G-protein-coupled receptor-associated sorting protein GASP1. Faseb J. 21, 802-811.
111. Mascarenhas, D.C., Gomes, K.S., Sorregotti, T., Nunes-de-Souza, R.L., 2017. Blockade of Cannabinoid CB1 Receptors in the Dorsal Periaqueductal Gray Unmasks the Antinociceptive Effect of Local Injections of Anandamide in Mice. Front. Pharmacol. 8, 695.
112. Mascia, F., Klotz, L., Lerch, J., Ahmed, M.H., Zhang, Y., Enz, R., 2017. CRIP1a inhibits endocytosis of G-protein coupled receptors activated by endocannabinoids and glutamate by a common molecular mechanism. J. Neurochem. 141, 577-591.
113. McMahon, H.T., Boucrot, E., 2011. Molecular mechanism and physiological functions of clathrin-mediated endocytosis. Nat. Rev. Mol. Cell. Biol. 12, 517-533.
114. Mechoulam, R., Parker, L.A., 2013. The endocannabinoid system and the brain. Annu. Rev. Psychol. 64, 21-47.
115. Meng, I.D., Manning, B.H., Martin, W.J., Fields, H.L., 1998. An analgesia circuit activated by cannabinoids. Nature 395, 381-383.
116. Micale, V., Di Marzo, V., Sulcova, A., Wotjak, C.T., Drago, F., 2013. Endocannabinoid system and mood disorders: Priming a target for new therapies. Pharmacol. Therapeut. 138, 18-37.
117. Mikasova, L., Groc, L., Choquet, D., Manzoni, O.J., 2008. Altered surface trafficking of presynaptic cannabinoid type 1 receptor in and out synaptic terminals parallels receptor desensitization. Proc. Natl. Acad. Sci. U. S. A. 105, 18596-18601.
118. Mills, I.G., 2007. The interplay between clathrin-coated vesicles and cell signallinge. Semin. Cell. Dev. Biol. 18, 459-470.
119. Milner, B., Squire, L.R., Kandel, E.R., 1998. Cognitive neuroscience and the study of memory. Neuron 20, 445-468.
120. Moore, C.A., Milano, S.K., Benovic, J.L., 2007. Regulation of receptor trafficking by GRKs and arrestins. Annu. Rev. Physiol. 69, 451-482.
121. Moreira, F.A., Kaiser, N., Monory, K., Lutz, B., 2008. Reduced anxiety-like behaviour induced by genetic and pharmacological inhibition of the endocannabinoid-degrading enzyme fatty acid amide hydrolase (FAAH) is mediated by CB1 receptors. Neuropharmacology 54, 141-150.
122. Morena, M., Patel, S., Bains, J.S., Hill, M.N., 2016. Neurobiological Interactions Between Stress and the Endocannabinoid System. Neuropsychopharmacology 41, 80-102.

123. Morgan, D.J., Davis, B.J., Kearn, C.S., Marcus, D., Cook, A.J., Wager-Miller, J., Straiker, A., Myoga, M.H., Karduck, J., Leishman, E., Sim-Selley, L.J., Czyzyk, T.A., Bradshaw, H.B., Selley, D.E., Mackie, K., 2014. Mutation of Putative GRK Phosphorylation Sites in the Cannabinoid Receptor 1 (CB1R) Confers Resistance to Cannabinoid Tolerance and Hypersensitivity to Cannabinoids in Mice. J. Neurosci. 34, 5152-5163.
124. Mu, J., Zhuang, S.Y., Kirby, M.T., Hampson, R.E., Deadwyler, S.A., 1999. Cannabinoid receptors differentially modulate potassium A and D currents in hippocampal neurons in culture. Journal of Pharmacology and Experimental Therapeutics 291, 893-902.
125. Munro, S., Thomas, K.L., Abushaar, M., 1993. Molecular Characterization of a Peripheral Receptor for Cannabinoids. Nature 365, 61-65.
126. Navarro, M., Hernandez, E., Munoz, R.M., delArco, I., Villanua, M.A., Carrera, M.R.A., deFonseca, F.R., 1997. Acute administration of the CB1 cannabinoid receptor antagonist SR 141716A induces anxiety-like responses in the rat. Neuroreport 8, 491-496.
127. Nguyen, P.T., Schmid, C.L., Raehal, K.M., Selley, D.E., Bohn, L.M., Sim-Selley, L.J., 2012. beta-arrestin2 regulates cannabinoid CB1 receptor signaling and adaptation in a central nervous system region-dependent manner. Biol. Psychiatry 71, 714-724.
128. Niehaus, J.L., Liu, Y., Wallis, K.T., Egertova, M., Bhartur, S.G., Mukhopadhyay, S., Shi, S., He, H., Selley, D.E., Howlett, A.C., Elphick, M.R., Lewis, D.L., 2007. CB1 cannabinoid receptor activity is modulated by the cannabinoid receptor interacting protein CRIP 1a. Mol. Pharmacol. 72, 1557-1566.
129. Nyhus, E., Curran, T., 2010. Functional role of gamma and theta oscillations in episodic memory. Neurosci. Biobehav. Rev. 34, 1023-1035.
130. Oldham, W.M., Hamm, H.E., 2008. Heterotrimeric G protein activation by G-protein-coupled receptors. Nat. Rev. Mol. Cell. Biol. 9, 60-71.
131. Patel, S., Hill, M.N., Cheer, J.F., Wotjak, C.T., Holmes, A., 2017. The endocannabinoid system as a target for novel anxiolytic drugs. Neurosci. Biobehav. Rev. 76, 56-66.
132. Pertwee, R.G., 2001. Cannabinoid receptors and pain. Progress in Neurobiology 63, 569-611.
133. Pertwee, R.G., 2009. Emerging strategies for exploiting cannabinoid receptor agonists as medicines. Br. J. Pharmacol. 156, 397-411.
134. Pertwee, R.G., 2012. Targeting the endocannabinoid system with cannabinoid receptor agonists: pharmacological strategies and therapeutic possibilities. Philos. T. R. Soc. B. 367, 3353-3363.
135. Picone, R.P., Kendall, D.A., 2015. From the Bench, Toward the Clinic: Therapeutic Opportunities for Cannabinoid Receptor Modulation. Mol Endocrinol 29, 801-813.
136. Pierce, K.L., Premont, R.T., Lefkowitz, R.J., 2002. Seven-transmembrane receptors. Nat. Rev. Mol. Cell. Bio. 3, 639-650.
137. Pin, J.P., Galvez, T., Prezeau, L., 2003. Evolution, structure, and activation mechanism of family 3/C G-protein-coupled receptors. Pharmacol. Therapeut. 98, 325-354.
138. Piomelli, D., 2003. The molecular logic of endocannabinoid signalling. Nat. Rev. Neurosci. 4, 873-884.

139. Pisani, A., Fezza, F., Galati, S., Battista, N., Napolitano, S., Finazzi-Agro, A., Bernardi, G., Brusa, L., Pierantozzi, M., Stanzione, P., Maccarrone, M., 2005. High endogenous cannabinoid levels in the cerebrospinal fluid of untreated Parkinson's disease patients. Ann. Neurol. 57, 777-779.
140. Pitler, T.A., Alger, B.E., 1992. Postsynaptic Spike Firing Reduces Synaptic Gaba(a) Responses in Hippocampal Pyramidal Cells. J. Neurosci. 12, 4122-4132.
141. Porsolt, R.D., Le Pichon, M., Jalfre, M., 1977. Depression: a new animal model sensitive to antidepressant treatments. Nature 266, 730-732.
142. Rey, A.A., Purrio, M., Viveros, M.P., Lutz, B., 2012. Biphasic effects of cannabinoids in anxiety responses: CB1 and GABA(B) receptors in the balance of GABAergic and glutamatergic neurotransmission. Neuropsychopharmacology 37, 2624-2634.
143. Rice, A.S., 2001. Cannabinoids and pain. Curr. Opin. Investig. Drugs 2, 399-414.
144. Richardson, J.D., Aanonsen, L., Hargreaves, K.M., 1998. Hypoactivity of the spinal cannabinoid system results in NMDA-dependent hyperalgesia. J. Neurosci. 18, 451-457.
145. Rinaldi-Carmona, M., Barth, F., Heaulme, M., Shire, D., Calandra, B., Congy, C., Martinez, S., Maruani, J., Neliat, G., Caput, D., et al., 1994. SR141716A, a potent and selective antagonist of the brain cannabinoid receptor. FEBS Lett. 350, 240-244.
146. Robbe, D., Montgomery, S.M., Thome, A., Rueda-Orozco, P.E., McNaughton, B.L., Buzsaki, G., 2006. Cannabinoids reveal importance of spike timing coordination in hippocampal function. Nat. Neurosci. 9, 1526-1533.
147. Robledo, P., Berrendero, F., Ozaita, A., Maldonado, R., 2008. Advances in the field of cannabinoid--opioid cross-talk. Addict Biol 13, 213-224.
148. Rodriguez de Fonseca, F., Cebeira, M., Ramos, J.A., Martin, M., Fernandez-Ruiz, J.J., 1994. Cannabinoid receptors in rat brain areas: sexual differences, fluctuations during estrous cycle and changes after gonadectomy and sex steroid replacement. Life Sci. 54, 159-170.
149. Rowland, N.E., Mukherjee, M., Robertson, K., 2001. Effects of the cannabinoid receptor antagonist SR 141716, alone and in combination with dexfenfluramine or naloxone, on food intake in rats. Psychopharmacology 159, 111-116.
150. Rozenfeld, R., Devi, L.A., 2008. Regulation of CB1 cannabinoid receptor trafficking by the adaptor protein AP-3. Faseb J. 22, 2311-2322.
151. Rubino, T., Vigano, D., Premolil, F., Castiglioni, C., Bianchessi, S., Zippel, R., Parolaro, D., 2006. Changes in the expression of G protein-coupled receptor kinases and beta-arrestins in mouse brain during cannabinoid tolerance - A role for Ras-ERK cascade. Mol. Neurobiol. 33, 199-213.
152. Shafrir, E., Gutman, A., 1993. Psammomys obesus of the Jerusalem colony: a model for nutritionally induced, non-insulin-dependent diabetes. J. Basic Clin. Physiol. Pharmacol. 4, 83-99.
153. Shonesy, B.C., Bluett, R.J., Ramikie, T.S., Baldi, R., Hermanson, D.J., Kingsley, P.J., Marnett, L.J., Winder, D.G., Colbran, R.J., Patel, S., 2014. Genetic Disruption of 2-Arachidonoylglycerol Synthesis Reveals a Key Role for Endocannabinoid Signaling in Anxiety Modulation. Cell Rep. 9, 1644-1653.
154. Scheen, A.J., Paquot, N., 2009. Use of cannabinoid CB1 receptor antagonists for the treatment of metabolic disorders. Best practice & research. Clinical endocrinology & metabolism 23, 103-116.

155. Schlicker, E., Kathmann, M., 2001. Modulation of transmitter release via presynaptic cannabinoid receptors. Trends Pharmacol. Sci. 22, 565-572.
156. Scholl, J.L., Afzal, A., Fox, L.C., Watt, M.J., Forster, G.L., 2019. Sex differences in anxiety-like behaviors in rats. Physiology & Behavior 211.
157. Schuske, K.R., Richmond, J.E., Matthies, D.S., Davis, W.S., Runz, S., Rube, D.A., van der Bliek, A.M., Jorgensen, E.M., 2003. Endophilin is required for synaptic vesicle endocytosis by localizing synaptojanin. Neuron 40, 749-762.
158. Schweitzer, P., 2000. Cannabinoids decrease the K+ M-current in hippocampal CA1 neurons. J. Neurosci. 20, 51-58.
159. Simiand, J., Keane, M., Keane, P.E., Soubrie, P., 1998. SR 141716, a CB1 cannabinoid receptor antagonist, selectively reduces sweet food intake in marmoset. Behavioural pharmacology 9, 179-181.
160. Simonin, F., Karcher, P., Boeuf, J.J.M., Matifas, A., Kieffer, B.L., 2004. Identification of a novel family of G protein-coupled receptor associated sorting proteins. J. Neurochem. 89, 766-775.
161. Smith, F.L., Cichewicz, D., Martin, Z.L., Welch, S.P., 1998. The enhancement of morphine antinociception in mice by Delta(9)-tetrahydrocannabinol. Pharmacol. Biochem. Beh. 60, 559-566.
162. Smith, J.S., Lefkowitz, R.J., Rajagopal, S., 2018. Biased signalling: from simple switches to allosteric microprocessors. Nat. Rev. Drug Discov. 17, 243-260.
163. Smrcka, A.V., 2008. G protein betagamma subunits: central mediators of G protein-coupled receptor signaling. Cell. Mol. Life Sci. 65, 2191-2214.
164. Squire, L.R., 2004. Memory systems of the brain: A brief history and current perspective. Neurobiol. Learn. Mem. 82, 171-177.
165. Stiedl, O., Radulovic, J., Lohmann, R., Birkenfeld, K., Palve, M., Kammermeier, J., Sananbenesi, F., Spiess, J., 1999. Strain and substrain differences in context- and tone-dependent fear conditioning of inbred mice. Behav. Brain. Res. 104, 1-12.
166. Stimpson, H.E.M., Toret, C.P., Cheng, A.T., Pauly, B.S., Drubin, D.G., 2009. Early-Arriving Syp1p and Ede1p Function in Endocytic Site Placement and Formation in Budding Yeast. Mol. Biol. Cell 20, 4640-4651.
167. Straiker, A., Dvorakova, M., Zimmowitch, A., MacKie, K., 2018. Cannabidiol inhibits endocannabinoid signaling in autaptic hippocampal neurons. Mol. Pharmacol. 94, 743-748.
168. Straiker, A., Mackie, K., 2005. Depolarization-induced suppression of excitation in murine autaptic hippocampal neurones. J. Physiol-London 569, 501-517.
169. Straiker, A., Wager-Miller, J., Mackie, K., 2012. The CB1 cannabinoid receptor C-terminus regulates receptor desensitization in autaptic hippocampal neurones. Br. J. Pharmacol. 165, 2652-2659.
170. Suenaga, T., Ichitani, Y., 2008. Effects of hippocampal administration of a cannabinoid receptor agonist WIN 55,212-2 on spontaneous object and place recognition in rats. Behav. Brain. Res. 190, 248-252.
171. Sugiura, T., Kondo, S., Sukagawa, A., Nakane, S., Shinoda, A., Itoh, K., Yamashita, A., Waku, K., 1995. 2-Arachidonoylglycerol: a possible endogenous cannabinoid receptor ligand in brain. Biochem. Biophys. Res. Commun. 215, 89-97.
172. Team, R Core., 2020. R: A language and environment for statistical computing. R Foundation for Statistical Computing, Vienna, Austria. URL https://www.R-project.org/.

173. Techlovská, Chambers, J.N., Dvo?áková, M., Petralia, R.S., Wang, Y.-X., Hájková, A., Nová, A., Franková, D., Prezeau, L., Blahos, J., 2014. Metabotropic glutamate receptor 1 splice variants mGluR1a and mGluR1b combine in mGluR1a/b dimers in vivo. Neuropharmacology 86, 329-336.
174. Toczek, M., Malinowska, B., 2018. Enhanced endocannabinoid tone as a potential target of pharmacotherapy. Life Sci. 204, 20-45.
175. Trevaskis, J., Walder, K., Foletta, V., Kerr-Bayles, L., McMillan, J., Cooper, A., Lee, S., Bolton, K., Prior, M., Fahey, R., Whitecross, K., Morton, G.J., Schwartz, M.W., Collier, G.R., 2005. Src homology 3-domain growth factor receptor-bound 2-like (endophilin) interacting protein 1, a novel neuronal protein that regulates energy balance. Endocrinology 146, 3757-3764.
176. Uezu, A., Horiuchi, A., Kanda, K., Kikuchi, N., Umeda, K., Tsujita, K., Suetsugu, S., Araki, N., Yamamoto, H., Takenawa, T., Nakanishi, H., 2007. SGIP1 alpha is an endocytic protein that directly interacts with phospholipids and Eps15. J. Biol. Chem. 282.
177. Varvel, S.A., Lichtman, A.H., 2002. Evaluation of CB1 receptor knockout mice in the Morris water maze. J. Pharmacol. Exp. Ther. 301, 915-924.
178. Vaughan, C.W., Connor, M., Bagley, E.E., Christie, M.J., 2000. Actions of cannabinoids on membrane properties and synaptic transmission in rat periaqueductal gray neurons in vitro. Mol. Pharmacol. 57, 288-295.
179. Velasco, E.R., Florido, A., Milad, M.R., Andero, R., 2019. Sex differences in fear extinction. Neurosci. Biobehav. Rev. 103, 81-108.
180. Viveros, M.P., Marco, E.M., File, S.E., 2005. Endocannabinoid system and stress and anxiety responses. Pharmacol Biochem Be 81, 331-342.
181. Walder, K.R., Fahey, R.P., Morton, G.J., Zimmet, P.Z., Collier, G.R., 2000. Characterization of obesity phenotypes in Psammomys obesus (Israeli sand rats). Int. J. Exp. Diabetes Res. 1, 177-184.
182. Walker, J.M., Huang, S.M., Strangman, N.M., Tsou, K., Sanudo-Pena, M.C., 1999. Pain modulation by release of the endogenous cannabinoid anandamide. Proc. Natl. Acad. Sci. U. S. A. 96, 12198-12203.
183. Weis, W.I., Kobilka, B.K., 2018. The Molecular Basis of G Protein-Coupled Receptor Activation. Annu. Rev. Biochem. 87, 897-919.
184. Welch, S.P., Stevens, D.L., 1992. Antinociceptive activity of intrathecally administered cannabinoids alone, and in combination with morphine, in mice. J. Pharmacol. Exp. Ther. 262, 10-18.
185. Welch, S.P., Thomas, C., Patrick, G.S., 1995. Modulation of cannabinoid-induced antinociception after intracerebroventricular versus intrathecal administration to mice: possible mechanisms for interaction with morphine. J. Pharmacol. Exp. Ther. 272, 310-321.
186. Whistler, J.L., Enquist, J., Marley, A., Fong, J., Gladher, F., Tsuruda, P., Murray, S.R., von Zastro, M., 2002. Modulation of postendocytic sorting of G-protein coupled receptors. Science 297, 615-620.
187. Wilhelm, B.G., Mandad, S., Truckenbrodt, S., Krohnert, K., Schafer, C., Rammner, B., Koo, S.J., Classen, G.A., Krauss, M., Haucke, V., Urlaub, H., Rizzoli, S.O., 2014. Composition of isolated synaptic boutons reveals the amounts of vesicle trafficking proteins. Science 344, 1023-1028.
188. Williams, C.M., Kirkham, T.C., 1999. Anandamide induces overeating: mediation by central cannabinoid (CB1) receptors. Psychopharmacology 143, 315-317.

189. Williams, C.M., Rogers, P.J., Kirkham, T.C., 1998. Hyperphagia in pre-fed rats following oral delta9-THC. Physiology & behavior 65, 343-346.
190. Wisler, J.W., Rockman, H.A., Lefkowitz, R.J., 2018. Biased G Protein-Coupled Receptor Signaling: Changing the Paradigm of Drug Discovery. Circulation 137, 2315-2317.
191. Woodhams, S.G., Chapman, V., Finn, D.P., Hohmann, A.G., Neugebauer, V., 2017. The cannabinoid system and pain. Neuropharmacology 124, 105-120.
192. Yeomans, J.S., Frankland, P.W., 1995. The acoustic startle reflex: neurons and connections. Brain research. Brain research reviews 21, 301-314.
193. Zimmer, A., Zimmer, A.M., Hohmann, A.G., Herkenham, M., Bonner, T.I., 1999. Increased mortality, hypoactivity, and hypoalgesia in cannabinoid CB1 receptor knockout mice. Proc. Natl. Acad. Sci. U. S. A. 96, 5780-5785.